Assessing the long-term risk of metal pollutants to honey bees: effects on the survival of adults, larvae, and mechanistic modeling

Thesis

Presented in Partial Fulfillment of the Requirements for the Degree Master of Science in the Graduate School of The Ohio State University

By

Dylan Frank Ricke

Graduate Program in Entomology

The Ohio State University

2022

Thesis Committee

Dr. Reed Johnson, Advisor

Dr. Mary Gardiner

Dr. James Strange

Abstract

Honey bees are exposed to an array of potentially toxic chemicals, which differ in aspects of their toxicity as well as their fate in the environment. In Chapter 1 of my thesis, I discuss the exposure and effects of toxic chemicals to honey bees through the lens of chemical kinetics. I also describe applications of kinetic modeling for the development of mechanistic models of colony exposure. In chapter 2, I demonstrate how kinetic modeling (toxicokinetic-toxicodynamic modeling) can be used to predict the long-term effects of chemical exposure on the survival of individual honey bees and the growth of their colonies. I focus on metal pollutants (As, Cd, Li, Pb, and Zn), which honey bees are exposed to in a range of human modified environments. I found that a toxicokinetic-toxicodynamic model (the General Unified Thresholds Model of Survival, GUTS) better predicted the survival of honey bees in the lab than a simple extrapolation of a standard (probit) model that is commonly used in honey bee risk assessments. When predicting the effects of metal exposure on colony growth, differences between modeling approaches were highly case-specific. In chapter 3, I focus on the exposure and effects of metals to immature honey bees. Specifically, I describe an experiment using queen-rearing boxes to measure the accumulation of metals into larval food (nurse jelly) and developing queen larvae. I also describe a laboratory study on the toxicity of different metals to honey bee larvae reared *in vitro*. I found that Cd and Li translocate into larval foods at a higher rate than has been observed for pesticides. Furthermore, when applied to the larval diet *in vitro*, As, Li, and Zn affected the survival of honey bee larvae at field-relevant concentrations.

Acknowledgments

I would like to thank my advisor, Dr. Reed Johnson. Reed gave me great latitude in the development of my research, and his enthusiasm for the practice of science is exemplary.

I also thank the members of my thesis committee. The four classes I've taken that were either instructed or co-instructed by Dr. Mary Gardiner were very helpful in my professional development as well as my understanding of insect ecology. Dr. Jamie Strange has remained a thoughtful voice during meetings and has done well as our department head during these eventful years.

I would also like to thank the fellow members of the Johnson lab. At this point, my thesis was directly aided by Chia-Hua Lin (methods development for Chapter 3), Jessica Lyons and Brandon Shannon (assisting in the execution of Chapter 3), Brittany Leyda and Brandon Shannon (assistance with toxicological assays in Chapter 2), and Katie Hutchison, Nicole Sammons, and Will Passifiume (performing the *in vitro* larval assays presented in Chapter 3).

Outside of the lab, I would like to thank Sarah Scott, who has welcomed my recurring questions related to bees and metals. Great thanks to Dr. Helen Hesketh of the UK Center for Ecology and Hydrology, who shared data from a paper of hers while I was developing the toxicological models in Chapter 2. I would also like to thank the other members of the virtual 2021 short course, Dynamical Modeling of Toxic Effects, which was offered by the University of Copenhagen and was instructed by the developers of a model of survival that is explored in Chapter 2. I thank personnel employed by Bayer

Crop Science (Dr. Daniel Schmehl, Dr. Vanessa Roeben, and Dr. Thomas Preuss), who met to discuss overlapping research interests and aspects of the modeling methodology presented in Chapter 2. Finally, I thank the Ohio State College of Food, Agriculture, and Life Sciences Internal Grants Program, which provided funding for the research presented in Chapter 3 through the SEEDS Competitive Grants Program.

Vita

2011.....Miami Palmetto Senior High School

Feb. 2015- Dec. 2016....K-12 math instructor, Mathnasium Math Learning Centers

2016.....Orchid lab intern, Fairchild Tropical Botanic Gardens

2016.....B.S. in Biology, New College of Florida

2017.....Entomology research intern, Archbold Biological Station

Nov. 2017- Feb. 2019 ...Lab manager, Dyer Lab, University of Georgia

August 2019.....Director's Associateship Award, The Ohio State University (OSU) College of Food, Agriculture, and Life Sciences (CFAES)

Feb. 2020.....OSU Competitive Grants Program (SEEDS) recipient

Aug. 2020-May 2021....Entomological Graduate Student Association (EGSA) Representative, Social Committee

Aug. 2020-May 2022....EGSA Representative, Entomology Seminar Committee

Aug. 2020-May 2022....Graduate Teaching Assistant, OSU

Nov. 2020.....First place team (OSU/University of Minnesota), Annual Entomological Student Debates Competition, The Entomological Society of America (ESA) Annual Conference

April 2021.....Best Research Poster, M.S. division, OSU-CFAES Annual Research Conference

Nov. 2021.....First place oral presentation, DeLong student seminar competition, OSU Dept. of Entomology

Nov. 2021.....Best M.S. research poster, PIE, pollinator division, ESA Annual Conference, Denver, CO

Publications

Ricke, D., C. Lin , R. Johnson. **2021**. Pollen Treated with a Combination of Agrochemicals Commonly Applied During Almond Bloom Reduces the Emergence Rate and Longevity of Honey Bee (Hymenoptera: Apidae) Queens. J. Insect Sci. 21(6): 5, 1-8. doi.org/10.1093/jisesa/ieab074.

Bernaola, L., M. Darlington, K. Britt, P. Prade, M. Roth, A. Pekarcik, M. Boone, D. Ricke, A. Tran, J. King, K. Carruthers, M. Thompson, J. J. Ternest, S. E. Anderson, S. W. Gula, K. C. Hauri, J. R. Pecenka, S. Grover, H. Puri, and S. G. Vakil. 2021. Technological Advances to Address Current Issues in Entomology: 2020 Student Debates. J. Insect Sci. 21(2): 18, 1-8. doi.org/10.1093/jisesa/ieab025.

Fields of Study

Major Field: Entomology

Table of Contents

List of Tables

List of Figures

Chapter 1. Literature review: The relevance of chemical kinetics for honey bee risk assessment

Abstract

The exposure of honey bees to toxic chemicals has received much research attention, but the risk posed to honey bee colonies in the field remains challenging to determine using routine risk assessment procedures. To that end, mechanistic risk assessment models are in development that can simulate chemical exposure and effects at the colony level. To be useful, such models must account for the differential fate of chemicals in the field, in colonies, and their effects on colony functioning over time. Here, I address each of these factors through the lens of chemical kinetics. Specifically, I discuss applications of chemical kinetics for modeling the environmental fate of toxic chemicals as it relates to colony exposure (kinetic fate modeling) and the effects of toxic exposure over time (toxicokinetic-toxicodynamic modeling). I conclude with a brief review of toxicokinetic studies at the molecular level and their potential application to honey bee risk assessment.

1.1 Introduction

The exposure of honey bees to potentially toxic chemicals remains a high-profile environmental issue with direct implications for agriculture (Calderone 2012, Reilly et al. 2020). Additionally, as a biomonitor (Niell et al. 2018, Smith et al. 2019) and a toxicological model species (Thompson and Pamminger 2019), the exposure and effects of toxic compounds on honey bees has implications for the conservation of other terrestrial arthropods.

There's growing evidence that field-relevant levels of toxic exposure can have adverse effects on the functioning of honey bees and their colonies (Fisher et al. 2021, Milone et al. 2021, Traynor, VanEngelsdorp, et al. 2021). However, the risk associated with a particular toxic chemical, or combination of chemicals, remains difficult to determine in real world scenarios (Henry et al. 2015, Carnesecchi et al. 2019, Cullen et al. 2019). This difficulty stems from gaps in our understanding of the processes leading to exposure (Simon-Delso et al. 2017, Sponsler and Johnson 2017) as well as the effects resulting from exposure (Grimm and Martin 2013). The existence of these knowledge gaps is unsurprising given the complexity of the situation. The exposure of honey bees to a given chemical will fluctuate over time. Toxic chemicals are differentially persistent, both in the field (Bonmatin et al. 2015, Gierer et al. 2019) and within colonies (Shimshoni et al. 2019). Some chemicals may also be persistent within the bodies of bees (Suchail et al. 2001, Mokkapati et al. 2022), which can result in time-cumulative effects that are not always predictable from short-term studies (Hesketh et al. 2016, Simon-Delso et al. 2018, Tosi et al. 2021). Finally, honey bees are frequently exposed to multiple toxic chemicals simultaneously, which opens the possibility of synergistic effects (Carnesecchi et al. 2019, Ostiguy et al. 2019).

These overlapping factors-- time-variable exposure, chemical persistence, time-cumulative toxicity, and the hazard arising from chemical mixtures-- comprise the honey bee "risk cup" (Fig. 1). The risk cup represents the combined risk (hazard x exposure) across all chemicals and routes of exposure.

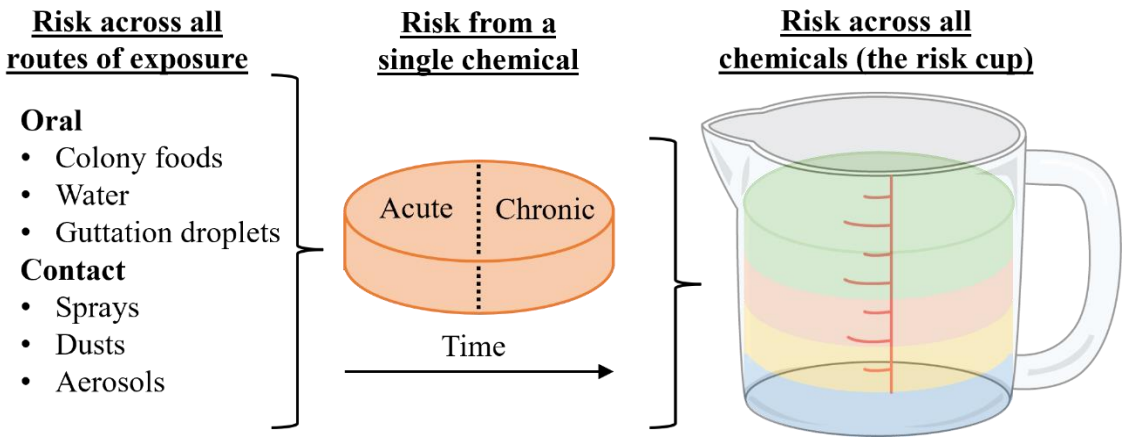

Figure 1. The honey bee risk cup (right) represents combined risk resulting from exposure to multiple toxic compounds (colored layers). The risk posed by a given substance (center) is the aggregate risk resulting from multiple potential sources of exposure (left), the intensity of that exposure over time (from acute to chronic), and the hazard (toxicity) associated with each chemical (not shown).

The risk cup concept is relevant to honey bee colonies, but difficult to implement in a standardized risk assessment process owing to its multifactorial nature and the many knowledge gaps in this area. For these reasons, current risk assessment models for pesticide registration (ex. Bee-REX) (USEPA 2014) make simplifying assumptions and reduce the number of factors under consideration. Rather than representing exposure over time, these models only consider worst-case *daily* rates of exposure. Although multiple life stages and exposure pathways are represented (Berenbaum 2016), there is currently no standardized approach for assessing the combined risk of chemical mixtures. In contrast with current approaches to honey bee risk assessment, mechanistic models are appealing because they can simulate the colony-level dynamics governing exposure (ex. foraging, food sharing) across the members of colonies (Sponsler and Johnson 2017) as well as the colony-level effects of exposure over time (Kuan et al. 2018, Schmolke et al.

2019). Such models are currently in development for honey bee risk assessment at the regulatory level (EFSA 2016, More et al. 2021).

Here, I discuss the relevance of chemical kinetics (hereafter, "kinetics") for addressing the components of the honey bee risk cup (Fig. 2). Kinetics is the basis of most chemical fate models used for chemical risk assessment, but has seen limited application for this purpose in models of honey bee exposure. Instead, models have tended to focus on aspects of honey bee's social biology affecting their exposure (Sponsler and Johnson 2017). Kinetic processes also determine the rate that toxic chemicals accumulate and are detoxified within individual organisms. This is the subject of the field of toxicokinetics (Grech et al. 2017). Survival models accounting for toxicokinetic factors stand to improve our ability to predict toxic effects over time at the individual and population levels (Ashauer and Escher 2010). These models present the most immediate opportunities for improving the risk assessment process for honey bees because they can leverage data generated during standard bioassays used to determine acute and chronic toxicity. I conclude with a discussion of toxicokinetic studies at the suborganismal level (i.e. at the chemical, cellular, and molecular levels). Research in this area stands to improve our ability to predict toxicity based on chemical structures (Carnesecchi et al. 2020), chemical sensitivities across taxa (López-Osorio and Wurm 2020), and the development of high-throughput *in vitro* models to complement existing chemical risk assessment practices (Haas and Nauen 2021).

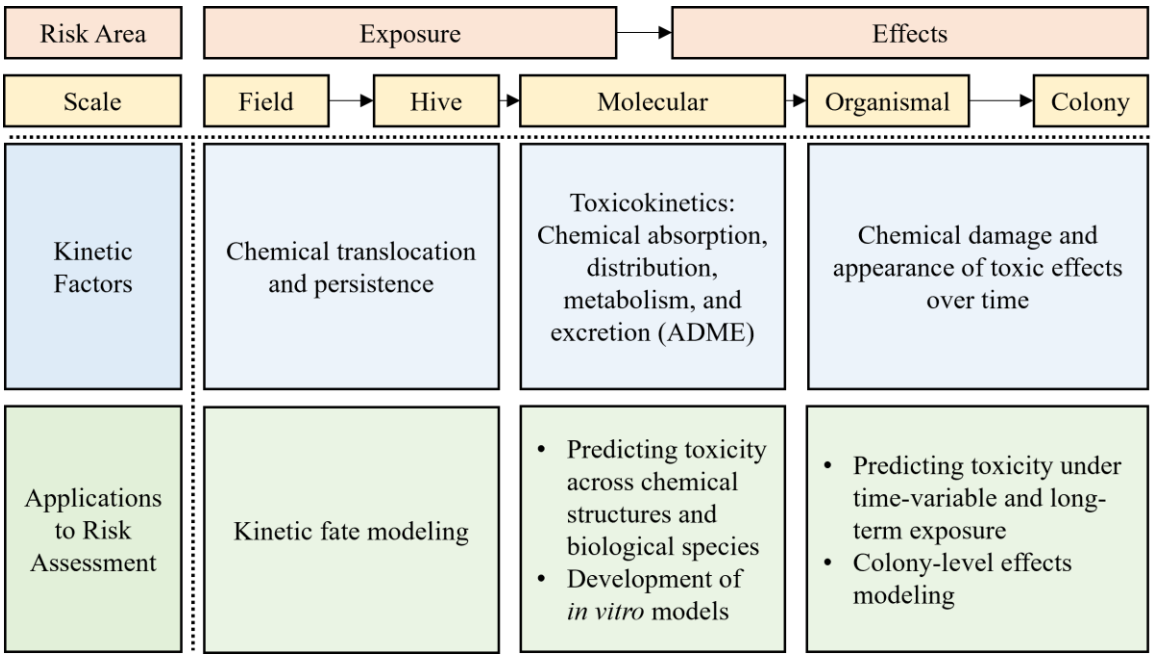

Figure 2. The relevance of toxicokinetics and its application to different aspects of honey bee risk assessment.

1.2 Kinetic fate

The kinetic fate of chemicals is the result of their movement between environmental compartments (soils, plants, colony matrices) and their persistence within those compartments. This is a complicated topic that will depend on chemical properties such as molecular weight, polarity, and vapor pressure, field variables, and the division of labor within colonies. Each of these factors have been discussed at length elsewhere (Bonmatin et al. 2015, Farha et al. 2016, Gierer et al. 2019). Here, I provide a brief review of these factors as they relate to colony exposure and exposure modeling, highlighting studies that have been published since the review of mechanistic models of exposure by Sponsler and Johnson (2017).

Modeling kinetic fate in the field

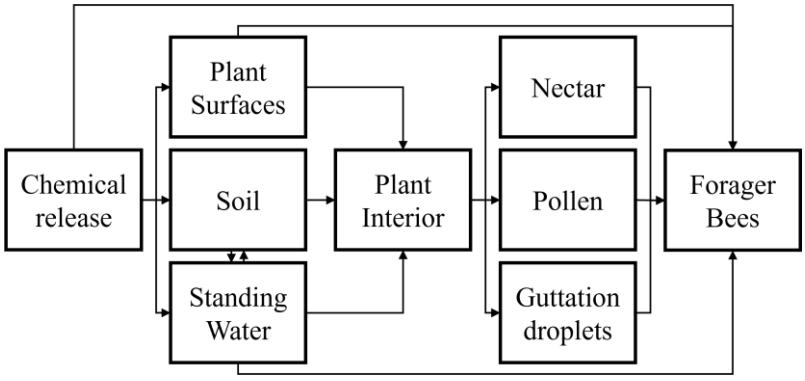

Figure 3. Routes of chemical exposure for honey bees foraging in the field.

Kinetic fate is an important consideration during honey bee risk assessment because chemical movement and persistence can vary widely across chemicals, studies, and environmental compartments. This variability is especially pronounced in the environment outside the hive (the field). In soils, for example, the half-lives of neonicotinoid insecticides can range from 100 to 1200 days, depending on the chemical and study (Bonmatin et al. 2015). In contrast, the soil half-lives of organophosphate insecticides are generally much lower ($\leq$ 30 days) (DiBartolomeis et al. 2019). The persistence of chemicals in soils, in combination with other factors like water solubility, allows them to translocate into the nectar and pollen of wildflowers, extending the period of time that colonies are exposed orally (Long and Krupke 2016). Within plants, pesticide half-lives are typically between 1 and 10 days, but some pesticides have in-plant half-lives as high as 150 days (Fantke and Juraske 2013). In addition to chemical properties, the persistence of chemicals across field components will vary with temperature

(volatilization), sunlight (photodegradation), humidity (hydrolysis), soil density (aerobic decomposition), and the presence of soil microbes (digestion) (Farha et al. 2016).

The EPA's Bee-REX model represents kinetic fate in a minimally mechanistic fashion, and only for pesticides applied as soil treatments. If field measurements of chemical residues in nectar and pollen are not available, a modified version of the soil-plant uptake model of Briggs et al. (1983) is used to predict the movement of pesticides into nectar and pollen (USEPA 2014). Chemical parameters in this model include the soil organic carbon-water partition coefficient (K_{oc}) and the octanol-water partition coefficient (K_{ow}). The values of the other parameters (soil organic content, water content, and density) are set by default to simulate a high exposure scenario (USEPA 2014). The EPA's implementation of this model is also designed to be conservative in predicting pesticide concentrations in nectar and pollen (resulting in worst-case predictions), which was confirmed with empirical data for five pesticides (FIFRA 2012). The Briggs model outperformed four other models when predicting the uptake of nonionic chemicals into plant shoots (Collins et al. 2006). However, the EPA's guidance document for honey bee risk assessment notes several limitations of the Briggs model: it was created to describe the uptake of chemicals into the shoots of a single plant species (barley) and had only been validated for neutral chemicals, for which translocation through plants will differ from those of ionic chemicals (USEPA 2014).

Kuan et al. (2018) present what is perhaps the most mechanistic model of chemical kinetics as it relates to honey bee exposure in the field. Like Bee-REX, they use the Briggs model to estimate pesticide concentrations in nectar and pollen following soil

application. Unlike Bee-REX, they model exposure over time. To represent the dissipation of pesticides in the field over time, they included two kinetic parameters, foliar half-life and aerobic soil half-life. Kinetic parameters are also included in the colony exposure model of Crenna et al. (2020), specifically the dissipation half-lives of pesticides in nectar and pollen. Each of these studies included a series of Monte Carlo simulations to capture the variability in model predictions resulting from variable combinations of chemical half-lives, as well as other model parameters. Similar methods may be used in future studies to determine kinetic parameters with the greatest influence on model outcomes and prioritization for subsequent research.

Modeling kinetic fate in the colony

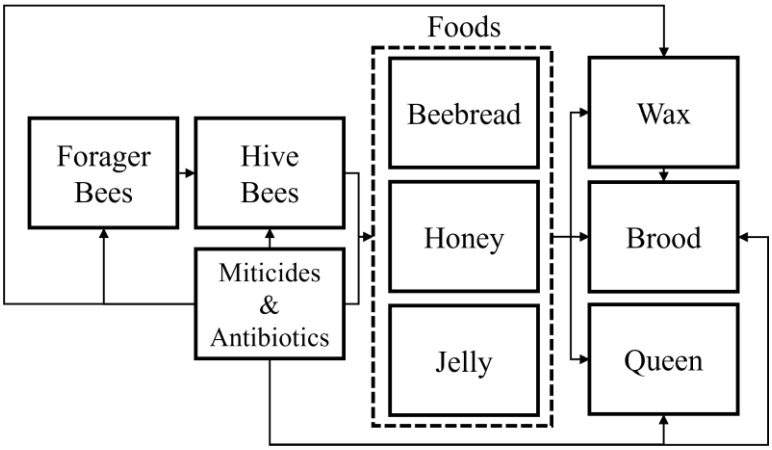

Figure 4. Routes of chemical exposure within colonies.

As in the field, the movement and persistence of chemicals within colonies varies widely across chemicals and compartments (colony matrices). For example,

neonicotinoids are unusually persistent in honey (Shimshoni et al. 2019). This may explain the widespread detection of neonicotinoids in honey samples from across the UK, despite having no registered use there for several years (Woodcock et al. 2018). Organophosphates, on the other hand, have lower persistence in honey, but greater persistence in wax (Shimshoni et al. 2019).

The best studied driver of chemical diffusion within colonies is lipid solubility. This largely determines the partitioning of chemicals between lipid-rich matrices, like colony wax (Shimshoni et al. 2019) and propolis (Simsek et al. 2021), versus lipid-insoluble matrices, like honey. Lipid solubility may also explain the relative affinity of chemicals for pollen relative to honey (de Oliveira et al. 2016) and the greater variety of chemicals that are typically measured from pollen samples collected in the field versus those measured from nectar or honey (Mullin et al. 2010, Ostiguy et al. 2019, Zioga et al. 2020). Although lipid solubility did not explain the relative translocation of pesticides from colony foods into nurse jelly (Böhme et al. 2018, 2019), it is an important consideration when predicting the diffusion of pesticides into jelly via contaminated wax (Kast and Kilchenmann 2022).

In addition to chemical properties like lipid solubility, the accumulation of toxic chemicals into the bodies of honey bees may also be an important parameter to include in kinetic fate models (Tremolada et al. 2011). Finally, several pesticides are known to form toxic metabolites within colonies, whose toxicity and persistence may differ from their parent compounds. For example, the miticide amitraz has a much shorter half-life than its

major metabolites, DMF and DMPF (Bommuraj et al. 2019), which are also differentially toxic to adult honey bees (Bommuraj et al. 2021).

The in-hive fate of chemicals is fertile ground for kinetic fate modeling because colony matrices differ widely in properties that affect the solubility of different chemicals (ex. lipid content) and there is less variability in environmental factors (ex. temperature and humidity) relative to conditions in the field. However, most colony exposure models do not represent in-hive exposure mechanistically. In Bee-REX, for example, pesticides in nectar and pollen are assumed to not degrade once within colonies. For nurse jelly, pesticides are assumed to occur at 1% of their concentration in nectar or pollen, whichever is greater. Recent studies suggest that the concentrations of pesticides in royal jelly are typically lower relative to colony foods (Böhme et al. 2019, Ricke et al. 2021). As such, the assumptions of Bee-REX result in worst-case estimates of daily exposure within colonies. To account for exposure over greater periods of time, kinetics will have to be included. For this reason, "in-hive pesticide residue dynamics" is considered a prerequisite for mechanistic models of exposure to be used for regulatory purposes in the European Union (EFSA 2016).

Perhaps the most mechanistic treatment of in-hive exposure is presented by Bonzini et al. (2011). They measured the accumulation of the miticide tau-fluvalinate into the bees, honey, and wax of colonies when applied to control the hive pest *Varroa destructor*. Measurements were then used to develop a predictive compartment model of the in-hive fate of tau-fluvalinate (Tremolada et al. 2011). Their model uses chemical properties including lipid solubility, organic carbon adsorption, and partial pressure to

calculate tau-fluvalinate's diffusion into hive wax, propolis, and honey. The results of a validation study corroborated their model, boding well for their general approach (Tremolada et al. 2011). Focusing on honey bees' social biology and food processing, Rumkee et al. (2017) modeled the distribution of pesticide-contaminated nectar among the honey cells of colonies. This model is certainly mechanistic, but does not incorporate chemical properties that may drive kinetics, such as persistence and diffusion across colony matrices.

Kinetic fate modeling going forward

Applications of kinetic fate modeling for honey bee risk assessment would benefit from more mechanistic research (Gierer et al. 2019). At present, most studies on colony exposure are observational and do not test mechanisms. This is reflective of the wider literature on the kinetic fate of chemicals in agricultural systems. For example, 18% of >800 studies reporting the dissipation half-lives of chemicals in plant components (leaves, fruits, roots, etc.) directly assessed the chemical properties that may explain observed differences across chemicals (Fantke and Juraske 2013). Notably, nectar and pollen were among the least represented plant matrices across studies (Fantke and Juraske 2013).

Kinetic fate modeling of honey bee exposure would benefit from a database of chemical properties, diffusion rates, and dissipation half-lives across chemicals and environmental compartments. Ideally, these parameters would be measured under standardized conditions. Shimshoni et al. (2019) provide an exemplary laboratory study

on the relative diffusion and persistence of 27 common pesticides in honey and beeswax as a function of their hydrophilicity, volatilization, and molar weight. Similar studies focusing on additional environmental compartments (pollen, soils) and breakdown processes (photodegradation, biodegradation) can be conducted to better characterize the kinetic processes throughout the full honey bee exposure pathway. Finally, more long-term studies of chemical fate in the field and within colonies will be necessary to inform and ultimately validate the predictions of kinetic fate models for honey bee protection (Zioga et al. 2020).

1.3 Toxicokinetic modeling at the organism level

In addition to mechanistic models of *exposure*, there's growing interest in mechanistic models of *toxic effects* for use in pesticide risk assessment (Grimm and Martin 2013, Vighi et al. 2019). These models represent the stepwise mechanisms leading from exposure to the appearance of toxic effects at the organism level (Fig. 5). These mechanisms are kinetic in nature and include the absorption, distribution, metabolization, and elimination of chemicals from the body (ADME), which make up the field of toxicokinetics (Grech et al. 2017). Within organisms, toxicants bind to their sites of action and cause damage, which is ultimately responsible for the toxic effects, such as mortality, that are the endpoints of bioassays. The formation and potential repair of damage is the subject of damage dynamics or toxicodynamics.

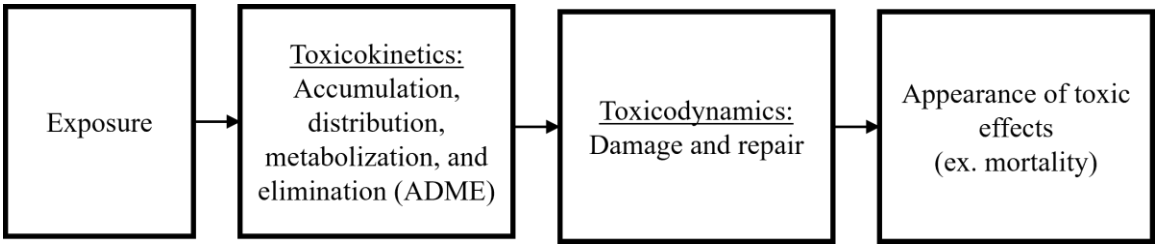

Figure 5. Mechanisms leading from exposure to toxicokinetics, toxicodynamics, and the appearance of toxic effects. TKTD models represent these stepwise mechanisms and associated parameters.

There are now a variety of toxicokinetic-toxicodynamic (TKTD) models available to represent the time course leading from chemical exposure to bioaccumulation, damage, and the appearance of toxic effects (Ashauer and Escher 2010, Jager et al. 2011). Although TKTD models represent processes that are suborganismal (e.g. bioaccumulation), there are minimally mechanistic TKTD models that can function with individual-level survival data, alone, making them amenable to data from standardized bioassays. These assays are conducted to calculate benchmarks of toxicity (LD_{50} values and no-observable-adverse-effect concentrations, or NOECs) during chemical risk assessments. The fact that TKTD models can function without information on chemical concentrations within organisms is noteworthy given the replication and technical expertise required to measure low concentrations of pesticides from bees during bioassays (Zaworra et al. 2019, Mokkapati et al. 2022). One such TKTD model, the General Unified Thresholds Model of Survival (GUTS) (Jager et al. 2011), was recently approved for aquatic risk assessment at the regulatory level in the European Union (Ockleford et al. 2018) and has been applied to bioassay data from honey bees in at least three studies (Hesketh et al. 2016, Heard et al. 2017, Robinson et al. 2017). This model is

a generalization of preexisting TKTD models and can operate with or without data on chemical concentrations within the organism (Jager et al. 2011).

TKTD models present unique advantages when analyzing data from bioassays (Ashauer and Escher 2010). Unlike standard dose-response models (ex. probit and logistic models), TKTD models use mortality data from all days over which the bioassay was conducted. This allows calculation of benchmarks of toxicity without relying entirely on the particular dose-response pattern at the last day of the assay. In addition, the parameters of TKTD models are typically rate constants that can be used to predict toxic effects over a range of untested exposure conditions. Standard dose-response models, by contrast, only provide a "static" picture of toxicity (holding either time or dosage constant) that require added assumptions for the purpose of extrapolation (Fig. 6).

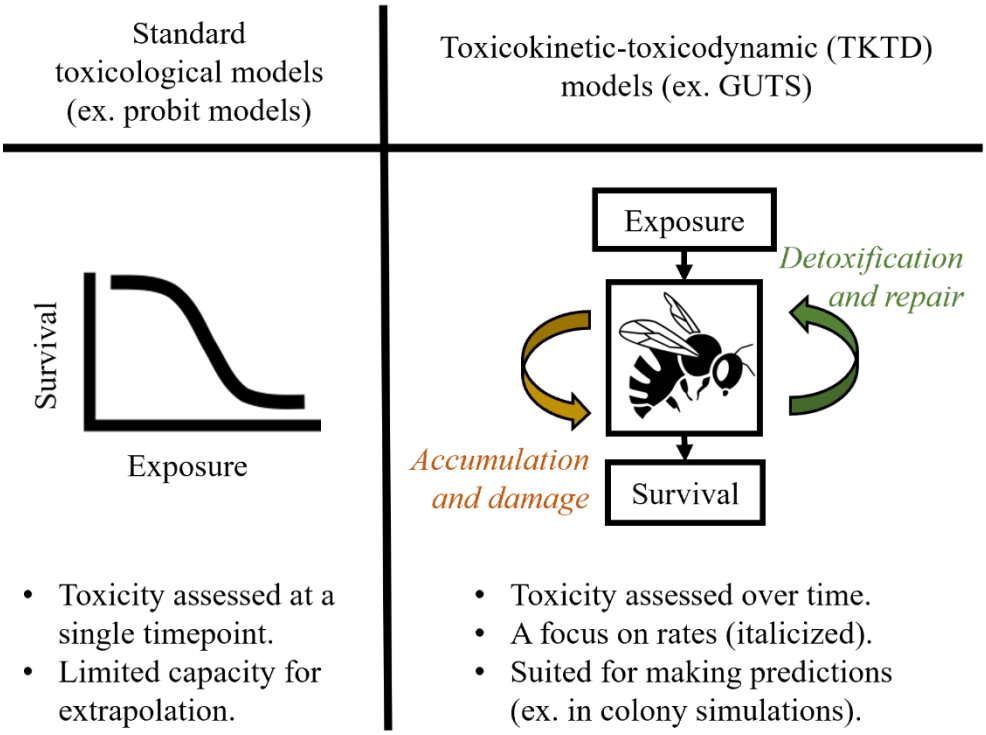

Figure 6. A comparison of standard toxicological models and TKTD models.

Toxicity over time

Because of their focus on toxicity over time as well as dosage, TKTD models can be used to predict toxic effects across a range of untested exposure scenarios. In that regard, they're most relevant for analyzing data from chronic toxicity assays. In the last decade, adult and larval honey bee chronic toxicity assays, lasting for ten and 22 days, respectively, were approved for use in the pesticide registration processes in the US and the European Union (OECD 2017, Schmehl et al. 2018). There remain a number of commonly-used pesticides for which chronic toxicity data from honey bees have not been generated during registration or reregistration, which occurs at least once every 15 years for pesticides registered in the US (USEPA 2021).

TKTD modeling can be used to improve the chronic risk assessment process for honey bees in two distinct ways. First, like acute toxicity assays, the data from chronic toxicity assays are currently only assessed at a single timepoint (usually the last day of the assay). This omits temporal information that may be important when dealing with toxicants that exhibit time-cumulative toxicity. Because TKTD models utilize data from all days of the assay, they can be used to characterize the degree of time-cumulative toxicity exhibited by a given chemical. The outputs of TKTD models can then be cross-validated with existing metrics of time-cumulative toxicity, such as the Haber constant (Cresswell 2018).

A second issue related to chronic toxicity testing is the duration of the assay. Standard chronic toxicity assays with adult honey bees are shorter ($\leq$10 days) than the typical honey bee lifespan (for summer bees: about one month, for winter bees: multiple months; Winston 1987). Because field-relevant concentrations of most chemicals do not produce measurable effects on honey bee survival over this duration, researchers often include concentrations that are higher than expected based on field studies. This may be sufficient to generate dose-response curves and to calculate the current benchmarks of toxicity, but it does not predict a chemical's effect on survival over the lifespan of the organism. TKTD models, by contrast, can be used to predict toxic effects over longer periods of time as well as lower exposure concentrations than those included in bioassays. This can also assist in identifying chemicals that may warrant more extended assays (>10 days) (Moncharmont et al. 2003, Simon-Delso et al. 2018, Tosi et al. 2021).

Methods for extrapolating standard dose-response models (ex. probit and logistic models) to predict the long-term effects of toxicants have been described (Sánchez-Bayo 2009). Similar approaches have been proposed for setting limits of exposure (Doull and Rozman 2000). Unlike TKTD models, these approaches lack a mechanistic basis, relying instead on transformations of the data and/or linear extension of the dose-response relationship over time (Belkebir et al. 2011). This overlooks TKTD processes within organisms (detoxification, elimination, damage repair) that may compensate for low levels of exposure over time. For example, based on a linear extrapolation of the data of Moncharmont et al. (2003), Rondeau et al. (2014) predicted that the long-term exposure of overwintering bees to just 0.25 ppb of imidacloprid would result in widespread mortality among the bees in a colony. However, in colonies exposed to sucrose solution containing 5 ppb of imidacloprid for 6 weeks (July-August), neither colony size nor longevity were reduced over the following ~7 months (September-April; Meikle et al. 2022). This occurred despite imidacloprid concentrations in honey persisting at concentrations between 2 and 5.9 ppb between November and February (supplementary material of Meikle et al. 2022).

TKTD modeling has already been used to extrapolate the results of 10-day chronic toxicity assays with honey bees over longer periods of exposure. Hesketh et al. (2016) found that the 10-day LC_{50} for the heavy metal cadmium was ~3X greater than its 30-day LC_{50} as estimated by GUTS. Extrapolating to the lifespan of winter bees (~90 days), the difference was roughly 10-fold, without accounting for differential rates of food consumption between summer and winter bees. By contrast, GUTS predicted more

similar LC_{50} values over time for the pesticides included in the study, indicative of lower levels of time-cumulative toxicity for those chemicals. A variety of TKTD studies with other organisms, primarily aquatic invertebrates, further demonstrate how lethal toxicity data can be used to predict toxic effects beyond the duration of bioassays (Brock et al. 2021).

Their ability to predict toxic effects over time also makes TKTD models applicable as modules in mechanistic models of honey bee exposure (Hörig et al. 2015). GUTS and related TKTD models have already been used to model the population dynamics of a variety of taxa under chemical stress, including *Daphnia magna* (Gergs et al. 2016), the mysid shrimp *Gammarus pulex* (Galic et al. 2014), and the earthworm *Eisenia fetida* (Roeben et al. 2020). Notably, most research on honey bee colony modeling has focused on the *exposure* of colonies to toxicants, with little if any exploration of how to model the subsequent *effects*. For this and other applications of population models in honey bee risk assessment, standardized exposure scenarios may be required (e.g. the FOCUS surface water scenarios used for aquatic risk assessment in the EU; Ockleford et al. 2018).

Mixture toxicity

In addition to assessing the toxicity of individual chemicals over time, TKTD modeling can be used to assess the toxicity of chemical mixtures. Again, mixture toxicity is highly relevant to honey bees: Large-scale surveys of commercial colonies in the US detected between 3 and 15 co-occurring pesticides on average, with over 100 unique

pesticides detected across studies (Mullin et al. 2010, Traynor et al. 2016, Ostiguy et al. 2019). In a given year, pesticides representing >9 modes of action have been detected from individual apiaries (Ostiguy et al. 2019). Particular combinations of chemicals are also known to have synergistic effects on honey bees, for example, sterol-biosynthesis inhibitors and other pesticides, including common apicultural miticides (Johnson et al. 2013, Carnesecchi et al. 2019). The potential for synergistic interactions significantly complicates the task of assessing the risk posed by chemical mixtures.

Existing metrics for quantifying the toxicity of chemical mixtures overlook the factor of time. Many studies have utilized a simple hazard quotient, sometimes referred to as the Toxic Unit (Rortais et al. 2017), calculated by adding the ratios of chemical concentrations then dividing by their LD_{50} or NOEC values (Stoner and Eitzer 2013). This quotient may be useful as a simple indicator of risk and it has been correlated with adverse colony-level outcomes (Traynor et al. 2016). However, it relies on point-estimates of toxicity with limited utility for predicting toxic effects over time. It also has not been applied consistently across studies, particularly the definition of quotient values indicating unacceptable levels of risk (Thompson 2021).

A very small number of studies have used pesticide usage data to quantify the combined toxicity of chemicals to honey bees across space and over large time intervals, which is known as toxicity loading (Goulson et al. 2018, Douglas et al. 2020). One study also considered the relative persistence of pesticides in the field (DiBartolomeis et al. 2019), providing a more mechanistic assessment of toxicity loading over time. Although metrics of toxicity loading may capture long-term and large-scale trends in chemical

abundance and their associated risk, like the hazard quotient approach, they rely on benchmarks of toxicity taken from a single timepoint in bioassays. Other metrics for assessing the toxicity of mixtures take synergistic interactions into account (ex. modified Toxic Units, Rortais et al. 2017), but do not consider time-cumulative toxicity (Carnesecchi et al. 2019). It should be noted that several mechanistic colony models exist that represent colony growth over multiple years, which may be suitable for conducting simulations of repeated and/or persistent exposure to chemical mixtures over time (Becher et al. 2014, Kuan et al. 2018).

Like standard approaches utilizing curve-fitting models, TKTD modeling can be used to test whether chemicals exhibit interactive effects in combination (Bart et al. 2021). To that end, TKTD modeling may provide special insights related to the modes of action of the chemicals in the mixture. In GUTS modeling, chemicals with similar modes of action are expected to produce similar forms of damage such that their combined effect can be predicted by adding their respective levels of damage (the concept of damage addition, Bart et al. 2021). As such, TKTD modeling can provide a cross-reference with existing concepts of mixture toxicity (concentration addition and independent action, Cedergreen et al. 2008). Toxic chemicals working through similar modes of action are also expected to have GUTS parameters that cluster together in parameter space, providing a novel screening-level diagnostic tool for determining probable modes of action across chemicals (Ashauer et al. 2015).

TKTD modeling in practice

TKTD models present practical advantages in comparison with standard dose-response models, including the ability to handle censored data, data with replicates of varying length, and data from assays with variable levels of exposure over time (Jager and Ashauer 2018a). However, TKTD modeling is not a panacea. Like existing methods, TKTD models will not be able to make accurate predictions with data from bioassays with insufficient dose-response information (e.g. all treatment groups exhibiting the same dose-response pattern). As with existing methods, treatments will have to be chosen carefully to balance field-relevance and the generation of informative data. Research designs and/or TKTD models may also have to be modified to account for factors that are not inherently toxicokinetic, such as ageing. Finally, exposure scenarios used in bioassays may need to be adjusted to optimize their application for TKTD modeling. For example, assays in which exposure occurs in one or two pulses can sometimes help to estimate particular TKTD parameters. Assay design will depend on the intended use for the data (i.e. generating certain benchmarks of toxicity, predicting toxicity over extended periods of exposure, time-variable exposure, etc.; Jager and Ashauer 2018b).

It must also be acknowledged that TKTD modeling is relatively data-intensive in comparison with approaches based on standard benchmarks of toxicity. Their application either requires TKTD parameters from previously fitted models or raw bioassay data for each chemical that could be used to estimate these parameters. Even if TKTD parameters were available for every chemical in isolation, the number of mixture studies required to test their interactions quickly becomes impractical. To simplify the problem, chemical

combinations can be prioritized according to their expected likelihood of exhibiting synergistic effects. This can potentially be achieved with high-throughput in silico docking studies (Mao et al. 2017, Carnesecchi et al. 2019). It may also be helpful to organize this effort in terms of chemical mechanisms of action (Ostiguy et al. 2019), as is done for the human risk cup (Reffstrup et al. 2010), bearing in mind that chemicals with the same mode of action may exhibit differential rates of synergy in combination with the same chemicals (Reid et al. 2020). TKTD parameters determined for chemicals representative of each group could then be compiled and used to assess the overall risk of field-relevant mixtures to honey bees over time via mechanistic modeling.

An assessment of mixture toxicity in the field as well as other applications of TKTD modeling with honey bees would benefit immensely from the availability of raw timeseries data generated from past toxicity assays. Currently, ecotoxicological databases focus on benchmarks of toxicity and chemical properties. These have proven useful for predicting toxicokinetic parameters and potentially the modes of action of chemicals in honey bees (Carnesecchi et al. 2020), but omit the temporal information contained in raw timeseries data. Long-term field studies measuring chemical residues from colonies will continue to be essential for model development (Zioga et al. 2020, Traynor, et al. 2021), combined with detailed pesticide usage data. The quality of such data is highly variable, both geographically and across pesticide categories, such as seed treatments (Hitaj et al. 2020). In the US, the most informative pesticide usage data is that collected annually by the California Department of Environmental Protection (“California Pesticide Information Portal” 2021).

1.4 Toxicokinetics at the suborganismal level

Toxicokinetic information at the suborganismal level can also be applied to risk assessment. Such data is not included as a standard part of the risk assessment process for honey bees, but is essential for the integration of toxicological data across the levels of biological organization. This integration is part and parcel of the development of *in vitro* models (e.g. cell cultures, enzyme assays), which may eventually be developed into high-throughput screening tools (Coecke et al. 2013). Importantly, this will require that *in vitro* measurements can be used to estimate risk at the organism level. This is the motivation for the development of adverse outcome pathways (AOPs), a conceptual framework for linking molecular events triggered by toxicants to their organism-level effects (Ankley et al. 2010). TKTD modeling will be essential to the development of AOPs because, unlike the parameters of standard dose-response models, they have explicit biological meaning (e.g. rates of chemical uptake, amounts of damage) that can be cross-checked between *in vivo* and *in vitro* models (Ashauer et al. 2015).

Below, we illustrate the utility of toxicokinetic information for honey bee risk assessment through a series of studies on neonicotinoids (LaLone et al. 2017). These studies illustrate how data from organism-level bioassays have been used to guide increasingly mechanistic studies, eventually leading to major insights on the toxicokinetics of chemicals within honey bees and across bee species (Fig. 7).

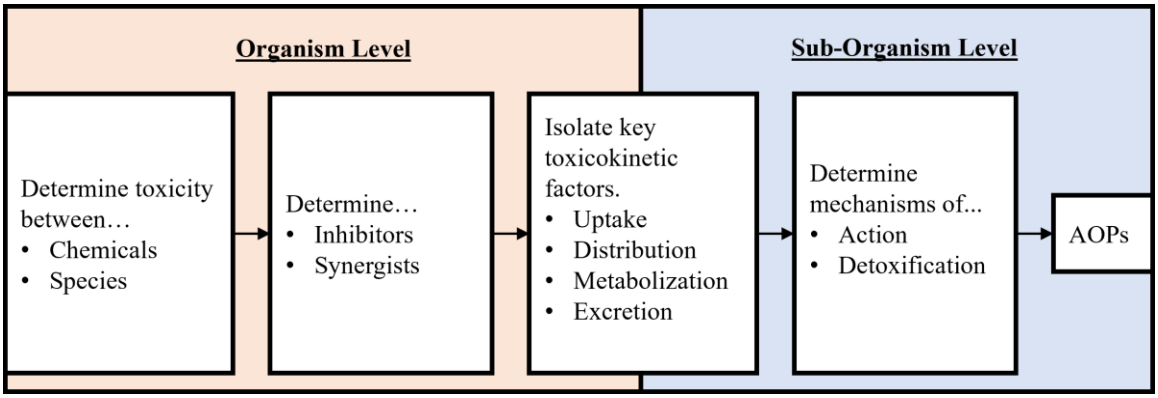

Figure 7. The development of toxicokinetic knowledge, beginning with organism-level studies (left), leading to increasingly mechanistic studies and elucidation of Adverse Outcome Pathways (AOPs) at the sub-organismal level (Ankley et al., 2010).

Most toxicokinetic research with honey bees below the organism level has been informed by organism-level bioassays. Through such assays, it is known that structurally-related but distinct classes of neonicotinoids (the *N*-cyanoamidine and *N*-nitroguanidine classes) exhibit marked differences in their toxicity to honey bees (Iwasa et al. 2004) and the buff-tailed bumble bee (*Bombus terrestris*) (Cresswell et al. 2014, Manjon et al. 2018). It was not known whether these differences in toxicity between chemical classes were due to the differential binding affinity of neonicotinoids to their sites of action (nicotinic acetylcholine receptors, nAChRs) or the relative activity of bee detoxification enzymes against either subclass of neonicotinoids. *B. terrestris* is also known to be more susceptible to imidacloprid than honey bees, and accumulated imidacloprid at a greater rate than honey bees in a lab study, but the causes for between-species differences in sensitivity (e.g. differential rates of feeding, toxicokinetic factors) were not clear (Cresswell et al. 2014). Using chemicals that are known to inhibit particular classes of detoxification genes, there was strong evidence that differences in the sensitivity of

honey bees to either class of neonicotinoids involved detoxification enzymes in the cytochrome monooxygenase (P450) family (Iwasa et al. 2004). Subsequent to these organism-level bioassays, researchers applied radio-labeled neonicotinoids from each neonicotinoid class to tissue samples of bee brains, finding no significant differences in their binding affinity to bee nAChRs (Manjon et al. 2018).

The CYP3 clade of P450s was previously shown to be important for detoxification across insects (Li et al. 2007) and was implicated in the differential tolerance of honey bees to different pesticides (Berenbaum and Johnson 2015). Manjon et al. (2018) expressed each gene in the honey bee CYP3 clade in an insect cell line, which they exposed to either thiacloprid (*N*-cyanoamidine) or imidacloprid (*N*-nitroguanidine) and measured rates of metabolism via LC-MS/MS. This approach identified a single P450, CYP9Q3, that was primarily responsible for the differential sensitivity of honey bees to these neonicotinoid classes. Orthologs of this gene were later identified from the genomes of the red mason bee (*Osmia bicornis*) and the buff tailed bumble bee and confirmed to efficiently metabolize *N*-cyanoamidine neonicotinoids *in vitro* (Beadle et al. 2019, Troczka et al. 2019). The P450 genes from each bee species also conferred resistance to these neonicotinoids when expressed in transgenic fruit flies (Manjon et al. 2018, Beadle et al. 2019, Troczka et al. 2019). Similar *in vitro* methods have also been used to identify honey bee P450 enzymes responsible for the detoxification of the butenolide insecticide flupyradifurone (Haas, Zaworra, et al. 2021) and synergistic effects, between pyrethroids and the miticide coumaphos (Johnson et al. 2009, Mao et al.

2011) and azole fungicides and a variety of pesticides, including the diamide insecticide chlorantraniliprole (Haas and Nauen 2021, Haas, Glaubitz, et al. 2021).

Kinetic factors other than detoxification by P450 enzymes also contribute to the differential toxicity of neonicotinoids in honey bees. Zaworra et al. (2019) demonstrated that imidacloprid translocates through the honey bee cuticle at a greater rate than thiacloprid and acetamiprid. The butenolide insecticide flupyradifurone, which has the same mechanism of action as neonicotinoids, had a slower uptake rate across the honey bee cuticle than two neonicotinoids in the same study, contributing to its lower overall toxicity relative to these chemicals (Haas, Zaworra, et al. 2021). Like imidacloprid, the *N*-cyanoamidine neonicotinoids acetamiprid and thiamethoxam form toxic metabolites, the latter including the neonicotinoid clothianidin (Nauen et al. 2003, Mokkapati et al. 2022).

In addition to developing new *in vitro* models, studies like those just described may eventually be used to validate predictive toxicological models incorporating chemical structures (Mao et al. 2011, Carnesecchi et al. 2020) and genomic data (López-Osorio and Wurm 2020). Toxicokinetic studies will also aid in the development of genetic biomarkers of honey bee stress. Measures of immune, stress, and detoxification gene expression together with organism-level effects have been reported in some studies and further investigation in this area is warranted (Christen and Fent 2017, Haas, Zaworra, et al. 2021).

1.5 Summary

Kinetics is relevant to each step of the honey bee risk assessment process, including exposure characterization (kinetic fate), the development of adverse outcome pathways (toxicokinetics), and hazard characterization (TKTD modeling). These kinetic factors will be essential for the continued development of mechanistic colony models to assess the impact of toxic exposure. Although mechanistic modeling requires more data than alternative modeling approaches, this challenge can be met through greater sharing of bioassay data and concerted research efforts to determine the kinetic properties of chemicals in different environmental compartments (soil, plants, floral resources, and hive matrices).

Chapter 2. Modeling the long-term (chronic) toxicity of major metal pollutants (As, Cd, Li, Pb, Zn) on honey bee survival and colony growth: A comparison of modeling approaches

Abstract

Honey bees are regularly exposed to metal pollutants in the environment. Metals never break down, allowing them to accumulate into honey bees and exert cumulative effects on honey bee health over time. Like other toxic chemicals, our understanding of the effects of metals on honey bees is largely based on relatively brief laboratory assays. Consequently, there's interest in modeling approaches that can leverage short-term toxicological data collected from individual honey bees to predict the cumulative effects of exposure on whole colonies. In the present study, I compared two approaches for predicting the effects of metals on honey bee survival: one utilizing a standard (probit) model of survival and another utilizing a toxicokinetic-toxicodynamic (TKTD) model (the General Unified Thresholds Model of Survival, GUTS). Specifically, I fitted each model to data from 10-day oral chronic toxicity assays with As, Cd, Li, Pb, and Zn. Fitted models were then used to predict the survival of honey bees in the laboratory under longer periods of exposure (> 10 days), which were validated for three of the metals (Cd, Li, and Zn). I found that GUTS outperformed probit modeling when predicting the survival of honey bees under exposure to Cd and Li, with equivocal results for Zn. Models were also used to predict the effects of each metal on colony growth, using a preexisting colony population model. The colony-level predictions of each modeling approach tended to overlap, with case-specific differences across metals. Based on my

results, I advise that colony modelers consider TKTD models when predicting honey bee survival and compare the predictions of contending models of survival when possible.

2.1 Introduction

Honey bees are regularly exposed to low (chronic) levels of a variety of potentially toxic chemicals in the environment, including metals (Johnson 2015, Solayman et al. 2016). As a class of toxicants, metals are uniquely persistent in environmental media (ex. soils) and are geographically widespread (Vareda et al. 2019). Metals are also known to bioaccumulate within exposed organisms, including honey bees (Di et al. 2016), which can result in cumulative effects on honey bee health over time, even at low levels of exposure (Hesketh et al. 2016, Hladun et al. 2016).

Honey bee colonies have long served as biomonitors of metal pollution (Bromenshenk et al. 1985, Leita et al. 1996, Conti and Botrè 2001) and related studies have shown that honey bees are exposed to metals by multiple routes. Metals in the air and soil are transferred into the nectar and pollen of growing plants, to which foraging honey bees are subsequently exposed (Leita et al. 1996, Quinn et al. 2011, Hladun, Parker, et al. 2013, Meindl and Ashman 2014, Xun et al. 2017, Borsuk et al. 2021). Flying bees also come into contact with airborne metals. Studies have shown that the metal loads on the bodies of foragers can be attributed to particular sources of metal emissions such as leaded gasoline and certain factories (Capitani et al. 2021, Papa et al. 2021). Metal loads also correlate with overall atmospheric particulate matter (Costa et al. 2019), though this correlation is sometimes weak (Steen et al. 2015, Goretti et al. 2020).

These metals are likely to be consumed during grooming or passed into the components of the colony, including colony foods, contributing to the colony's oral exposure.

The above routes of exposure result in metal levels in colony foods (beebread and honey) that sometimes reach parts-per-million (mg/kg) concentrations (Appendix A; Solayman et al. 2016). These concentrations are typically below regulatory limits based on human exposure (Monchanin, Devaud, et al. 2021), though some studies report metal concentrations from honey at certain sites that may pose human health concerns if consumed very frequently, either alone (Devillers et al. 2002, Gutiérrez et al. 2015, Bosancic et al. 2020) or when assessed in combination with pesticide residues (Bommuraj et al. 2019). Notably, metal concentrations in the bodies of honey bees are often 1-2 orders of magnitude greater than in beebread or honey (Appendix A), indicative of bioaccumulation. This has led some researchers to refer to honey bees as biofilters of metals from honey (Dżugan et al. 2018, Borsuk et al. 2021). The accumulation of metals into honey bees has also been measured directly in the lab (Hladun, Kaftanoglu, et al. 2013, Di et al. 2016) and some studies have measured the accumulation of metals into colonies over time, either in the field (Leita et al. 1996) or under netted enclosures in a semi-field study (Hladun et al. 2016).

Metals pose risk to honey bees in the field

There is strong evidence that metals can affect honey bee health at field-relevant levels of exposure. Colony-level studies have found correlations between increased metal loads within colonies and decreased colony growth or brood production (Bromenshenk et

al. 1991, Hladun et al. 2016). These studies are corroborated by field studies with non-*Apis* bees, finding reductions to colony size and brood production in nests containing greater concentrations of certain metals (Moroń et al. 2014, Sivakoff et al. 2020).

At the individual level, the effects of metals are most pronounced for honey bee brood (Hladun, Kaftanoglu, et al. 2013, Di et al. 2016, 2020). This is discussed in greater detail in Chapter 3. For adult honey bees, exposure to metals at field-relevant concentrations can have neurotoxic effects, including reductions to appetitive learning (Hladun et al. 2012, Burden et al. 2016, 2019) and acetylcholinesterase activity (Al-Naggar et al. 2020). Metal exposure also affects the expression rates of genes involved in the detoxification of xenobiotics, including a detoxification gene specific to metals (metallothionein) and genes involved in the scavenging of reactive oxygen species (Nikolić et al. 2016, 2019, Purać et al. 2019, Gizaw et al. 2020). Studies with a variety of other invertebrates have also found that metals have negative health effects at field-relevant levels of exposure, often below regulatory levels set on the basis of human exposure (Monchanin, Devaud, et al. 2021).

Metals and time-reinforced toxicity

Metal bioaccumulation results in toxic effects that also accumulate over time. If the increase in toxicity over time cannot be explained by dosage alone, it is said to be reinforced by time or exhibit time-reinforced toxicity (TRT; Holder 2016). TRT is not unique to metals and will occur at some rate for any toxicant that bioaccumulates in a toxic form, binds irreversibly to target receptors, causes self-perpetuating damage, or

creates persistent toxic metabolites (Holder 2016). TRT is usually assessed with data from lethal toxicity assays. The most common metric of TRT is the Haber constant, which is the slope of a chemical's estimated LC_x values (ex. LC_{50} values) over time on a log-log scale (Cresswell 2017). This constant has been proposed as a benchmark of TRT for use in honey bee risk assessment (Cresswell 2018).

TRT is ultimately a function of chemical accumulation (governed by its toxicokinetics) and the formation of damage (toxicodynamics). There's growing interest in applications of toxicokinetic-toxicodynamic (TKTD) models that take these mechanisms into explicit consideration (Vighi et al. 2019). Such models have historically been validated with metals and have been used to model metals' effects at the individual and population levels, primarily for aquatic risk assessment (Grech et al. 2017).

TKTD models are appealing because they represent the toxicity of chemicals over time. In contrast, standard dose-response models that are used in honey bee risk assessment (ex. probit models) are only used to analyze data from the last day of bioassays (EFSA 2013, USEPA 2014, OECD 2017). This is sufficient to calculate the current benchmarks of toxicity (LC_{50} values and no-observable-adverse-effect concentrations, or NOECs), but omits temporal information that may be important when dealing with toxicants that exhibit TRT.

The parameters of TKTD models typically include rate constants (ex. rates of chemical uptake) that can be used to predict the effects of chemicals over untested conditions of exposure (durations and concentrations). Standard dose-response models, on the other hand, require added assumptions for the purpose of extrapolation. Methods

for extrapolating standard dose-response models have been used to predict honey bee survival at the individual level (Sánchez-Bayo 2009) and in colony-level risk assessment models (Kuan et al. 2018, Schmolke et al. 2019, Bulson et al. 2021). To our knowledge, the predictions of standard dose-response models and TKTD models have only been compared in one population modeling study, focusing on the mysid shrimp *Gammarus pulex* (Galic et al. 2014).

In the present study, the chronic lethal toxicity of five metal pollutants (As, Cd, Li, Pb, and Zn) to honey bees was assessed via standard (10-day) chronic toxicity assays (Fig. 8). The results were used to calibrate standard dose-response models (probit models) and a TKTD model (the General Unified Thresholds Model of Survival, GUTS; Jager et al. 2011). Calibrated models were then used to predict survival over 16 days of exposure at lower concentrations, which were subsequently validated by conducting longer assays with three of the metals (Cd, Li, and Zn). Going forward, we use the term “corroborate” rather than "validate,” in the parlance of (Jager and Ashauer 2018b). We hypothesized that the TKTD model, GUTS, would be better at predicting the results of corroboration assays than the probit modeling approach.

We also compared the colony-level predictions of each modeling approach. Using a simple colony population model (Khoury et al. 2011), probit and GUTS models were used to predict the effects of each metal on the population growth of colonies over 150 days of exposure. We hypothesized that GUTS would tend to predict lower rates of colony growth over time. We then repeated our simulations after re-fitting the models to the longer datasets generated during model corroboration, with the hypothesis that

models fitted to the longer datasets would predict lower rates of survival over time. Finally, Haber constants were calculated for each metal and compared with a metric of TRT known as depuration/repair time (DRT_x). This metric is the hypothetical time required for a chemical's damage within the organism to fall by a given percentage, denoted by x (Ockleford et al. 2018). Chemicals exhibiting less TRT are expected to have lower DRT_x values, indicative of rapid depuration of the chemical from the body and/or damage recovery.

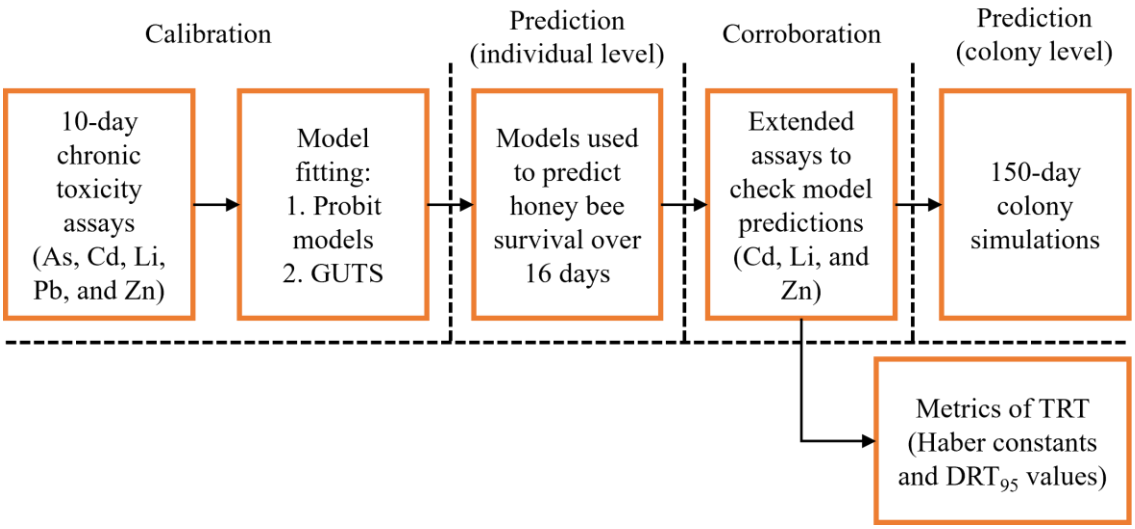

Figure 8. Overview of experimental methodology. GUTS = General Unified Thresholds Model of Survival. TRT = time-reinforced toxicity. DRT = depuration/repair time.

2.2 Methods

2.2.1 Selection of metals

Five metals (As, Cd, Li, Pb, and Zn) were included in this study (Table 1). All five metals are released into urban areas through vehicle emissions, construction,

manufacturing, and improper waste disposal (Wuana and Okieimen 2011, Vareda et al. 2019). In agricultural areas, they may be introduced as contaminants of fertilizers, biosolids, wastewater irrigation, and pesticides (He et al. 2005, Wuana and Okieimen 2011). Agricultural areas may also contain traces of As, Cd, and Pb from metal-based insecticides that were widely used in the past (Wuana and Okieimen 2011, Codling et al. 2015). Biologically important metals, including Zn, are currently applied to crops as micronutrients in fertilizers and foliar sprays (Fageria et al. 2002) or as the active ingredients of bactericides (Naranjo et al. 2020). Finally, Li in the form of Li salts have received attention as potential treatments against *Varroa destructor*, a mite which parasitizes honey bee colonies (Ziegelmann et al. 2018). The persistence of Li within colonies is not well understood and may have long-term effects on adult honey bees following feeding.

			Concentrations reported from colony components (mg/kg)		
Metal	**LC_{50} (mg/L)**	**Assay length (h)**	**Honey[4]**	**Pollen or Bee Bread**	**Bee bodies**
As	4.03[1]	240	ND-0.10	≤ 0.01 - 1.38[5]	≤ 1.51E-3[6] - 13.9[7]
Cd	3.697[1]	96	1.7E-5 - 0.373	≤ 0.003[5] - 2.3[8]	≤ 4.5E-4[9] - 3.19[10]
Li	~173.5[3]	~432	NA	NA	≤ 0.01 - 0.05[12]
Pb	345[2]	72	6.3E-4 -3.232	≤ 0.1[5] - 4.6[8]	≤ 0.00125[13] - 11.23[14]
Zn	290*	240	0.23-73.60	≤ 7.13[14] - 108.2[8]	≤ 8.56[9] - 210.55[15]

Table 1. Toxicological data from past studies reporting the toxicity and exposure of each metal to honey bees. A more detailed table of concentrations from each study is presented in Appendix A. **The 10-day LC_{50} value for Zn was estimated using data from a preliminary study in the Summer of 2020. Sources: [1]Hesketh et al. (2016), [2]Di et al. (2016), [3]Ziegelmann et al. (2018), [4]Solayman et al. (2016), [5]Morgano et al. (2010), [6]Matin et al. (2016), [7]Bromenshenk et al. (1991), [8]Leita et al. (1996), [9]Silici et al. (2016), [10]Tomzyk et al. (2020), [12]Van der Steen et al. (2012), [13]Conti and Botrè (2001), [14]Al-Naggar et al. (2013), [15]Goretti et al. (2020).

2.2.2 Toxicity assays

Preparation of experimental solutions

For calibration assays, five concentrations of each metal were selected that were expected to produce a range of effects on survival over ten days, including little to no effect (the lowest concentration for each metal) to complete mortality (the highest two concentrations) (Table 2).

Metal	Compound	Range of Concentrations (mg/L)	Replicates per Concentration
As	$Na_2HAsO_4 \cdot 7H_2O$	0.3125 - 5	4 - 5
Cd	$CdCl_2$	2.5 - 60	4 - 5
Li	LiCl	86.5-1734	4 - 6
Pb	$Pb(NO_3)_2$	250 - 4000	4 - 6
Zn	$Zn(CH_3CO_2)_2$	250 - 2000	3 - 4

Table 2. The range of concentrations and number of replicates for each metal included in calibration assays. Concentrations are in terms of metal ions in solution. There were six treatment groups per metal, including negative controls.

Stock solutions were prepared by adding metal compounds (Table 2) to the appropriate volume of 50% sucrose solution in water (w/w) to achieve the desired concentrations of metal ions in solution. The mass of each metal compound for the desired volume of stock solution was calculated with the following equation in Excel:

$$mg_{compound} = \frac{mg_{ion}}{mL_{solution}} x \frac{mg_{compound}}{mg_{ion}} x \frac{mL_{solution}}{1}$$

To prepare experimental solutions at the desired concentrations, stock solutions were serially diluted with 50% sucrose solution according to the following equations:

$$mL_{solution1} = \frac{mL_{solution2} Conc_{solution2}}{Conc_{solution1}}$$

$$mL_{sucrose} = mL_{solution2} - mL_{solution1}$$

Calibration assays (10 days)

Assays were performed from June through August of 2021 at the Ohio State University Wooster campus. For each trial, a hive frame with emerging honey bees was taken from a healthy colony and stored in an incubator (60-80% RH, 34°C, Model

HH030-AA, Darwin Chambers, St. Louis, MO, USA). None of the colonies were treated with antibiotics in the previous four years, but colonies had been treated with formic acid and oxalic acid at some point over the previous years for Varroa mite control.

To set up each trial, newly emerged bees were anaesthetized at -20°C for 5 min then transferred in groups of 20 into 177 cm^3 ice cream cups (Uniq Brand, Gilbert, AZ; Fig. 9). Newly emerged bees were collected from the incubator every day to ensure that all bees were $\leq$ 1 day old. Each cup received a sterile 3 mL plastic syringe to serve as an *ad libitum* feeder, containing its respective metal at one of five concentrations or no metal (negative controls).

On each day of the 10-day assay, the number of living and dead honey bees were counted and the weight of feeders were measured. Feeders were refilled as needed to ensure that no feeder ran out of solution during a given trial. To account for syrup loss due to evaporation, evaporation cups containing no bees were included in five of the 10-day calibration trials and all nine of the 20-day corroboration trials. One evaporation cup was included on each shelf of the incubator during these trials, amounting to 148 measures of daily evaporation.

Figure 9. The setup of chronic toxicity assays. Brood frames from healthy colonies (left) were stored in the incubator (center) and used to provision same-age adult honey bees, which were divided in groups of 20 into ice cream cups (right). Each cup received sucrose solution treated with one of five metals (As, Cd, Li, Pb, or Zn) or no metal (negative controls). Survival and food consumption was recorded daily for the duration of each assay (10-day calibration assays or 20-day corroboration assays).

Corroboration assays (20 days)

After completing the 10-day calibration assays, longer (20-day) corroboration assays were conducted with three of the metals (Cd, Li, and Zn) from August 10th-31st, 2021. These assays were conducted with the same methodology as 10-day assays with the same measurements taken on each day. However, the corroboration assays included some concentrations that were lower than those included in the calibration assays. Trials with each concentration were replicated three times (Table 3).

Metal	Compound	Range of Concentrations (mg/L)	Treatment Groups (#)	Replicates per Concentration
Cd	$CdCl_2$	0.25 - 5	5	3
Li	LiCl	14 - 173.5	6	3
Zn	$Zn(C_2H_3O_2)_2$	100 - 2000	6	3

Table 3. The range of concentrations and number of replicates of each metal included in corroboration assays.

2.2.3 Model calibration

Using data from calibration assays for each metal, probit models of survival over concentration on day 10 were fitted with the *glm* function in the R package 'stats' (R Core Team 2021). Datapoints were weighted according to the number of honey bees in each cup (mean = 20.01, SD = 0.81). All other arguments to *glm* were kept at their default values. LC_{50} values and their 95% confidence intervals were estimated with the *LC_probit* function in the R package 'ecotox' (Hlina et al. 2021).

GUTS models were fitted to survival data with the *survFit* function in the R package 'morse' (Delignette-Muller et al. 2017, Baudrot et al. 2021). Specifically, the reduced version of GUTS (GUTS-RED) was used (see Appendix B for a description of GUTS and its parameters). To cross-check the parameter values estimated by 'morse,' GUTS parameters were also estimated using the OpenGUTS software (version 1.1; Jager 2021). This software does not rely on prior information during model fitting and can be considered a more conservative parameter estimation approach. OpenGUTS was also used to determine the death mechanism (stochastic death, SD, or individual tolerances, IT) that produced the best fit to the data for each metal (Appendix B). In 'morse' and OpenGUTS, all settings and function arguments were kept at their default values. Because mortality in the negative control groups was nearly zero throughout the 10-day calibration assays, baseline mortality (h_b) was set to zero during model fitting. This resulted in three parameter estimates belonging to GUTS-RED-SD (k_d, b_{ext}, and z_{ext}) and GUTS-RED-IT (k_d, m_{ext}, and F_s) for each metal. LC_{50} values for each metal and version of GUTS were then calculated with the *LCx* function in 'morse.'

The above was repeated using data from the 20-day corroboration assays. This allowed a comparison of model outputs when fitted to data of differing length (10 days or >10 days). To limit the effect of ageing on our analysis, data from corroboration trials were omitted once mortality in any of the negative control cups reached 20%. For each metal, this occurred on day 16. During model fitting, baseline mortality (h_b) was preset to the average daily rate of mortality observed in the negative control group for each metal. For Cd, Li, and Zn, this was equal to daily death rates of 0.4, 0.5, and 0.5%, respectively.

2.2.4 Survival predictions, individual level

The survival of honey bees was predicted differently depending on the survival model being implemented. GUTS-RED predictions were generated using the *predict_ode* function in 'morse.' For the probit models, metal concentrations were used to predict the expected rate of survival from the probit dose-response curve for each metal on day 10 (Fig. 10). Because probit models were fitted with data from a single timepoint (the last day of the 10-day calibration assays), they could only be used to predict survival over 10 days of exposure. To convert these 10-day survival predictions into daily rates, they were simply divided by 10. This approach was performed with survival probabilities spanning the 95% confidence region of each probit prediction.

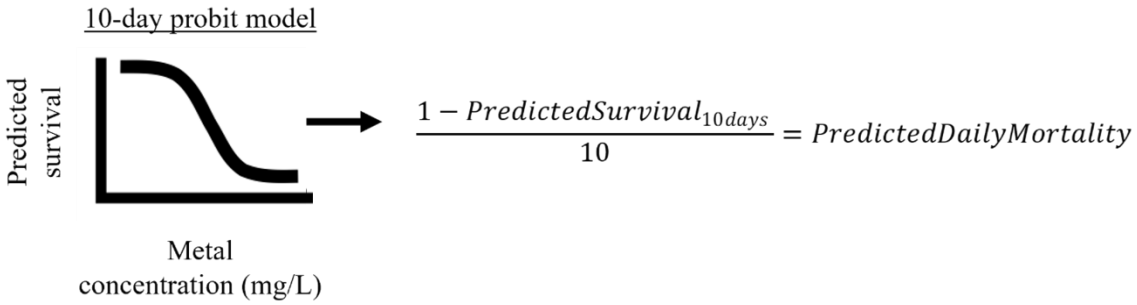

Figure 10. Approach for extrapolating probit models to predict survival. Survival was predicted by taking the expected rate of survival over 10 days from the model's dose-response curve. These values were converted into daily rates of survival by diving them by 10.

The accuracy of predictions made with probit and GUTS models were quantified with root-mean-square errors, which were calculated with the *accuracy* function in the R package 'forecast' (Hyndman and Khandakar 2008). To test the relative accuracy of each model for statistical significance, two-sided Diebold-Mariano tests were performed between the residual errors of each model, using the function *dm.test*, also in 'forecast'.

2.2.5 Survival predictions, colony level

Colony modelling

An established colony population model (Khoury et al. 2011) was used to predict the colony-level effects of oral exposure to each metal via honey. Since its original publication, the Khoury model has been adapted for a number of studies on the colony-level effects of different honey bee stressors, including pesticide exposure, food limitation, and impaired brood tending (Myerscough et al. 2017, Holder et al. 2018, Zeaiter and Myerscough 2020).

The Khoury model is a relatively simple colony population model comprised of just two differential equations (Fig. 11). The first equation represents the rate that brood emerge to adulthood, which increases with the colony's total population size (N), up to the value of the parameter L, the queen's maximum egg laying rate. The emergence rate approaches L as a function of a second parameter, w. A second equation calculates the proportion of hive bees that are recruited to foraging at each timestep. When no foragers are present, the rate of recruitment is at its maximum possible value, represented by the parameter α. Recruitment is counterbalanced by the inhibition of recruitment by existing foragers, controlled by the parameter σ.

For this study, a version of the original Khoury model was written in R using the R package 'deSolve' (Soetaert et al. 2010). Each parameter in the model was set to the default values used in the original publication (Khoury et al. 2011). Model outputs were cross-checked with those reported in the original publication to ensure that it was correctly implemented. The Khoury model was then modified to simulate the oral exposure of adult bees to metals in colony honey (Fig. 11).

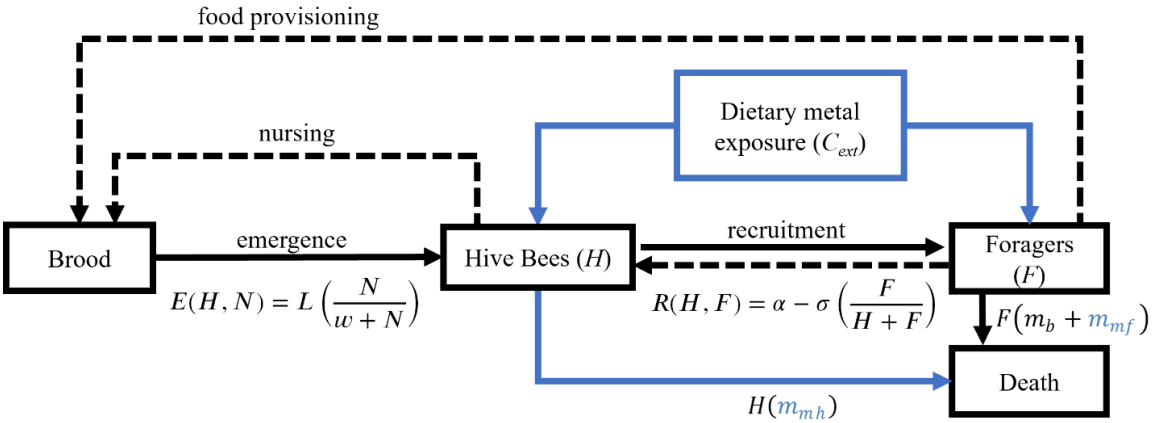

Figure 11. The colony population model used for the present study. Our modifications are given in blue. Figure modified with permission from Khoury et al. (2011).

In the original Khoury model, only foragers die, at a daily rate determined by the parameter for baseline mortality, m_b. For the present study, two additional death rate parameters, m_{mh} and m_{mf}, were introduced to represent average daily rates of metal-induced mortality among hive bees and foragers, respectively. The level of exposure at each timepoint was represented with the GUTS parameter C_{ext}. The EPA's Bee-REX model was used to estimate the relative oral exposure of foragers and hive bees (USEPA 2014). Foragers were assumed to consume 292 mg of nectar per day whereas hive bees were assumed to consume 100 mg per day, which is the average level of consumption in Bee-REX for workers performing in-hive duties. Using these values, the daily exposure of hive bees in our simulations were calculated by multiplying the level of exposure experienced by foragers (C_{ext}) by 100/292. Because Bee-REX assumes that adult bees consume little pollen relative to nectar or honey, metal exposure in our model was assumed to originate entirely from contaminated honey.

Colony simulations

The modified Khoury model was used to simulate the growth of colonies over 200 days. In each simulation, no exposure took place for the first 50 days. For control simulations, no exposure continued until day 200. For exposure simulations, oral exposure via honey occurred from day 50 to day 200. Modelling was performed with each metal across a range of concentrations. The lowest concentrations for As, Cd, Pb, and Zn were the mean concentrations measured in honey (Solayman et al. 2016). For Li, we used the lowest concentration that was shown to be effective for control of *V.*

destructor (2mM LiCl, or ~ 13.9 mg/L Li) (Ziegelmann et al. 2018). A series of simulations were then run for each metal in which metal concentrations were increased incrementally until the predicted population size of simulated colonies reached zero by day 200.

Survival at each timestep of the colony simulations were calculated differently depending on the modeling approach being implemented. Probit predictions were calculated in the same manner as before (section 2.2.4), using the average concentration of each metal in honey over the previous ten days to predict survival at each timestep. To implement GUTS in the colony model, metal exposure at each timestep (C_{ext}) was substituted into the GUTS equation for scaled damage (D_{ext}) using values for the dominant rate constant (K_d) that had been estimated for each metal during model fitting.

$$D_{ext,t} = K_d\left(C_{ext} - D_{ext,t-1}\right)$$

In the context of our colony model, D_{ext} represents the damage experienced by adult bees throughout the colony. Because damage is represented at the colony level, it was reduced at each timestep by a factor equal to the number of adult bees that had died at that timestep. This was necessary to ensure that the damage experienced by previously-exposed bees that had died wasn't being reapplied to bees that later emerged. Average damage was also reduced at each timestep to account for the proportion of newly-emerged bees in the colony that had yet to be exposed and therefore had not incurred any damage.

$$D_{ext,corrected} = D_{ext} - D_{ext}\left(\frac{Bees_t - Bees_{t-1}}{Bees_{t-1}}\right)$$

To translate damage into rates of survival, D_{ext} was substituted into the GUTS equation for the hazard rate (h_z), using values for the killing rate parameter, b_{ext}, and the tolerance threshold. z_{ext}, that were previously estimated for each metal during model fitting.

$$h_z = b_{ext} max(0, D_{ext} - z_{ext}) + h_b$$

GUTS parameters, like the parameters of probit models, come with uncertainty, represented by their 95% confidence intervals. To account for the uncertainty surrounding the estimates of each GUTS parameter, a series of Monte Carlo simulations were conducted in which parameter values were randomly sampled from the 95% confidence region of the posterior distribution of each parameter (Fig. 12). Sampling was not conducted uniformly. Rather, the probability of sampling a given value depended on the density of the posterior distribution at that value. Each simulation was repeated 1000 times, using different combinations of randomly sampled parameter values.

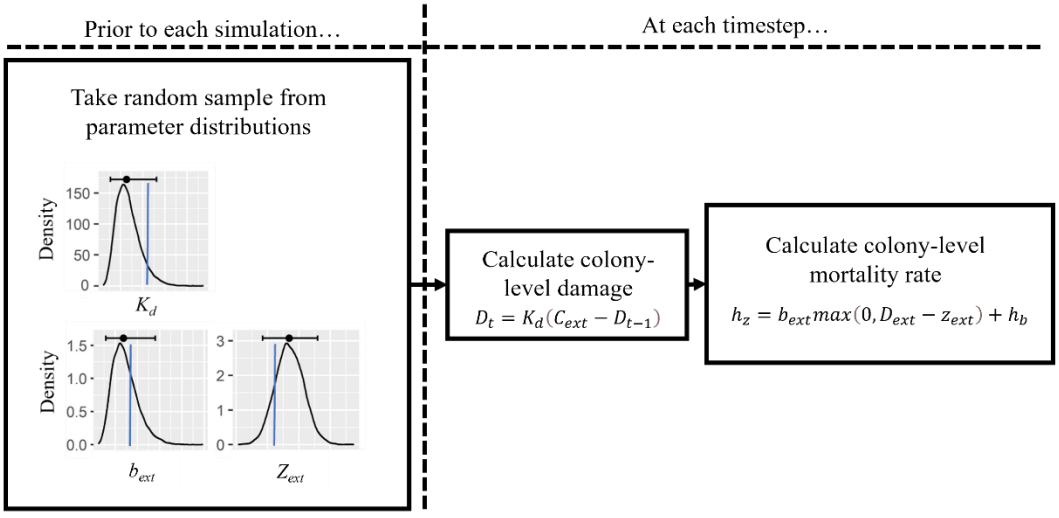

Figure 12. The implementation of GUTS parameters during colony modeling.

2.2.6 Metrics of TRT

Haber Constants

Cresswell (2018) describes the Haber constant and its derivation graphically. Briefly, survival data from each treatment group in the assay is used to generate logit models of survival over time. These models are then used to estimate the time required for 50% of the test population to die at each concentration (lethal effect times, or LT_{50} values). The resulting LT_{50} values are plotted over their respective concentrations on a log-log plot and the slope of the resulting line of best fit is equal to the Haber constant. In the absence of TRT, this slope is expected to be equal to -1, with more negative values indicating increasing levels of TRT.

The Excel protocol of Cresswell (2017) was replicated in R and used to calculate Haber constants for each metal, pooling the data from calibration and corroboration assays. The outputs of the R code were cross-checked against the outputs of the original protocol to ensure that it was properly replicated. For each metal, an F test was performed using the *linearHypothesis* function in the R package 'car' (Fox and Weisberg 2019) to determine whether Haber constants (slopes) were significantly different from -1, indicative of time-dependent effects on toxicity. Pairwise differences between Haber constants belonging to each metal were also compared through a series of Tukey's HSD tests, which were implemented using the *lstrends* function in the R package 'lsmeans' (Lenth 2016).

Depuration/repair times

The depuration/repair time (DRT_x) is an alternative metric of TRT specific to GUTS that represents the time for chemical damage to fall by a given percentage, denoted by *x*, in the absence of exposure (Ockleford et al. 2018). Using GUTS-RED, DRT_x is calculated with the following equation:

$$DRT_x = \frac{-ln(x)}{k_d}$$

The European Food Safety Authority recommends using the DRT_{95} (Ockleford et al. 2018). For each metal, DRT_{95} values were calculated with k_d values estimated in OpenGUTS, using GUTS models fitted to data from calibration assays. Because the lower bound of k_d could not be estimated for each metal in OpenGUTS, only the upper estimates of DRT_{95} values could be calculated.

2.3 Results

2.3.1 Calibration assays

In accordance with guidelines for conducting honey bee chronic toxicity assays (OECD 2017), none of the control groups in the calibration assays exhibited mortality >15% by the end of day 10. There was a clear dose-response relationship for all metals throughout calibration assays: at each timepoint, average rates of survival were lower at higher metal concentrations (Fig. 13). Raw food consumption data is provided in Appendix C, Fig. 30.

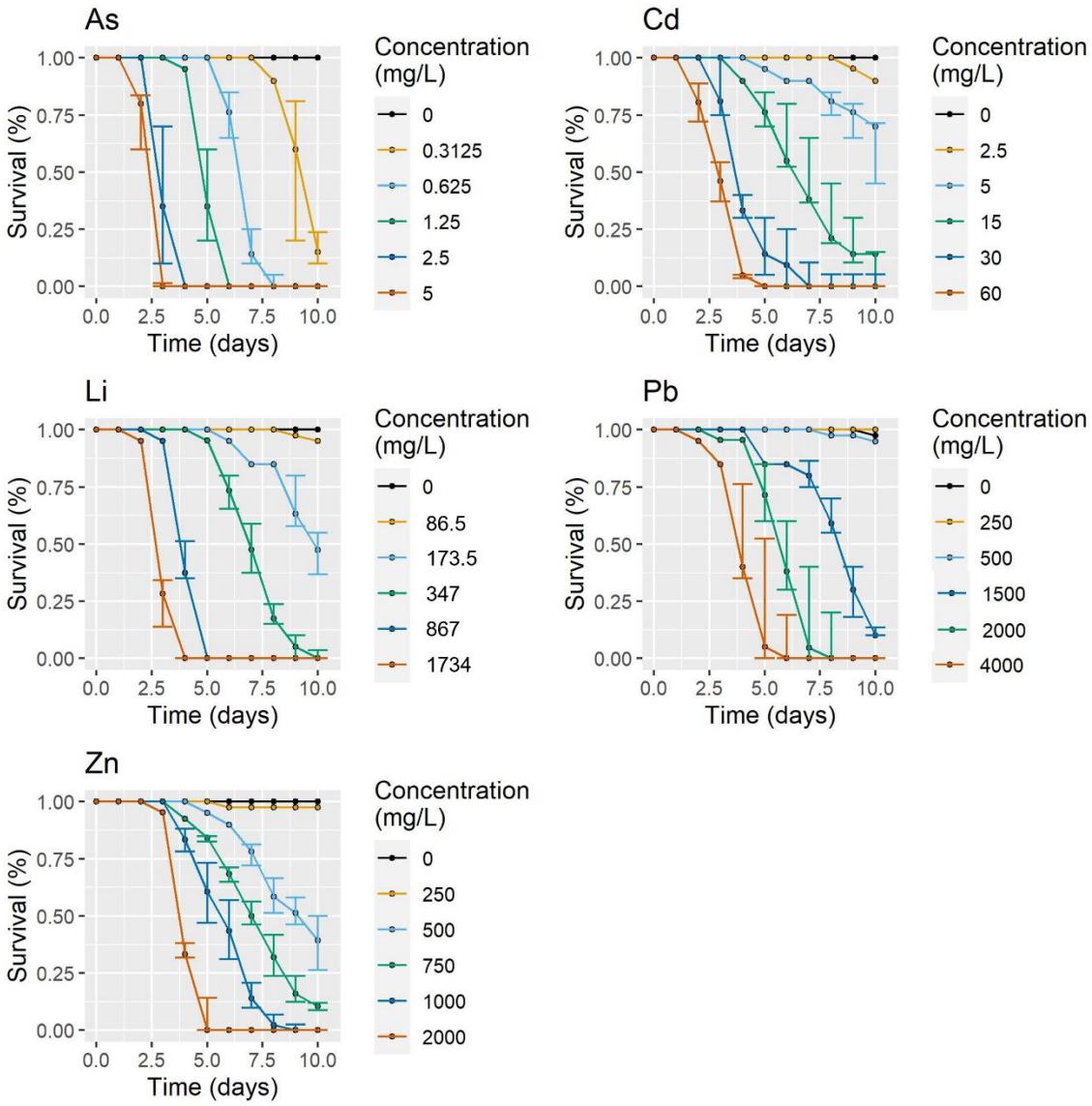

Figure 13. Rates of survival over time for each metal and concentration during calibration assays. Points and error bars represent medians and interquartile ranges, respectively. Error bars are only provided for timepoints with mortality ≥15% to improve legibility.

For each metal, GUTS-SD provided a better fit to the data than GUTS-IT (Table 4).

	As		Cd		Li		Pb		Zn	
Criteria	**SD**	**IT**	**SD**	**IT**	**SD**	**IT**	**SD**	**IT**	**SD**	**IT**
R^2	9.5E-01	8.3E-01	9.8E-01	9.4E-01	9.7E-01	8.9E-01	9.8E-01	9.6E-01	9.9E-01	9.5E-01
- Log likelihood	7.6E+02	1.0E+03	7.19E+02	7.7E+02	7.1E+02	8.6E+02	6.9E+02	7.2E+02	6.2E+02	6.5E+02
AIC	1.5E+03	2.0E+03	1.4E+03	1.6E+03	1.4E+03	1.7E+03	1.4E+03	1.4E+03	1.2E+03	1.3E+03
NRMSE	2.0E+01	3.4E+01	8.1E+00	1.3E+01	1.3E+01	2.4E+01	6.0E+00	9.6E+00	5.2E+00	1.1E+01

Table 4. Goodness-of-fit criteria for each GUTS model (GUTS-RED-SD and GUTS-RED-IT) and metal, fitted to the calibration data in the software OpenGUTS. GUTS-SD outperformed GUTS-IT in all cases (higher R^2 values and lower values for all other criteria).

In OpenGUTS, the lower bound for the dominant rate constant could not be estimated for any metal or version of GUTS, but the lower and upper bounds of all other parameters could be estimated (Table 5). All GUTS parameters could be estimated using the R package 'morse,' whose estimates are provided in Appendix C, Table 19.

GUTS Model	**Parameter**	**Unit**	**As**	**Cd**	**Li****	**Pb**	**Zn**
SD	Dominant rate* (*kd*)	day^{-1}	ND-4.3E-3	ND-2.4E-2	ND-5.1E-3	ND-2.1E-2	ND-1.8E-2
	Killing rate (bw)	mg L^{-1}	3.1E-3	2.8E-2	10.92	10.53	3.405
	Threshold (z)	mg L^{-1} day^{-1}	119	2.303	0.03253	0.04524	0.07323

Table 5. Median parameter estimates of GUTS-SD for each metal, fitted to the calibration data. Values were estimated in the OpenGUTS software. *The lower bound of the dominant rate constant could not be estimated for any metal ("ND" = not determined). **The values of GUTS parameters for Li are in terms of mg/L of LiCl, whose concentrations were used when fitting GUTS models.

Probit models for each metal are presented in Fig. 14. Exact values for all LC_{50} estimates are provided in Appendix C, Table 20.

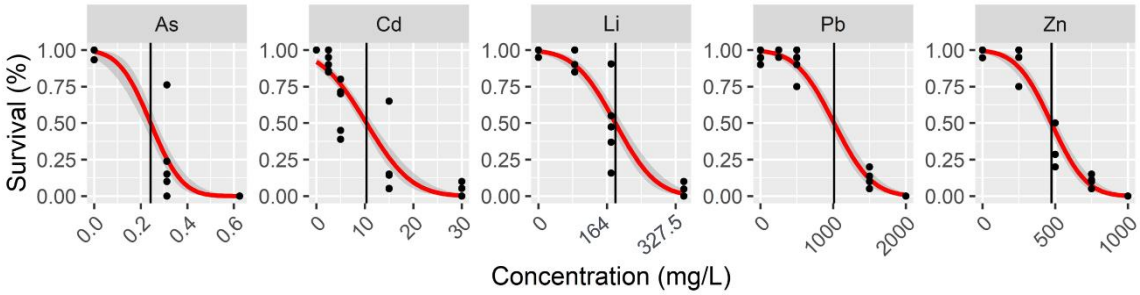

Figure 14. Probit models fitted to the calibration data on day 10. Red curves are median predicted levels of survival. Shaded regions span the 95% confidence intervals for each model. Black lines indicate the estimated LC_{50} values for each metal.

2.3.2 Corroboration assays

As with the calibration data, the corroboration data exhibited a clear relationship between survival and concentration, with higher concentrations resulting in lower rates of survival (Fig. 15). Raw survival data including data beyond day 16 are provided in Appendix C, Fig. 31. Raw food consumption data are provided in Appendix C, Fig. 32.

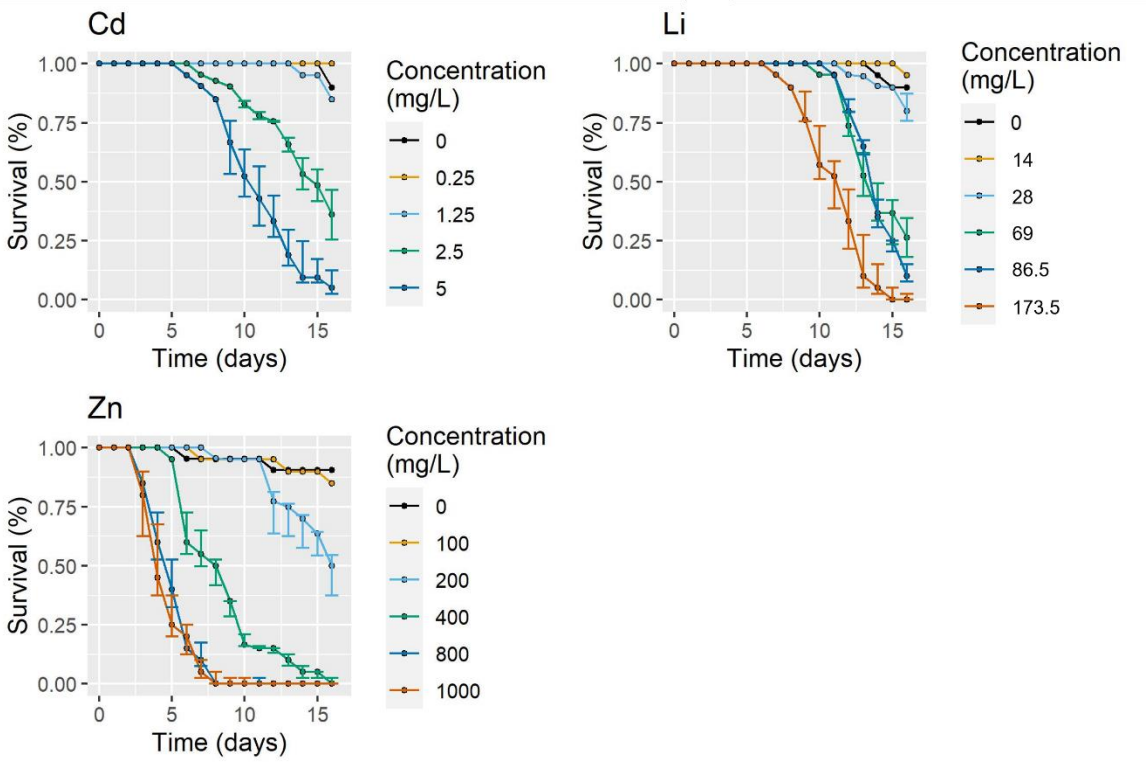

Figure 15. Rates of survival over time for each metal and concentration during corroboration assays. Data were omitted once survival in any control group reached 80% (day 16). Points and error bars represent medians and interquartile ranges, respectively. Error bars are only provided for timepoints with mortality ≥15% to improve legibility.

Probit models of the corroboration data on day 16 are presented in Fig. 16. Exact values for all LC50 estimates are provided in Appendix C, Table 20.

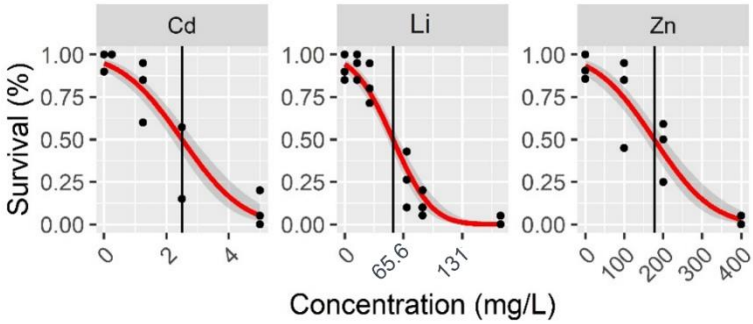

Figure 16. Probit models fitted to the corroboration data at day 16. Red curves are median predicted levels of survival. Shaded regions span the 95% confidence intervals for each model. Black lines indicate the estimated LC_{50} values for each metal.

For all metals included in corroboration assays, the predictions of GUTS-SD had lower residual errors than the probit approach (Fig. 17, Table 6). Differences in the residual errors between models were significantly different for all metals, except when comparing the errors between the probit approach and GUTS-SD for Zn (Table 6).

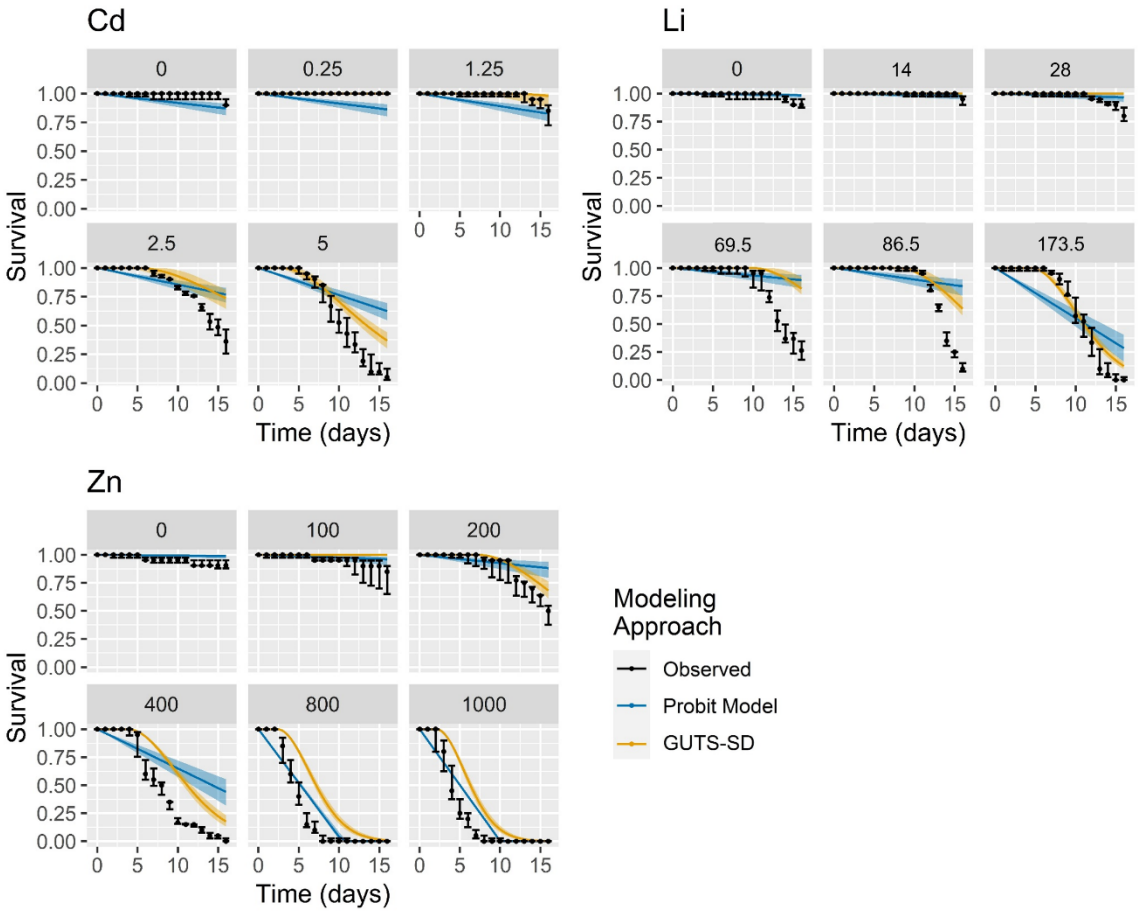

Figure 17. Observed and predicted rates of survival for each metal and concentration included in corroboration assays. Points and error bars represent median rates of survival and their interquartile ranges. Shaded regions span the 95% confidence intervals of predictions made by each modeling approach.

	Root-Mean-Square Errors	
Metal	**Probit Approach**	**GUTS-SD**
Cd	17.24	11.87*
Li	17.42	11.72*
Zn	19.76	18.08

Table 6. Root-mean-square errors for each model fitted to the corroboration data. GUTS-SD had lower error for all metals. Asterisks indicate errors that were significantly lower than those of the competing model (pairwise Diebold-Mariano tests, $p < 0.05$). For Cd, Li, and Zn, p-values were 0.0051, 0.0017, and 0.3553, respectively.

2.3.3 LC_{50} estimates

LC_{50} estimates made using the data from day 16 of corroboration assays were all lower than those made with data from day 10 of calibration assays (Fig. 18). Although the median LC_{50} estimates made with GUTS-SD tended to be lower than those made with probit models, this was not consistent, and their 95% confidence intervals overlapped for all metals except As (Fig. 18). Exact LC_{50} estimates are presented in Appendix C, Table 20.

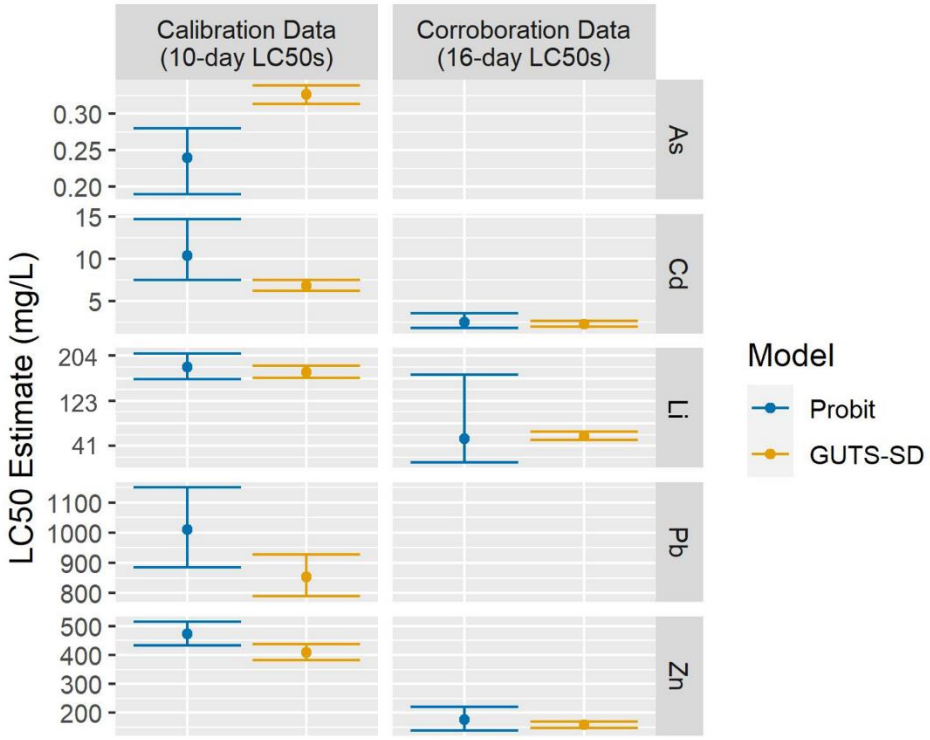

Figure 18. 10- and 16-day LC_{50} values for each metal, estimated with data from calibration assays or corroboration assays, respectively. Points are median estimates and error bars span the 95% confidence interval for each estimate.

2.3.4 Colony-level predictions

At the lowest levels of exposure simulated, the predictions of each modeling approach overlapped (Fig. 19). The confidence intervals surrounding model predictions only diverged at the highest concentrations simulated (>50X field-relevant concentrations).

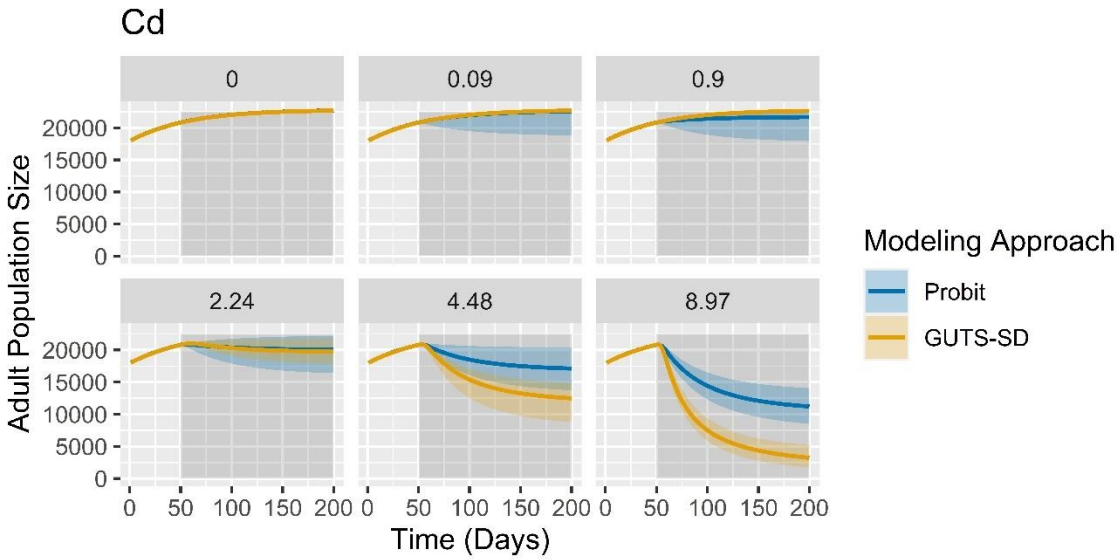

Figure 19. An example of the colony-level predictions of each modeling approach, using models fitted to calibration data for Cd. In each simulation, exposure took place at a constant level from day 50 to day 200 (shaded in grey). Note that the lowest level of exposure (0.09 mg/L) is equal to the mean concentration of Cd measured from honey (Solayman et al. 2016).

Regardless of the data used to fit the models (calibration data or corroboration data), probit models predicted toxic effects occurring at lower levels of exposure than GUTS-SD (Fig. 20). However, GUTS-SD tended to predict lower final population sizes across the concentrations simulated (Table 7).

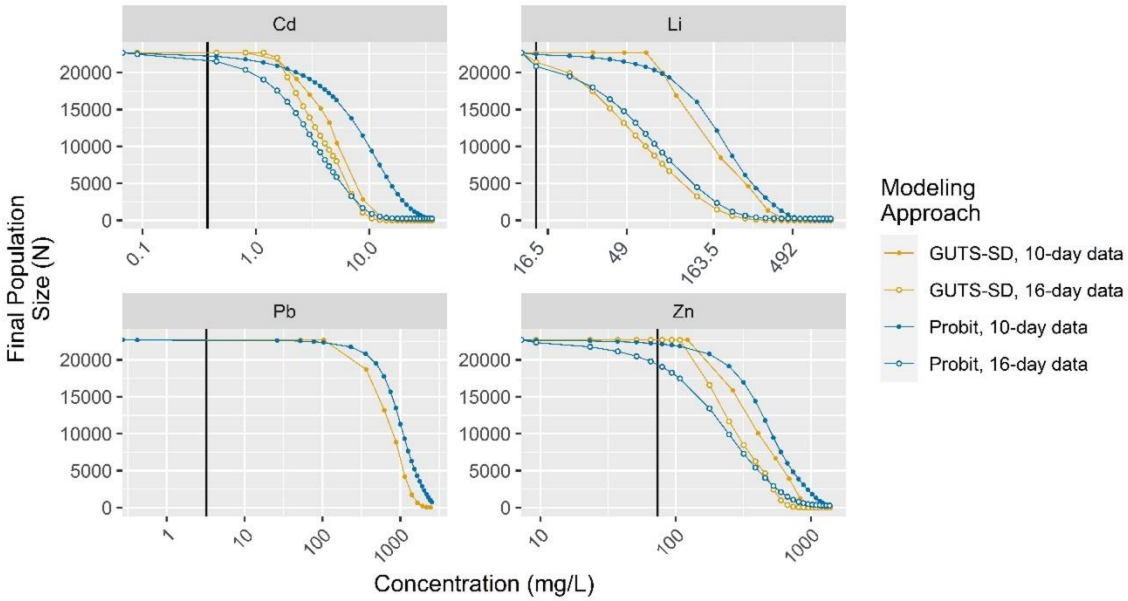

Figure 20. Median final population sizes from colony simulations for Cd, Li, Pb, and Zn across a range of concentrations. Predictions were either made with GUTS-SD (orange) or probit models (blue) and were either fitted to the 10-day calibration data (filled circles) or 16-day corroboration data (open circles). For Cd, Pb, and Zn, black vertical lines indicate the highest concentrations measured in honey (Solayman et al. 2016). For Li, the black line indicates the lowest concentration effective against Varroa mite in the study of (Ziegelmann et al. 2018).

		Concentration resulting in N ≤ 10,000 (mg/L)	
Metal	**Data Used**	**Probit**	**GUTS -SD**
As	Calibration	0.26	0.32
Cd	Calibration	10.31	5.93
	Corroboration	3.7	4.47
Li	Calibration	212.75	164.73
	Corroboration	80.27	64.19
Pb	Calibration	1106.7	884.08
Zn	Calibration	514.85	434.89
	Corroboration	248.05	290.17

Table 7. Concentrations of each metal resulting in final adult population sizes (N) ≤10,000. The lowest concentration in each row is highlighted in red.

For As, the predictions of the probit approach varied widely depending on the day at which the data were taken from bioassays (day 9 or day 10, Fig. 21).

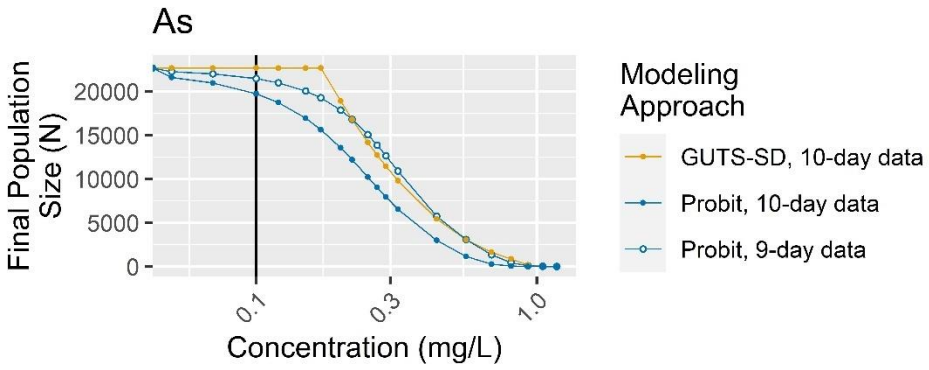

Figure 21. Median final population sizes from colony simulations for As, made with probit models fitted to data from day 9 or day 10 of calibration assays. The black vertical line indicates the highest concentration of As measured from honey (Solayman et al. 2016).

2.3.5 Metrics of TRT

All Haber constants were less than -1, but only those of As, Cd, and Li were significantly less than -1, indicative of TRT (Wald test, $p << 0.05$, Fig. 22, Table 8). Haber constants suggested that Cd exhibits the greatest TRT, followed by As, Li, Zn, and Pb. However, none of the Haber constants were significantly different from each other (Tukey's HSD test, $p > 0.05$, Appendix C Table 21).

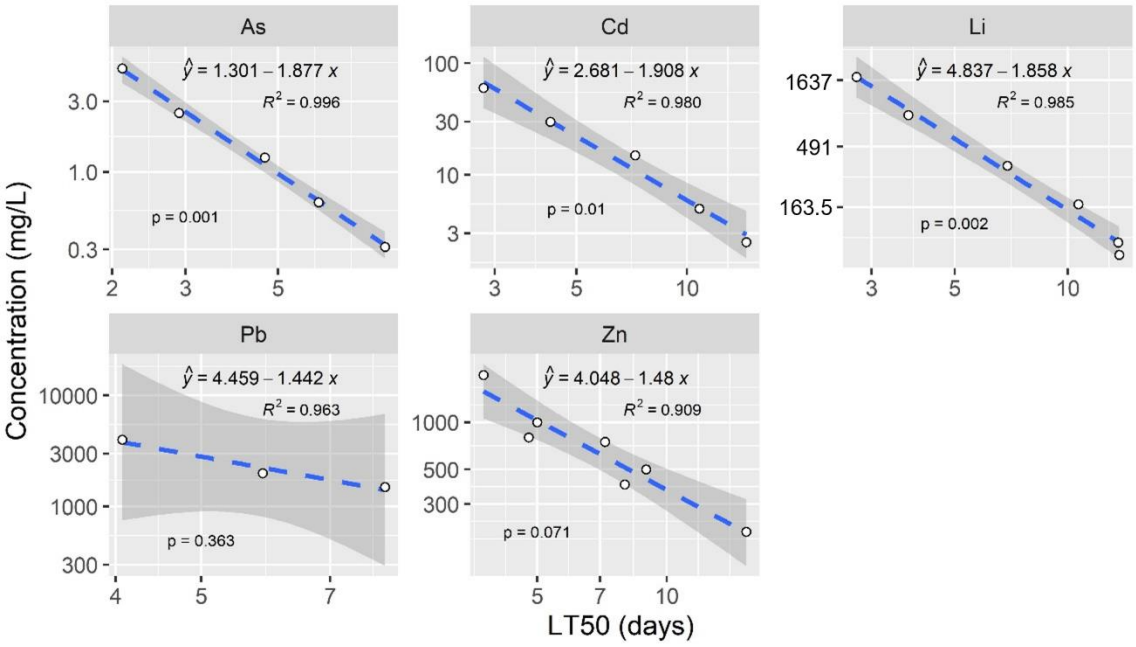

Figure 22. Estimated LC_{50} values over time for each metal, pooling data from calibration assays and corroboration assays. Haber constants are equal to the slopes of each line of best-fit (Table 8). All slopes except those of Pb and Zn were significantly different from -1 (Wald test, $p < 0.05$), indicative of TRT, but slopes were not significantly different from each other (Tukey's HSD test, $p > 0.05$).

Metal	Haber Constant	P value	Lower CL	Upper CL	SE	df
As	-1.88	0.001	-2.23	-1.528	0.165	16
Cd	-1.91	0.010	-2.21	-1.605	0.143	16
Li	-1.86	0.002	-2.12	-1.592	0.126	16
Pb	-1.44	0.363	-2.28	-0.602	0.396	16
Zn	-1.48	0.071	-1.83	-1.127	0.167	16

Table 8. Haber constants for each metal. Haber constants (slopes) that are significantly different from -1 are indicative of TRT (F tests, $p < 0.05$).

Because the lower bound of k_d could not be estimated for any metal in OpenGUTS, only the lower bound of DRT_{95} values could be calculated. These DRT_{95} values suggested that As exhibits the greatest time-cumulative toxicity, followed by Li,

Zn, Cd, and Pb (Table 9). This ranking differs from that produced using Haber constants (Cd, As, Li, Zn, and Pb) (Table 8).

Metal	Assay	DRT_{95} (days)
As	Calibration	694.9-ND
Cd	Calibration	125.1-ND
	Corroboration	155.5-ND
Li	Calibration	587.9-ND
	Corroboration	420.4-ND
Pb	Calibration	144.7-ND
Zn	Calibration	165.9-ND
	Corroboration	35.82-357.7

Table 9. DRT_{95} values calculated for each metal, using GUTS-SD models fitted in OpenGUTS.

2.4 Discussion

Honey bees are frequently exposed to persistent toxic chemicals such as metals, but methods for predicting their long-term effects remain largely unexplored. In the present study, we found that the TKTD model GUTS-RED-SD predicted the survival of honey bees exposed to Cd, Li, and Zn more accurately than a simple extrapolation of a standard (probit) dose-response model, and this was statistically significant for Cd and Li (Table 6). Notably, the differences between the predictions of GUTS-RED-SD and probit models would not be evident by simply comparing their LC_{50} estimates, which overlapped for all metals but As (Fig. 18). Instead, differences were due to the ability of GUTS to account for time-cumulative toxicity. This produces a more realistic, S-shaped dose-response curve, and results in increased rates of mortality over time.

When predicting the effects of each metal on colony growth, differences between modeling approaches were less clear cut. GUTS-RED-SD tended to predict lower rates of colony growth for the higher levels of exposure that were simulated, but this depended on the length of the data used to fit the models (10-day calibration data or 16-day corroboration data) (Fig. 20, 21, Table 7). At lower levels of exposure, the probit approach predicted lower rates of survival (Fig. 20, Fig. 21). This pattern is related to the fact that GUTS is a threshold model: toxic effects will not be predicted unless exposure is sufficient to cause damage that exceeds the organism's estimated tolerance threshold. At the lower concentrations that we simulated, damage did not reach this threshold for any metal, except Li when fitted to the 16-day corroboration data (Fig. 20). Probit models, on the other hand, make no threshold assumption, but they require added assumptions for the purpose of extrapolation. As illustrated in Fig. 19, our probit extrapolation approach assumes that the rate of mortality will be constant (linear) under constant levels of exposure, and this will be equal to the average predicted rate of mortality on the day of the assay used to fit the model. This comes with the implicit assumption that toxicity is not reinforced by time, but *constant* with time. For chemicals that exhibit TRT, this will result in lower predicted rates of mortality over increasing periods of exposure. On the other hand, although our probit extrapolation approach does not account for TRT, over longer assays, it will naturally predict lower rates of mortality because higher average rates of mortality will be calculated by the last day (for a given concentration). This is an artifact of relying on averages and may or may not result in more accurate predictions relative to TKTD modeling.

The relative predictions of probit models and GUTS-RED-SD differed between metals. Notably, for As, the probit approach predicted much lower rates of colony growth than the corresponding GUTS model (Fig. 21), but this difference was reduced when the probit model was fitted to data from day 9 of the calibration assay, rather than day 10. These differences between days are related to the As concentrations used: on day 10, only one As concentration (0.3125 mg/L) exhibited rates of survival between 0 and 1 (Fig. 13), providing limited dose-response data for probit analysis, whereas more dose-response information was present on day 9. GUTS modeling, by contrast, uses all available timepoints, which obviates this issue.

For all metals, lower rates of colony growth were predicted when models were fitted to the 16-day data versus the 10-day data. This occurred because some of the concentrations in the corroboration assays took longer than 10 days to produce an effect and therefore would have appeared benign under shorter durations of exposure. Considering this, we recommend that colony modelers use data from assays that match as closely as possible the conditions of exposure that they intend to simulate. For models of long-term exposure, this will require extended assays such as those performed by (Tosi et al. 2021) and (Simon-Delso et al. 2018). It may be possible to use shorter assays, but this will require an added margin of safety. Because of the considerable effort required to conduct long-term bioassays, applications of TKTD modeling in this area would benefit from an open-source database of raw timeseries data from past bioassays.

We stress that our colony model is not intended for risk assessment *per se*. We developed it for the sole purpose of comparing the predictions made with standard dose-

response models (here, probit models) and the TKTD model GUTS. Because our model does not include sublethal effects or brood effects, it will necessarily underestimate the overall effects of each metal on colony growth. This is supported by laboratory studies showing that honey bee larvae can have LC_{50} values two orders of magnitude lower than those of adults (Hladun, Kaftanoglu, et al. 2013, Di et al. 2016). Indeed, our model only predicted effects on colony growth at very large concentrations relative to those that have been measured from colony honey (Fig. 20, 21), whereas empirical studies with actual colonies have found negative effects on colony growth at field-relevant concentrations (Hladun et al. 2016). As such, the predictions of our model are best treated as indictors of risk rather than literal predictions, and could potentially be used to calculate risk quotients like those presented in previous colony risk models (Crenna et al. 2020).

A defining characteristic of our model is that it represents both exposure and effects at the colony level. This is in contrast with colony models representing the exposure of multiple cohorts of bees, either implicitly in the form of additional subroutines or explicitly via agent-based modeling (Becher et al. 2014). Population modeling studies with GUTS have used agent-based models, reflecting the individual-level nature of GUTS (Martin et al. 2013, Gergs et al. 2016, Roeben et al. 2020). We acknowledge the fact that exposure in colonies is ultimately an individual-level phenomenon and the effect of a toxicant will depend on the specific distribution of exposures among the members of the colony (Sponsler and Johnson 2017). We believe that our colony-level approach is still informative because in large populations, such as those in honey bee colonies, individual-level survival probabilities should approximate

the population-level average (i.e. the law of large numbers). This is implicit to standard bioassays with honey bees, which are conducted with groups of bees rather than individuals. Because we modeled exposure at the colony level, we reduced damage at each time step to account for changes to the colony population (either newly-dead or newly-emerged bees). This does not guarantee that our model's outputs are equivalent with a corresponding agent-based model. This is a complex topic that could be explored in future modeling studies utilizing agent-based models.

Our long-term assays provide added evidence that metal pollutants pose high risk to honey bees in the field. The LC_{50} values for As and Cd overlapped with concentrations that have been reported from pollen and the bodies of bees in some studies (Table 1). For Zn, this was only true for LC_{50} values calculated from the longer, 16-day assays. For Li, we observed greater mortality in bees fed 1059 mg/L of LiCl (~173.4 mg/L Li) than would be expected from a previous study (Ziegelmann et al. 2018), indicating that this concentration is not safe to apply to colonies for Varroa control. In contrast, our 10-day LC_{50} estimates for Cd and Pb were higher than previous estimates, despite our assays lasting longer than previous studies (Di et al. 2016). Differences with other studies may be related to the Pb compounds used ($Pb(NO_3)_2$ versus $PbCl_2$), the genetic stock of the honey bees (Laurino et al. 2013), and the time of year that the bees were collected (Smirle and Winston 1987).

Finally, we calculated two metrics of TRT, the Haber constant and the DRT_{95}, for each metal. The former has been proposed as a metric of TRT for honey bee risk assessment (Cresswell 2018) and has been calculated with data from bioassays with

honey bees in a number of studies, including neonicotinoid insecticides (Rondeau et al. 2014, Sánchez-Bayo and Tennekes 2020, Bommuraj et al. 2021), the phenylpyrazole insecticide fipronil (Holder et al. 2018), miticides and their metabolites (Bommuraj et al. 2021), the fungicide boscalid (Simon-Delso et al. 2018), and the butenolide insecticide flupyradifurone (Tosi et al. 2021). The DRT_{95} is specific to GUTS modeling and has not been applied to data from honey bee bioassays to our knowledge. Because OpenGUTS could not estimate the lower bound of the dominant rate constant (k_d) for any metal, only the lower bound of DRT_{95} values could be calculated. We may have been able to estimate both bounds of k_d if assays were designed to include pulses of exposure, rather than continuous exposure (Baudrot and Charles 2019), but we chose the latter because it was closer to the exposure scenarios that we intended to simulate. There were no apparent problems estimating k_d or any other parameter using the R package 'morse,' which was used to make survival predictions, and GUTS models fitted with 'morse' or OpenGUTS produced visually identical fits to the calibration data (not shown).

We did not find that the Haber constant and the lower bound of DRT_{95} estimates agreed when ranking the metals by TRT (Tables 8 and 9). Furthermore, Haber constants were only significantly different from -1, which is indicative of TRT, for three of the metals (As, Cd, and Li). It would be interesting to compare these metrics of TRT across a greater range of chemicals to see if they can distinguish between chemicals that are known to exhibit varying levels of TRT. This could be done with existing data from honey bee bioassays, including our own data, which is available on FigShare (10.6084/m9.figshare.19357973).

Conclusion

Metal pollution is widespread, posing the risk of bioaccumulation and resultant, time-cumulative effects for a variety of wild and managed species, including honey bees. We found that the survival model GUTS-RED-SD outcompeted a standard (probit) modeling approach when predicting the survival of honey bees in the laboratory under exposure to Cd and Li. GUTS-RED-SD also had lower error for a third metal, Zn. However, the relative predictions of either modeling approach were highly case-specific when implemented in the background of a simple colony population model. Consistently, longer assays resulted in lower survival predictions. We therefore recommend that colony modelers use data from longer assays when predicting survival under chronic conditions of exposure, as well as comparing the predictions of contending models when possible. Finally, we found that two metrics of TRT, the Haber constant and the DRT_{95}, diverged when ranking each metal by TRT. This finding should be taken with caution, as we could only estimate the lower bound of the DRT_{95}. Additional research is necessary to determine the sensitivity of metrics of TRT for comparing across chemicals and under what conditions different metrics are likely to diverge.

Chapter 3. The accumulation of metal pollutants into royal jelly and their effects on the survival of larval honey bee workers and queens

Abstract

Honey bees are exposed to metal pollutants in human-modified environments, including cities and agricultural areas. Previous studies have shown that metals are more toxic to honey bee larvae than adults, but the exposure of larvae to metals in their diet (worker-produced jelly secretions) is unknown. This knowledge gap is especially important because jelly is the primary component of the queen's diet throughout her larval and adult life. In the present study, a queen-rearing experiment was conducted to measure the rates that Cd and Li translocate from colony food, sucrose solution, into royal jelly and developing queen larvae. The survival of exposed queens was then tracked to their emergence as adults and 7 days following emergence. Separately, an experiment was conducted in which worker larvae were reared *in vitro* to measure the effects of As, Li, and Zn on worker survival throughout development. These metals were selected to complement data from previous studies with Cd and Pb. We found that Cd and Li accumulated into both royal jelly and queen larvae at 1-10% of the concentration present in sucrose solution. Based on these translocation rates and the results of *in vitro* larval assays, it appears that metals have lethal effects on honey bee larvae at field-relevant concentrations. Additional research will be necessary to quantify the concentrations of metals in nurse jelly and their effects on brood production under field conditions, as well as their long-term sublethal effects on adult queens exposed as larvae.

3.1 Introduction

The honey bee society is organized around the gathering of food and the rearing of brood. Foragers collect nectar and pollen, which are consumed by adult bees that produce the jelly secretions that are consumed by the adult queen and both worker and queen larvae (Winston 1987). The nectar and pollen collected by foragers are frequently contaminated with toxic chemicals (Ostiguy et al. 2019), including metals (Johnson 2015, Solayman et al. 2016, Smith et al. 2019), but their translocation into the jelly secretions that make up the larval diet is largely unstudied. This is a major knowledge gap because queens and worker larvae feed primarily on nurse jelly (royal jelly and worker jelly, respectively) and their exposure has long-term implications for the success of colonies (vanEngelsdorp et al. 2013, Traynor et al. 2016, Traynor, VanEngelsdorp, et al. 2021).

Studies indicate that honey bee larvae are disproportionately susceptible to metals in their diet. The 50% lethal effect concentrations (LC_{50}) of Pb, Cd, Cu, and Se in the larval diet were found to be 1-2 orders of magnitude lower than those of adult bees (Hladun, Kaftanoglu, et al. 2013, Di et al. 2016). Effects on larval survival coincided with reductions to larval growth, which also occurred at lower concentrations (Di et al. 2016). Exposure to metals during the larval stage can also have carryover effects in adulthood. Larval exposure to field-relevant levels of Pb resulted in reduced head size and cognitive ability in adult worker bees (Monchanin, Blanc-Brude, et al. 2021). Acute exposure to Mn during development led to precocious foraging and premature death in adults (Søvik et al. 2015). Metals' effects on larval development likely contribute to negative correlations observed between metal loads within colonies, colony growth, and brood

production in field and semi-field studies (Bromenshenk et al. 1991, Hladun et al. 2016). These studies are corroborated by field studies with non-*Apis* bees where reductions in brood production in colonies or nests containing greater concentrations of certain metals have been observed (Moroń et al. 2014, Sivakoff et al. 2020).

Although metals are uniquely hazardous to honey bee larvae, the risk posed by metals in the field is not clear because metal concentrations in jelly, the primary component of the larval diet, has hardly been investigated. Existing studies suggest that nurse jelly sometimes contains higher concentrations of metals than honey. Leita et al. (1996) found that the concentrations of Cd, Pb, and Zn were 1.5-7X greater in jelly relative to honey. For 8 of the 9 metals included in their study, Stocker et al. (2005) measured 5-20-times higher concentrations in jelly relative to honey. In contrast, (Matuszewska et al. 2021) measured higher concentrations of As, Pb, and Cd in pollen relative to jelly, by a factor of 2-30, with marginal differences in the concentrations of Zn and Cr. Metals typically occur at higher concentrations in pollen compared to honey (Appendix A), and jelly may tend to exhibit an intermediate level of metal contamination, but the generality of this interpretation is unclear.

In the present study, the translocation of two metals, Cd and Li, from sucrose solution into royal jelly and developing queens was measured using a bulk queen-rearing approach. This approach allowed for the concentrations of metals in the diet of bees rearing queens to be controlled and made it possible to collect enough queen larvae and royal jelly for analysis of metal concentrations. A subset of developing queen cells were monitored to determine the effects of metal treatments on rates of adult queen emergence

and survival to 7 days following emergence. Finally, the effects of three metals, As, Li, and Zn, on larval survival was assessed through *in vitro* rearing of worker larvae to compare the effects of these metals to similar experiments conducted with Cd, Cu (Di et al. 2020) and Pb (Di et al. 2016).

3.2 Methods

3.2.1 Selection of metals

As, Cd, and Zn are major metal pollutants of human-modified environments, occurring at elevated levels in agricultural systems as well as urban areas (He et al. 2005, Wuana and Okieimen 2011). The heavy metal Cd has been measured in honey, pollen, and royal jelly of colonies located in contaminated environments at concentrations as high as 0.375, 1.40, and 3.5 mg/kg, respectively (Leita et al. 1996, Al-Naggar et al. 2013, Solayman et al. 2016). These concentrations exceed the larval LC_{50} of 0.275 mg/L for Cd, which was determined when Cd was fed to larvae from day 4 to day 10 of development (Di et al. 2016). The metalloid As has been measured from the honey and pollen stores of colonies at concentrations as high as 0.10 and 1.38 mg/kg, respectively (Conti and Botrè 2001, Solayman et al. 2016). The concentration of As has been measured in royal jelly collected directly from colonies at a concentration of 0.02 mg/kg, (Murashova et al. 2019) and it has been found in human dietary supplements containing royal jelly at concentrations as high as 0.244 mg/kg (Dolan et al. 2003). Finally, Zn has been measured from honey, pollen stores, and royal jelly at concentrations as high as 73,

108, and 96 mg/kg, respectively (Leita et al. 1996, Stocker et al. 2005, Solayman et al. 2016).

Less is known about the exposure of colonies to Li in contaminated environments (but see García et al. 2006, Hernández et al. 2005, Van Der Steen et al. 2012). However, Li exposure is relevant to honey bees because Li salts have recently gained attention as potential miticides for the treatment of *Varroa destructor*, a mite that parasitizes honey bee colonies (Ziegelmann et al. 2018). Li is toxic to *Varroa* mites via contact (Kolics, Mátyás, et al. 2020) and orally when feeding on honey bees that have been fed Li (Ziegelmann et al. 2018). It has been suggested to feed colonies with sucrose containing LiCl at concentrations as high as 25 mM (~173.4 mg/L Li) to control *Varroa* mites (Hannus et al. 2017, Ziegelmann et al. 2018). This concentration is lethal when fed directly to honey bee larvae reared *in vitro* (Hannus et al. 2017). As such, Li salts are only considered appropriate for use in colonies containing low levels of brood, which occurs when colonies are preparing to overwinter (Hannus et al. 2017, Kolics, Specziár, et al. 2020). Nonetheless, the concentration of Li that larvae may be exposed to through jelly, and the effect of Li exposure on larval development in colonies in which it has been applied as a *Varroa* control, warrants further study.

3.2.2 Queen-rearing experiment

Trials

Queen-rearing trials were conducted in the summers of 2020 and 2021 at the Ohio State University Wooster campus. Queens were reared in modified queen rearing boxes (hereafter “queen boxes”) using existing protocols (Spivak et al. 1994, Johnson and

Percel 2013, Ricke et al. 2021) (Fig. 23). Each queen box was provisioned with 200 g of pollen (BetterBee, Greenwich, NY) and 1.5 liters of 50% (w/w) sucrose solution. Sucrose solutions containing 173.5 mg/L of Li or 50 mg/L of Cd were prepared by adding LiCl or $CdCl_2$ to sucrose solution to achieve concentrations of 1060 mg/L of LiCl or 81.53 mg/L of $CdCl_2$. This concentration of LiCl was previously shown to be efficacious for *Varroa* control and exhibited marginal effects on the survival of adult honey bees over ten days of feeding (Ziegelmann et al. 2018). A concentration of 50 mg/L of Cd was chosen because this was expected to result in a measurable amount of Cd in royal jelly samples by the time queen cells were dissected (day 4 of each trial).

Metal	Concentration (mg/L)	Metal Compound	Queen Boxes (2020)	Queen Boxes (2021)	Total Queen Boxes	Queen boxes included in survival study (2021)
Control	0	None	3	7	10	4
Cd	50	$CdCl_2$	2	7	9	4
Li	173.5	LiCl	3	7	10	4

Table 10. Metal treatments and number of queen rearing boxes receiving each treatment across years.

Each queen box received thirty worker larvae between 24-48 h old, which were grafted into base mount JZ-BZ queen cups on queen cell bar frames (Mann Lake Ltd., Hackensak, MN) (Fig. 23). Each queen box also received approximately 1.1 kg of nurse bees, which were shaken from multiple healthy colonies into a ventilated swarm box prior to being distributed into queen boxes. Queen boxes were weighed before and after distributing nurses into them to ensure that the weight of nurses across boxes were within

100 g of each other. All hives used in this study were managed according to standard beekeeping practices (Honey Bee Health Coalition 2019) and no synthetic miticides that accumulate into colony wax were used or applied to hive equipment in the years preceding the study.

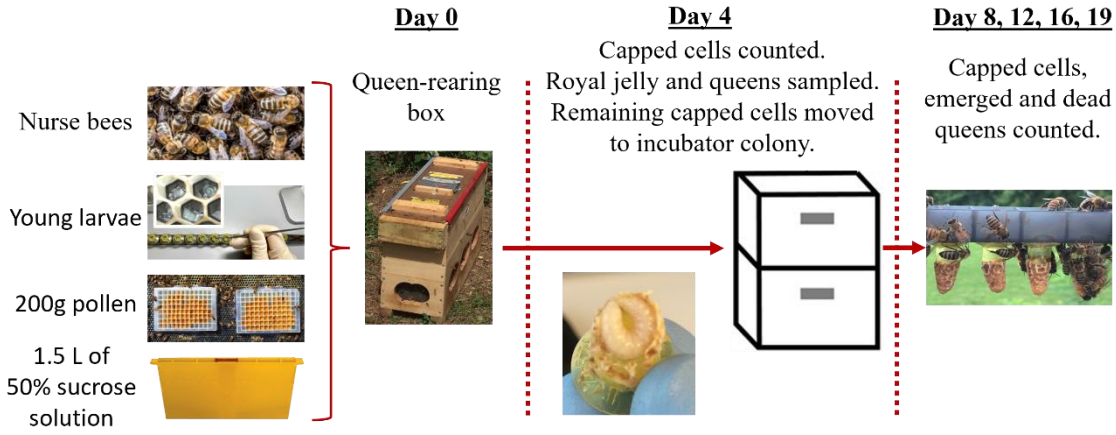

Figure 23. Experimental methodology of queen-rearing trials. In 2020, trials were terminated on day 4. In 2021, trials continued to day 19.

In 2020, trials were terminated on day 4 and all queen cells were dissected to collect queen larvae and royal jelly. Samples from each queen box were pooled and stored at -20°C for metal analysis. Queen larvae were dehydrated for 72h at 50°C and homogenized with a mortar and pestle. Parchment paper was placed between the mortar and pestle to prevent cross-contamination between samples, and the mortar was cleaned and dried between samples. All samples including royal jelly were sent to the Trace Elements Research Laboratory (TERL) at the Ohio State University Columbus campus for metal analysis. There, samples were digested in boiling nitric acid (95%) for at least 30 min and analyzed via ICP-OES (Hladun et al. 2016).

In the summer of 2021, extended assays lasting 19 days were performed. In that year, only the cells that were not capped by day 4 were dissected for metal analysis. If at least 50% of cells in control queen boxes were capped on day 4, trials continued. This occurred for 4 trials (Table 10). During these trials, capped cells were counted and distributed into new queen frames. Cells belonging to different treatment groups were moved into queen frames in alternating order, starting from the center of frames. These frames were then placed into strong incubating colonies in the top box and separated from the resident queen by at least two boxes above a queen excluder. On day 8, cells that were still capped were moved into plastic queen cages to isolate queens that would later emerge. The survival of queen cells to emergence was then monitored every four days until day 19.

Analyses

The rate that each metal translocated from treated sucrose solution into jelly and queen samples was calculated by dividing the concentration of each metal occurring in each sample by the nominal concentration applied to sucrose solution. Differences between the translocation rates of each metal into jelly and queens was then compared with a Kruskal-Wallis rank sums test using the *kruskal.test* function in the R package 'stats' (R Core Team 2021).

Four trials from 2021 were included in the survival analysis, representing 120 queens per treatment. Kaplan-Meier survival estimates were calculated for each group using the *survfit* function in the R package 'survival' (Therneau 2021). To compare

overall survival rates between groups, pairwise log-rank tests were performed with a Bonferroni correction using the *pairwise_survdiff* function in the package 'survminer' (Kassambara et al. 2021).

3.2.3 *In vitro* larval rearing

In vitro larval assays were conducted at the Waterman Agricultural Research and Natural Resources Laboratory (WANRL) at the Ohio State University in Columbus, OH, in the summer of 2021. Assays followed the protocol of (Schmehl et al. 2016). Because the effects of Cd on larval survival had been studied previously (Di et al. 2016), we focused on As, Li, and Zn (Table 11). For each treatment, an aqueous stock solution containing the respective metal at 51X the highest desired concentration was prepared. For each trial, 74.4 uL of stock solution was diluted with 3.72 mL of untreated diet solution. This was serially diluted with additional diet solution to achieve the remaining concentrations for each metal (Table 11).

Treatment	Concentrations (mg/L)	Metal Compound
As	0, 0.05, 0.5, 5	$Na_2HAsO_4 \cdot 7H_2O$
Li	0, 8.7, 17.5, 173.5	LiCl
Zn	0, 30, 100, 250	$Zn(CH_3CO_2)_2$

Table 11. Metal treatments used during *in vitro* larval rearing.

Each larval plate was divided into 3-4 groups of 12-18 wells, depending on the availability of larvae on a given day and the number of treatments being prepared (Fig.

24). Larvae aged to 4 days were grafted into plates and their development (larval/pupal) and survival (dead/alive) was monitored daily for the following 15 days. Each group either received the negative control treatment consisting of royal jelly, glucose, fructose, yeast extract, and water ("Diet C", Schmehl et al. 2018) or a metal treatment. Treatments were replaced every day for the first five days post-grafting (prior to pupation). Only one metal was applied to a given plate. The placement of treatment groups on each plate was randomized between plates. All larvae in a given plate were collected from the same brood frame. Each treatment was replicated at least 3 times (Table 12).

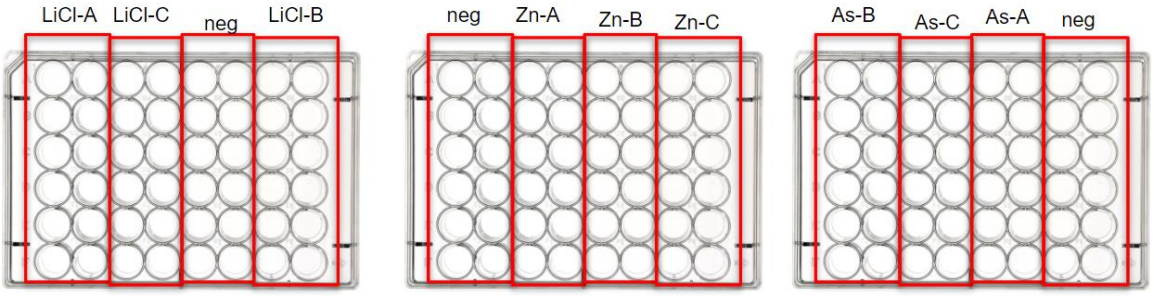

Figure 24. Examples of larval rearing plates for each metal (As, Li, or Zn). In a typical plate, 12 larvae were treated with a given metal at a given concentration (A, B, C) or no metal (neg). The placement of treatment groups was randomized between trials.

Metal	Concentration (mg/L)	Replicates	Larvae
As	0	5	59
	0.05	4	48
	0.5	3	36
	5	4	60
Li	0	5	69
	8.7	4	52
	17.5	8	52
	173.5	8	52
Zn	0	3	59
	30	3	36
	100	3	36
	250	3	36

Table 12. The number of replicates and larvae included in each treatment group.

Analysis

Kaplan-Meier survival estimates and pairwise comparisons of survival rates between *in vitro* treatments groups were generated for each metal using the *survdiff* and *pairwise_survdiff* functions in the R packages 'survival' and 'survminer,' respectively (Kassambara et al. 2021, Therneau 2021). In addition, LC_{50} estimates for each treatment group were estimated by fitting probit models to the survival data for each treatment group, using the *glm* function in the R package 'stats.'

3.3 Results

Metal translocation into royal jelly and queens

During ICP-OES, limits of detection were 0.1-0.4 and 0.1-3.5 mg/kg for Cd and Li, respectively. These limits were determined based on the performance of the ICP-OES machine on metal standards prior to analyzing each batch of samples. Metal concentrations were below limits of detection for all samples taken from control boxes,

except for eight jelly samples that were collected in 2020 that contained detectable levels of Li. The mean Li concentration in these samples was 3.46 mg/kg, whereas the mean concentration of jelly samples from boxes treated with Li was 12.34 mg/kg. None of the boxes that these samples were collected from were included in the survival analysis.

On average, Li concentrations in jelly and queen samples were 7.11% (n=10) and 29.83% (n=8) of the concentration applied in sucrose solution, respectively (Fig. 25, Table 13). Cd concentrations in jelly (n=9) and queen samples (n=6) were 3.75% and 1.40% those in the sucrose solution. Including Cd samples taken during preliminary trials in 2020, in which sucrose solution was also treated with 100 mg/L of Cd, jelly (n=11) and queen (n=9) samples contained 3.98% and 1.36% as much Cd as was applied in sucrose solutions, respectively.

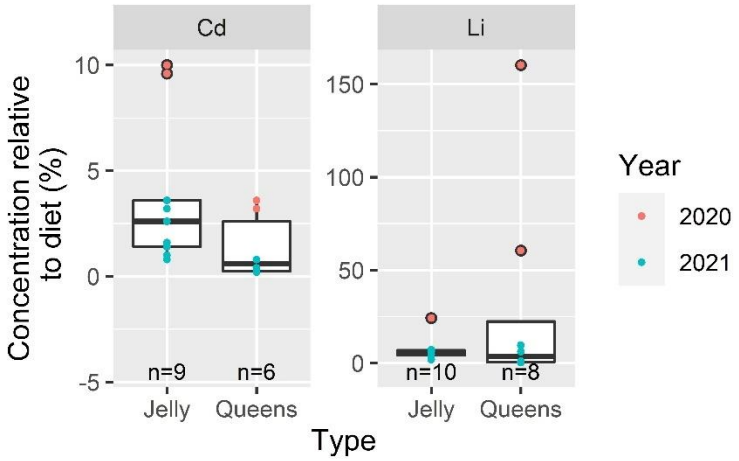

Figure 25. The concentrations of each metal in jelly and queen samples relative to concentrations applied to experimental sucrose solutions.

For both metals, translocation rates into jelly and queens were not significantly different ($p > 0.05$, Kruskal-Wallis rank sums tests, Table 13).

Treatment	Jelly (%)	Queens (%)	p	df	χ^2
50 mg/L Cd	3.75 (n=9)	1.40 (n=6)	0.4601	1	0.54574
173.5 mg/L Li	7.11 (n=10)	29.83 (n=8)	0.05718	1	3.6172

Table 13. Results of Kruskal-Wallis rank sums tests comparing the translocation rates of each metal into jelly and queens. Differences between translocation rates into jelly and queens were not statistically significant for either metal ($p > 0.05$).

Queen survival

There was a pronounced effect of each metal treatment on queen survival, resulting in nearly all queens dying by the end of trials (Fig. 26, Table 14). This occurred despite most queen cells containing jelly on day 4 that had not been consumed. Most capped cells that had been treated with metals were subsequently uncapped by nurses and emptied by day 8.

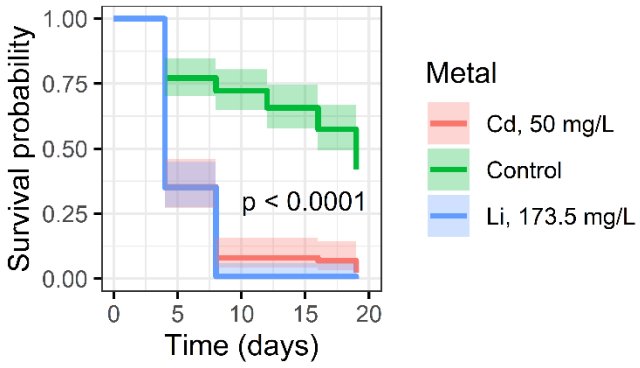

Figure 26. Kaplan-Meier survival curves for each metal treatment applied to queen-rearing boxes. Lines represent median survival estimates and shaded regions span the 95% confidence interval of survival predictions. The p value is the result of a log-rank test comparing the overall rates of survival across all treatment groups.

Metal	Day 4	Day 8	Day 12	Day 16	Day 19
Control	0.75±0.02	0.69±0.02	0.48±0.08	0.47±0.08	0.45±0.09
Cd	0.46±0.10	0.22±0.07	0.02±0.02	0.02±0.02	0.02±0.02
Li	0.37±0.05	0.03±0.02	0.00±0.00	0.00±0.00	0.00±0.00

Table 14. Mean rates of survival ± standard errors for each metal and timepoint during queen-rearing trials.

Rates of survival were significantly different when comparing each metal treatment with the negative control group (pairwise log-rank tests, $p << 0.05$), but survival rates were not significantly different when comparing between metal treatments (Table 15).

	Cd	Control
Control	< 2E-16	-
Li	0.82	< 2E-16

Table 15. P values from pairwise log-rank tests between the overall rates of survival between each metal treatment included in queen-rearing trials.

In vitro larval rearing

There was a dose-dependent effect of each metal on larval survival *in vitro* (log-rank tests, $p < 0.05$, Fig. 27). However, only certain treatment groups had significantly lower survival compared with the negative control groups (pairwise log-rank tests, $p < 0.05$, Table 16). Significant differences relative to negative controls occurred for As applied at 0.5 and 5 mg/L, Li applied at 173.5 mg/L, and Zn applied at 250 mg/L (Table 16).

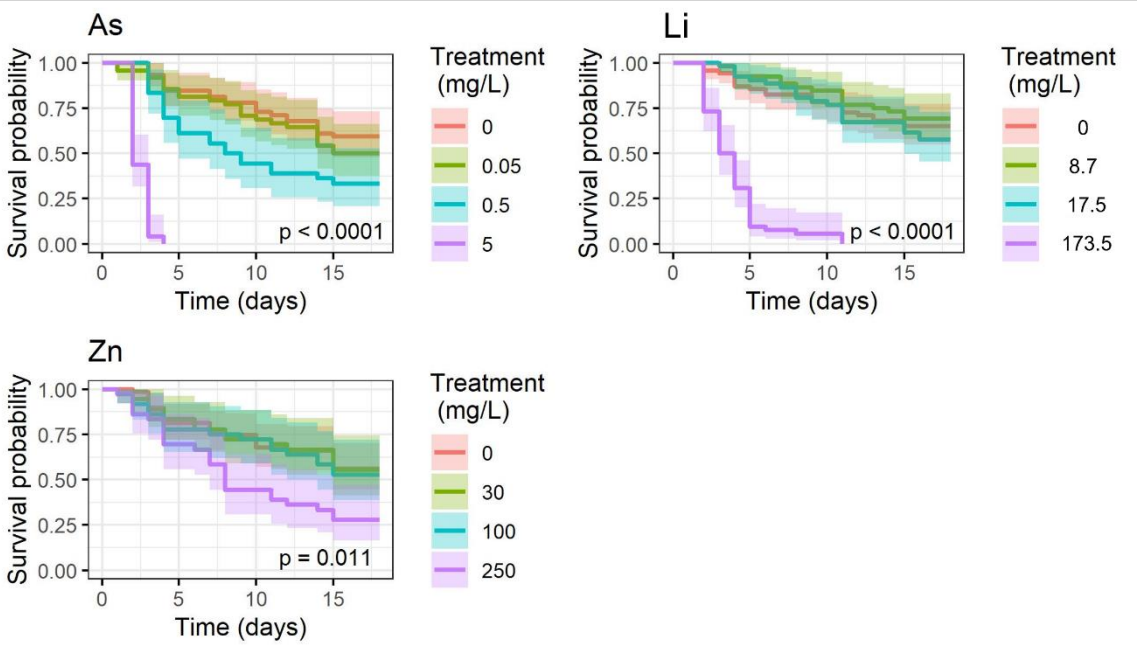

Figure 27. Kaplan-Meier survival curves for each metal and treatment group included in *in vitro* larval assays. Lines represent median survival estimates and shaded regions span the 95% confidence interval of survival predictions for each treatment group. P values were calculated from log-rank tests comparing the overall rate of survival across all treatment groups for each metal.

Metal	Concentration (mg/L)	P value
As	0.05	0.3721
	0.5	0.0067
	5	<2E-16
Li	8.7	0.56
	17.5	0.56
	173.5	<2E-16
Zn	30	0.955
	100	0.912
	250	0.018

Table 16. P values from multiple pairwise log-rank tests comparing the survival of each *in vitro* metal treatment group with their respective negative control groups.

Metal	Age at End of Trials (d)	LC_{50}
As	23	0.15 (0-0.44)
Cd*	10	0.275 (0.13-0.54)
Cu*	10	6.97 (3.09-22.21)
Li	23	29.9 (23.9-37.9)
Pb*	10	1.12 (0.46-2.46)
Zn	23	82.71

Table 17. Larval LC_{50} estimates for each metal, generated with data from larval *in vitro* worker assays. *LC_{50} estimates for Cd, Cu, and Pb were taken from the studies of (Di et al. 2016, 2020).

Metal	Standard Error	χ^2	df
As	0.074	10.19	18
Li	20.83	50.38	57
Zn	27.84	16.36	16

Table 18. Goodness of fit criteria for probit models fitted to *in vitro* larval rearing data.

3.4 Discussion

Honey bee larvae are more sensitive to metal exposure than adults, but the concentrations of metals in the primary component of their diet, nurse jelly, is largely unknown. In the first four days of queen-rearing trials, we found that Li and Cd translocated from sucrose solution into royal jelly at rates of 1-10% (Fig. 25). A higher rate was found for Li in queens (~25%), but differences between the concentrations of Li in jelly and queens were not statistically significant (Table 13). In addition, we found that sucrose solution containing 173.5 mg/L of Li (or 1060 mg/L of LiCl) resulted in almost complete queen mortality before adult emergence (Fig. 26). High mortality was also observed for queen boxes fed 50 mg/L of Cd. In trials in which worker larvae were reared

in vitro, As, Li, and Zn all affected larval survival at concentrations that have been measured from jelly, colony foods, or the bodies of bees in contaminated sites (Table 16, Appendix A). These trials add to the small body of knowledge on the larval toxicity of metals (Table 17).

The translocation rate of Li into queens that we observed (~7%) is similar to the translocation rate into worker larvae reported by Prešern et al. (2020) (~4%). In their study, colonies were also fed sucrose solution containing 173.5 mg/L of Li, at a rate of 1 L per day for three consecutive days. They did not measure jelly concentrations or track the survival of brood in treated colonies. However, they did measure the accumulation of Li into adult bees and observed increased mortality among them in the 7 days following treatment. In the present study, we confirm that this same concentration has severe effects on queen development, resulting in near-complete mortality by the 10^{th} day of larval development. High larval mortality had previously been shown to occur *in vitro* when worker larvae were directly fed with sucrose containing Li at the same concentration (Hannus et al. 2017), but its effects on bee development *in vivo* had not been reported to our knowledge.

In queen boxes treated with 173.5 mg/L of Li, royal jelly contained Li at concentrations of ~12 mg/L. Although we observed high mortality during queen-rearing trials under these conditions, effects of Li on the survival of worker larvae were only observed when larvae were fed concentrations >17.5 mg/L (Fig. 27). These differences between *in vitro* and queen-rearing assays suggest that the high mortality observed during queen-rearing trials resulted from LiCl's direct toxicity to queen brood as well as indirect

effects on the brood-tending capacity of nurse bees. Previous studies have shown that the exposure of nurses to pesticides can have developmental effects on their hypopharyngeal glands, which produce royal jelly (Berenbaum and Liao 2019). In recent queen-rearing experiments, this has been directly linked to reductions in both the quantity of royal jelly produced and its metabolomic profile (Milone et al. 2021).

In addition to affecting jelly production, toxic exposure can affect the brood-tending behavior of nurse bees (Berenbaum and Liao 2019). In queen boxes treated with metals, we found that most cells that were capped on day 4 were subsequently uncapped and emptied by day 8. This was previously observed when larvae were exposed to chronic levels of the neonicotinoid clothianidin and appeared to be triggered by pheromone signals produced by treated larvae (Schuehly et al. 2021). Queen exposure during development can also affect worker behaviors later in life. For example, queens exposed as larvae to common in-hive pesticides via beeswax produced mandibular pheromones as adults that were less attractive to workers than those of untreated queens (Walsh et al. 2020). The lifelong effects of metal exposure during development on honey bee physiology, social interactions, and reproduction is an interesting avenue for future studies. In addition to using whole colonies or small nucleus colonies (Milone and Tarpy 2021), research in this area may utilize novel methods for measuring queen egg-laying and larval development in the lab (Fine et al. 2018).

In the study of Hladun et al. (2016), which lasted for 60 days, the metal concentrations in worker pupae were ~5-75X greater than was applied in sucrose solution. This is much higher than the translocation rates observed in this study. The

discrepancy may be due to the longer duration of their study, which allowed metals to accumulate to a higher final concentration relative to experimental treatments, or to the lower concentrations applied, which would be less likely to affect the feeding rate and resulting accumulation. Additionally, this study sampled worker brood rather than queen brood. It was previously shown that pesticides are transferred at a higher rate into worker jelly than queen jelly (Böhme et al. 2018, 2019) and the same may hold for metals. However, the concentration of one metal, Zn, has been found to be higher in royal jelly relative to worker jelly (Wang et al. 2016). Zn is an essential metal in the honey bee diet and its concentration in jelly may be regulated differently than metals that have no known biological function (ex. Cd) (Stocker et al. 2005). Hladun et al. (2016) also found that queens in experimental colonies exhibited higher concentrations of all metals in their study relative to control queens, indicative of metal contamination of royal jelly, though this was only significant for 2 of 4 metals tested. In the study of Kolics et al. (2021), Li concentrations were below the limit of detection in queens sampled 28 days after treatment with sucrose solution containing 173.5 mg/L of Li, which likely resulted from the elimination of Li from the body.

Our study and previous studies warn against the overapplication of Li to control *Varroa* mites in colonies containing brood. Previous studies have also shown that Li treatments can contaminate hive products that are consumed by humans. In the study of Kolics et al. (2021), 1 L of sucrose solution containing 173.5 mg/L of Li was fed to colonies on a single day. Li concentrations in uncapped honey, bee bread, and worker bodies returned to control levels within ~15 days following treatment. Although

uncapped honey contained very low Li concentrations after this time (< 0.25 mg/kg), Li persisted in honey that had been capped shortly during or after colonies were treated, at a mean concentration of 22.40 mg/kg. Honey containing Li at this concentration can result in Li exposure to human consumers exceeding the daily dietary allowance determined by Schrauzer (2002) (14.3 ug/kg of body weight). A human weighing 63.5 kg would only need to consume ~30 mL at this concentration to reach this threshold. The accumulation of Li into hive products can potentially be mitigated through alternative modes of Li delivery, such as lithiated contact strips (Kolics, Mátyás, et al. 2020).

In addition to metals, larvae are also disproportionately susceptible to a variety of common pesticides (Zhu et al. 2014, Tomé et al. 2020). Like metals, the translocation of pesticides into nurse jelly is only partially understood. The translocation rates we observed for Cd and Li are 1-2 orders of magnitude greater than the translocation rates of pesticides applied to queen-rearing boxes in pollen (Böhme et al. 2018, 2019, Ricke et al. 2021). The greater translocation rates we measured are likely the result of the greater persistence of metals relative to pesticides and the fact that metals in this study were applied in sucrose solution rather than pollen, which is consumed at a lower rate by hive bees (USEPA 2014).

3.5 Conclusion

Metal pollution is common in human-modified environments, posing risk to honey bees and other terrestrial arthropods. We determined the rates that Cd and Li translocate into nurse jelly over the course of four days and measured their effect on the

survival of queen larvae. The effects of Li on queen development provide additional cause for caution regarding application of Li salts as a control for *Varroa*. Additionally, the effects of As, Li, and Zn on the survival of worker larvae reared *in vitro* demonstrate that larvae are uniquely susceptible to a variety of metals. Future studies should measure the exposure and effects of larvae to metals in field colonies, as well as the more long-term effects of exposure during development on queen fitness.

References

(California Pesticide Information Portal) California Department of Pesticide Regulation. **2021**. California Pesticide Information Portal. (https://calpip.cdpr.ca.gov/county.cfm?ds=PUR).

Al-Naggar, Y. A., E. A. Naiem, A. I. Seif, and M. H. Mona. **2013**. Honey bees and their products as bio-indicator of environmental pollution with heavy metals. Mellifera. 20: 10–20.

Al-Naggar, Y., K. Dabour, S. Masry, A. Sadek, E. Naiem, and J. P. Giesy. **2020**. Sublethal effects of chronic exposure to CdO or PbO nanoparticles or their binary mixture on the honey bee (Apis millefera L.). Environ. Sci. Pollut. Res. 27.

Ankley, G. T., R. S. Bennett, R. J. Erickson, D. J. Hoff, M. W. Hornung, R. D. Johnson, D. R. Mount, J. W. Nichols, C. L. Russom, P. K. Schmieder, J. A. Serrrano, J. E. Tietge, and D. L. Villeneuve. **2010**. Adverse outcome pathways: A conceptual framework to support ecotoxicology research and risk assessment. Environ. Toxicol. Chem. 29: 730–741.

Ashauer, R., and C. D. Brown. **2008**. Toxicodynamic assumptions in ecotoxicological hazard models. Environ. Toxicol. Chem. 27: 1817–21.

Ashauer, R., and B. I. Escher. **2010**. Advantages of toxicokinetic and toxicodynamic modelling in aquatic ecotoxicology and risk assessment. J. Environ. Monit.

Ashauer, R., I. O'Connor, A. Hintermeister, and B. I. Escher. **2015**. Death Dilemma and Organism Recovery in Ecotoxicology. Environ. Sci. Technol. 49: 10136–10146.

Bart, S., T. Jager, A. Robinson, E. Lahive, D. J. Spurgeon, and R. Ashauer. **2021**. Predicting mixture effects over time with toxicokinetic-toxicodynamic models (GUTS): Assumptions, experimental testing, and predictive power. Environ. Sci. Technol. 55: 2430–2439.

Baudrot, V., and S. Charles. **2019**. Recommendations to address uncertainties in environmental risk assessment using toxicokinetic-toxicodynamic models. Sci. Rep. 9.

Baudrot, V., S. Charles, M. L. Delignette-Muller, W. Duchemin, B. Gouseen, N. Kehrein, G. Kon-Kam-King, C. Lopes, P. Ruiz, A. Singer, and P. Veber. **2021**. morse: Modelling Tools for Reproduction and Survival Data in Ecotoxicology.

Beadle, K., K. S. Singh, B. J. Troczka, E. Randall, M. Zaworra, C. T. Zimmer, A. Hayward, R. Reid, L. Kor, M. Kohler, B. Buer, D. R. Nelson, M. S. Williamson, T. G. E. Davies, L. M. Field, R. Nauen, and C. Bass. **2019**. Genomic insights into neonicotinoid sensitivity in the solitary bee Osmia bicornis. PLoS Genet. 15: 1–19.

Becher, M. A., V. Grimm, P. Thorbek, J. Horn, P. J. Kennedy, and J. L. Osborne. **2014**. BEEHAVE: A systems model of honeybee colony dynamics and foraging to explore multifactorial causes of colony failure. J. Appl. Ecol. 51: 470–482.

Belkebir, E., C. Rousselle, C. Duboudin, L. Bodin, and N. Bonvallot. **2011**. Haber's rule duration adjustments should not be used systematically for risk assessment in public health decision-making. Toxicol. Lett. 204: 148–55.

Berenbaum, M. R. 2016. Does the Honey Bee "risk Cup" Runneth Over? Estimating Aggregate Exposures for Assessing Pesticide Risks to Honey Bees in

Agroecosystems. J. Agric. Food Chem.
Berenbaum, M. R., and R. M. Johnson. **2015**. Xenobiotic detoxification pathways in honey bees. Curr. Opin. Insect Sci. 10: 51–58.
Berenbaum, M. R., and L. H. Liao. **2019**. Honey Bees and Environmental Stress: Toxicologic Pathology of a Superorganism. Toxicol. Pathol. 47: 1076–1081.
Böhme, F., G. Bischoff, C. P. W. Zebitz, P. Rosenkranz, and K. Wallner. **2018**. From field to food—will pesticide-contaminated pollen diet lead to a contamination of royal jelly? Apidologie. 49: 112–119.
Böhme, F., G. Bischoff, C. P. W. Zebitz, P. Rosenkranz, and K. Wallner. **2019**. From field to food II–will pesticide-contaminated pollen diet lead to a contamination of worker jelly? J. Apic. Res. 58: 542–549.
Bommuraj, V., Y. Chen, M. Birenboim, S. Barel, and J. A. Shimshoni. **2021**. Concentration- and time-dependent toxicity of commonly encountered pesticides and pesticide mixtures to honeybees (Apis mellifera L.). Chemosphere. 266: 128974.
Bommuraj, V., Y. Chen, H. Klein, R. Sperling, S. Barel, and J. A. Shimshoni. **2019**. Pesticide and trace element residues in honey and beeswax combs from Israel in association with human risk assessment and honey adulteration. Food Chem. 299: 125123.
Bonmatin, J. M., C. Giorio, V. Girolami, D. Goulson, D. P. Kreutzweiser, C. Krupke, M. Liess, E. Long, M. Marzaro, E. A. Mitchell, D. A. Noome, N. Simon-Delso, and A. Tapparo. **2015**. Environmental fate and exposure; neonicotinoids and fipronil. Environ. Sci. Pollut. Res. 22: 35–67.
Bonzini, S., P. Tremolada, I. Bernardinelli, M. Colombo, and M. Vighi. **2011**. Predicting pesticide fate in the hive (part 1): Experimentally determined τ-Fluvalinate residues in bees, honey and wax. Apidologie. 42: 378–390.
Borsuk, G., A. Sulborska, E. Stawiarz, K. Olszewski, D. Wiącek, N. Ramzi, A. Nawrocka, and M. Jędryczka. **2021**. Capacity of honeybees to remove heavy metals from nectar and excrete the contaminants from their bodies. Apidologie. 52: 1098–1111.
Bosancic, B., M. Zabic, D. Mihajlovic, J. Samardzic, and G. Mirjanic. **2020**. Comparative study of toxic heavy metal residues and other properties of honey from different environmental production systems. Environ. Sci. Pollut. Res. 27.
Briggs, G. G., R. H. Bromilow, A. A. Evans, and M. Williams. **1983**. Relationships between lipophilicity and the distribution of non-ionised chemicals in barley shoots following uptake by the roots. Pestic. Sci. 14: 492–500.
Brock, T., M. Arena, N. Cedergreen, S. Charles, S. Duquesne, A. Ippolito, M. Klein, M. Reed, I. Teodorovic, P. J. van den Brink, and A. Focks. **2021**. Application of General Unified Threshold Models of Survival Models for Regulatory Aquatic Pesticide Risk Assessment Illustrated with an Example for the Insecticide Chlorpyrifos. Integr. Environ. Assess. Manag. 17: 243–258.
Bromenshenk, J. J., S. R. Carlson, J. C. Simpson, and J. M. Thomas. **1985**. Pollution monitoring of Puget Sound with honey bees. Science. 227: 632–634.
Bromenshenk, J. J., J. L. Gudatis, S. R. Carlson, J. M. Thomas, and M. A.

Simmons. **1991**. Population dynamics of honey bee nucleus colonies exposed to industrial pollutants. Apidologie. 22: 359–369.

Bulson, L., M. A. Becher, T. J. McKinley, and L. Wilfert. **2021**. Long-term effects of antibiotic treatments on honeybee colony fitness: A modelling approach. J. Appl. Ecol. 58.

Burden, C. M., C. Elmore, K. R. Hladun, J. T. Trumble, and B. H. Smith. **2016**. Acute exposure to selenium disrupts associative conditioning and long-term memory recall in honey bees (Apis mellifera). Ecotoxicol. Environ. Saf. 127: 71–79.

Burden, C. M., M. O. Morgan, K. R. Hladun, G. V. Amdam, J. J. Trumble, and B. H. Smith. **2019**. Acute sublethal exposure to toxic heavy metals alters honey bee (Apis mellifera) feeding behavior. Sci. Rep. 9: 4253.

Calderone, N. W. 2012. Insect pollinated crops, insect pollinators and US agriculture: Trend analysis of aggregate data for the period 1992-2009. PLoS One. 7: e37235.

Capitani, G., G. Papa, M. Pellecchia, and I. Negri. **2021**. Disentangling multiple PM emission sources in the Po Valley (Italy) using honey bees. Heliyon. 7: e06194.

Carnesecchi, E., C. Svendsen, S. Lasagni, A. Grech, N. Quignot, B. Amzal, C. Toma, S. Tosi, A. Rortais, J. Cortinas-Abrahantes, E. Capri, N. Kramer, E. Benfenati, D. Spurgeon, G. Guillot, and J. L. C. M. Dorne. **2019**. Investigating combined toxicity of binary mixtures in bees: Meta-analysis of laboratory tests, modelling, mechanistic basis and implications for risk assessment. Environ. Int. 133 pt. B: 105256.

Carnesecchi, E., C. Toma, A. Roncaglioni, N. Kramer, E. Benfenati, and J. L. C. M. Dorne. **2020**. Integrating QSAR models predicting acute contact toxicity and mode of action profiling in honey bees (A. mellifera): Data curation using open source databases, performance testing and validation. Sci. Total Environ. 735: 139243.

Cedergreen, N., A. M. Christensen, A. Kamper, P. Kudsk, S. K. Mathiassen, J. C. Streibig, and H. Sørensen. **2008**. A review of independent action compared to concentration addition as reference models for mixtures of compounds with different molecular target sites. Environ. Toxicol. Chem.

Christen, V., and K. Fent. **2017**. Exposure of honey bees (Apis mellifera) to different classes of insecticides exhibit distinct molecular effect patterns at concentrations that mimic environmental contamination. Environ. Pollut. 226: 48–59.

Codling, E. E., R. L. Chaney, and C. E. Green. **2015**. Accumulation of Lead and Arsenic by Carrots Grown on Lead-Arsenate Contaminated Orchard Soils. J. Plant Nutr. 38: 509–525.

Coecke, S., O. Pelkonen, S. B. Leite, U. Bernauer, J. G. M. Bessems, F. Y. Bois, U. Gundert-Remy, G. Loizou, E. Testai, and J. M. Zaldívar. **2013**. Toxicokinetics as a key to the integrated toxicity risk assessment based primarily on non-animal approaches. Toxicol. Vitr. 27: 1570–7.

Collins, C. D., I. Martin, and M. Fryer. **2006**. Evaluation of models for predicting plant uptake of chemicals from soil, Environ. Agency.

Conti, M. E., and F. Botrè. **2001**. Honeybees and their products as potential bioindicators of heavy metals contamination. Environ. Monit. Assess. 69: 267–282.

Costa, A., M. Veca, M. Barberis, A. Tosti, G. Notaro, S. Nava, M. Lazzari, A.

Agazzi, and F. Maria Tangorra. **2019**. Heavy metals on honeybees indicate their concentration in the atmosphere. a proof of concept. Ital. J. Anim. Sci. 18: 309–315.

Crenna, E., O. Jolliet, E. Collina, S. Sala, and P. Fantke. **2020**. Characterizing honey bee exposure and effects from pesticides for chemical prioritization and life cycle assessment. Environ. Int. 138: 105642.

Cresswell, J. E. 2017. Protocol for evaluating whether a test substance shows bioaccumulative properties using Haber's Law.

Cresswell, J. E. 2018. Three cardinal numbers to safeguard bees against pesticide exposure: LD50, NOEC (revised) and the Haber exponent. *In* HAZARDS Pestic. TO BEES.

Cresswell, J. E., F. X. L. Robert, H. Florance, and N. Smirnoff. **2014**. Clearance of ingested neonicotinoid pesticide (imidacloprid) in honey bees (Apis mellifera) and bumblebees (Bombus terrestris). Pest Manag. Sci. 70: 332–337.

Cullen, M. G., L. J. Thompson, J. C. Carolan, J. C. Stout, and D. A. Stanley. **2019**. Fungicides, herbicides and bees: A systematic review of existing research and methods. PLoS One. 14: e0225743.

Delignette-Muller, M. L., P. Ruiz, and P. Veber. **2017**. Robust Fit of Toxicokinetic-Toxicodynamic Models Using Prior Knowledge Contained in the Design of Survival Toxicity Tests. Environ. Sci. Technol. 51: 4038–4045.

Devillers, J., J. C. Doré, M. Marenco, F. Poirier-Duchêne, N. Galand, and C. Viel. **2002**. Chemometrical analysis of 18 metallic and nonmetallic elements found in honeys sold in France. J. Agric. Food Chem. 50: 5998–6007.

Di, N., K. R. Hladun, K. Zhang, T. X. Liu, and J. T. Trumble. **2016**. Laboratory bioassays on the impact of cadmium, copper and lead on the development and survival of honeybee (Apis mellifera L.) larvae and foragers. Chemosphere. 152: 530–538.

Di, N., K. Zhang, K. R. Hladun, M. Rust, Y. F. Chen, Z. Y. Zhu, T. X. Liu, and J. T. Trumble. **2020**. Joint effects of cadmium and copper on Apis mellifera forgers and larvae. Comp. Biochem. Physiol. Part - C Toxicol. Pharmacol. 237: 108839.

DiBartolomeis, M., S. Kegley, P. Mineau, R. Radford, and K. Klein. **2019**. An assessment of acute insecticide toxicity loading (AITL) of chemical pesticides used on agricultural land in the United States. PLoS One. 14: e0220029.

Dolan, S. P., D. A. Nortrup, P. M. Bolger, and S. G. Capar. **2003**. Analysis of dietary supplements for arsenic, cadmium, mercury, and lead using inductively coupled plasma mass spectrometry. J. Agric. Food Chem. 51.

Douglas, M. R., D. B. Sponsler, E. V. Lonsdorf, and C. M. Grozinger. **2020**. County-level analysis reveals a rapidly shifting landscape of insecticide hazard to honey bees (Apis mellifera) on US farmland. Sci. Rep. 10: 797.

Doull, J., and K. K. Rozman. **2000**. Using Haber's Law to define the margin of exposure. Toxicology. 149: 1–2.

Dżugan, M., M. Wesołowska, G. Zaguła, M. Kaczmarski, M. Czernicka, and C. Puchalski. **2018**. Honeybees (Apis mellifera) as a biological barrier for contamination of honey by environmental toxic metals. Environ. Monit. Assess. 190: 101.

EFSA. **2013**. Guidance on the risk assessment of plant protection products on bees (Apis mellifera, Bombus spp. and solitary bees). EFSA J. 11: 3295.

EFSA. **2016**. Statement on the suitability of the BEEHAVE model for its potential use in a regulatory context and for the risk assessment of multiple stressors in honeybees at the landscape level. EFSA J. 13: 4125.

Fageria, N. K., C. Baligar, and R. B. Clark. **2002**. Micronutrients in crop production. Adv. Agron.

Fantke, P., and R. Juraske. **2013**. Variability of pesticide dissipation half-lives in plants. Environ. Sci. Technol. 47: 3548–3562.

Farha, W., A. M. Abd El-Aty, M. M. Rahman, H. C. Shin, and J. H. Shim. **2016**. An overview on common aspects influencing the dissipation pattern of pesticides: a review. Environ. Monit. Assess.

FIFRA. **2012**. White Paper in Support of the Proposed Risk Assessment Process for Bees Submitted to the FIFRA Scientific Advisory Panel for Review and Comment Office of Chemical Safety and Pollution Prevention Office of Pesticide Programs Environmental Fate and Effects.

Fine, J. D., H. Y. Shpigler, A. M. Ray, N. J. Beach, A. L. Sankey, A. Cash-Ahmed, Z. Y. Huang, I. Astrauskaite, R. Chao, H. Zhao, and G. E. Robinson. **2018**. Quantifying the effects of pollen nutrition on honey bee queen egg laying with a new laboratory system. PLoS One. 13.

Fisher, A., G. DeGrandi-Hoffman, B. H. Smith, M. Johnson, O. Kaftanoglu, T. Cogley, J. H. Fewell, and J. F. Harrison. **2021**. Colony field test reveals dramatically higher toxicity of a widely-used mito-toxic fungicide on honey bees (Apis mellifera). Environ. Pollut. 269: 115964.

Fox, J., and S. Weisberg. **2019**. An {R} Companion to Applied Regression, Third Edition, 3rd ed. SAGE Publishing, Thousand Oaks, CA.

Galic, N., R. Ashauer, H. Baveco, A. M. Nyman, A. Barsi, P. Thorbek, E. Bruns, and P. J. Van den Brink. **2014**. Modeling the contribution of toxicokinetic and toxicodynamic processes to the recovery of Gammarus pulex populations after exposure to pesticides. Environ. Toxicol. Chem. 33: 1476–88.

García, J. C. R., R. I. Rodríguez, R. M. P. Crecente, J. B. García, S. G. Martín, and C. H. Latorre. **2006**. Preliminary chemometric study on the use of honey as an environmental marker in Galicia (northwestern Spain). J. Agric. Food Chem. 54.

Gergs, A., F. Gabsi, A. Zenker, and T. G. Preuss. **2016**. Demographic Toxicokinetic-Toxicodynamic Modeling of Lethal Effects. Environ. Sci. Technol. 50: 6017–6024.

Gierer, F., S. Vaughan, M. Slater, H. M. Thompson, J. S. Elmore, and R. D. Girling. **2019**. A review of the factors that influence pesticide residues in pollen and nectar: Future research requirements for optimising the estimation of pollinator exposure. Environ. Pollut. 249: 236–247.

Gizaw, G., Y. H. Kim, K. H. Moon, J. B. Choi, Y. H. Kim, and J. K. Park. **2020**. Effect of environmental heavy metals on the expression of detoxification-related genes in honey bee Apis mellifera. Apidologie. 51: 664–674.

Goretti, E., M. Pallottini, R. Rossi, G. La Porta, T. Gardi, B. T. Cenci Goga, A. C. Elia, M. Galletti, B. Moroni, C. Petroselli, R. Selvaggi, and D. Cappelletti. **2020**.

Heavy metal bioaccumulation in honey bee matrix, an indicator to assess the contamination level in terrestrial environments. Environ. Pollut. 256: 113388.

Goulson, D., J. Thompson, and A. Croombs. **2018**. Rapid rise in toxic load for bees revealed by analysis of pesticide use in Great Britain. PeerJ. 2018: e5255.

Grech, A., C. Brochot, J. Lou Dorne, N. Quignot, F. Y. Bois, and R. Beaudouin. **2017**. Toxicokinetic models and related tools in environmental risk assessment of chemicals. Sci. Total Environ. 578: 1–15.

Grimm, V., and B. T. Martin. **2013**. Mechanistic effect modeling for ecological risk assessment: where to go from here? Integr. Environ. Assess. Manag. 9: e58-63.

Gutiérrez, M., R. Molero, M. Gaju, J. van der Steen, C. Porrini, and J. A. Ruiz. **2015**. Assessment of heavy metal pollution in Córdoba (Spain) by biomonitoring foraging honeybee. Environ. Monit. Assess. 187: 651.

Haas, J., J. Glaubitz, U. Koenig, and R. Nauen. **2021**. A mechanism-based approach unveils metabolic routes potentially mediating chlorantraniliprole synergism in honey bees, Apis mellifera L., by azole fungicides. Pest Manag. Sci. 78: 965–973.

Haas, J., and R. Nauen. **2021**. Pesticide risk assessment at the molecular level using honey bee cytochrome P450 enzymes: A complementary approach. Environ. Int. 147: 106372.

Haas, J., M. Zaworra, J. Glaubitz, G. Hertlein, M. Kohler, A. Lagojda, B. Lueke, C. Maus, M.-T. Almanza, T. G. E. Davies, C. Bass, and R. Nauen. **2021**. A toxicogenomics approach reveals characteristics supporting the honey bee (Apis mellifera L.) safety profile of the butenolide insecticide flupyradifurone. Ecotoxicol. Environ. Saf. 217: 112247.

Hannus, S., P. Rosenkranz, and B. Ziegelmann. **2017**. Lithium metal salt for use in treatment of varroa destructor mite infestation of honey bees.

He, Z. L., X. E. Yang, and P. J. Stoffella. **2005**. Trace elements in agroecosystems and impacts on the environment. J. Trace Elem. Med. Biol. 19: 125–40.

Heard, M. S., J. Baas, J. Lou Dorne, E. Lahive, A. G. Robinson, A. Rortais, D. J. Spurgeon, C. Svendsen, and H. Hesketh. **2017**. Comparative toxicity of pesticides and environmental contaminants in bees: Are honey bees a useful proxy for wild bee species? Sci. Total Environ. 578: 357–365.

Henry, M., N. Cerrutti, P. Aupinel, A. Decourtye, M. Gayrard, J. F. Odoux, A. Pissard, C. Rüger, and V. Bretagnolle. **2015**. Reconciling laboratory and field assessments of neonicotinoid toxicity to honeybees. Proc. R. Soc. B Biol. Sci. 282: 20152110.

Hesketh, H., E. Lahive, A. A. Horton, A. G. Robinson, C. Svendsen, A. Rortais, J. L. Dorne, J. Baas, D. J. Spurgeon, and M. S. Heard. **2016**. Extending standard testing period in honeybees to predict lifespan impacts of pesticides and heavy metals using dynamic energy budget modelling. Sci. Rep. 6: 37655.

Hitaj, C., D. J. Smith, A. Code, S. Wechsler, P. D. Esker, and M. R. Douglas. **2020**. Sowing uncertainty: what we do and don't know about the planting of pesticide-treated seed. Bioscience.

Hladun, K. R., N. Di, T. X. Liu, and J. T. Trumble. **2016**. Metal contaminant accumulation in the hive: Consequences for whole-colony health and brood

production in the honey bee (Apis mellifera L.). Environ. Toxicol. Chem. 35: 322–329.

Hladun, K. R., O. Kaftanoglu, D. R. Parker, K. D. Tran, and J. T. Trumble. **2013**. Effects of selenium on development, survival, and accumulation in the honeybee (Apis mellifera L.). Environ. Toxicol. Chem. 32: 2584–92.

Hladun, K. R., D. R. Parker, K. D. Tran, and J. T. Trumble. **2013**. Effects of selenium accumulation on phytotoxicity, herbivory, and pollination ecology in radish (Raphanus sativus L.). Environ. Pollut. 172: 70–75.

Hladun, K. R., B. H. Smith, J. A. Mustard, R. R. Morton, and J. T. Trumble. **2012**. Selenium toxicity to honey bee (apis mellifera l.) pollinators: Effects on behaviors and survival. PLoS One. 7: e34137.

Hlina, B. L., O. Birceanu, C. S. Robinson, H. Dhiyebi, and M. P. Wilkie. **2021**. The relationship between thermal physiology and lampricide sensitivity in larval sea lamprey (Petromyzon marinus). J. Great Lakes Res. 47: S272–S284.

Holder, P. J. 2016. Little and often makes much: identifying the time-reinforced toxicity of pesticides and their impacts on bees.

Holder, P. J., A. Jones, C. R. Tyler, and J. E. Cresswell. **2018**. Fipronil pesticide as a suspect in historical mass mortalities of honey bees. Proc. Natl. Acad. Sci. U. S. A. 115: 13033–13038.

Honey Bee Health Coalition. **2019**. Best management practices for hive health, A guide for beekeepers.

Hörig, K., C. Maus, A. Nikolakis, H.-T. Ratte, M. Roß-Nickoll, W. Schmitt, T. G. Preuss, B. Cropscience, and H.-T. Ratte. **2015**. The advantage of a toxicokinetic model of the honey bee colony in the context of the risk assessment of plant protection products, p. 51. *In* Julius-Kühn-Archiv.

Hyndman, R. J., and Y. Khandakar. **2008**. Automatic time series forecasting: The forecast package for R. J. Stat. Softw. 27.

Iwasa, T., N. Motoyama, J. T. Ambrose, and R. M. Roe. **2004**. Mechanism for the differential toxicity of neonicotinoid insecticides in the honey bee, Apis mellifera. Crop Prot. 23: 371–378.

Jager, T. 2021. Robust Likelihood-Based Approach for Automated Optimization and Uncertainty Analysis of Toxicokinetic-Toxicodynamic Models. Integr. Environ. Assess. Manag. 17: 388–397.

Jager, T., C. Albert, T. G. Preuss, and R. Ashauer. **2011**. General unified threshold model of survival - A toxicokinetic-toxicodynamic framework for ecotoxicology. Environ. Sci. Technol. 45: 2529–2540.

Jager, T., and R. Ashauer. **2018a**. Modelling survival under chemical stress: A comprehensive guide to the GUTS framework, 2nd ed. Toxicodynamics Ltd., York, UK.

Jager, T., and R. Ashauer. **2018b**. How to Evaluate the Quality of Toxicokinetic—Toxicodynamic Models in the Context of Environmental Risk Assessment. Integr. Environ. Assess. Manag. 14: 604–614.

Johnson, R. M. 2015. Honey Bee Toxicology. Annu. Rev. Entomol. 60: 415–34.

Johnson, R. M., L. Dahlgren, B. D. Siegfried, and M. D. Ellis. **2013**. Acaricide ,

Fungicide and Drug Interactions in Honey Bees (Apis mellifera). 8: e54092.
Johnson, R. M., and E. G. Percel. **2013**. Effect of a Fungicide and Spray Adjuvant on Queen-Rearing Success in Honey Bees (Hymenoptera: Apidae). J. Econ. Entomol. 106: 1952–1957.
Johnson, R. M., H. S. Pollock, and M. R. Berenbaum. **2009**. Synergistic interactions between in-hive miticides in Apis mellifera. J. Econ. Entomol. 102: 474–9.
Kassambara, A., M. Kosinski, P. Biecek, and F. Scheipl. **2021**. survminer: drawing survival curves using "ggplot2".
Kast, C., and V. Kilchenmann. **2022**. An in vitro model for assessing the toxicity of pesticides in beeswax on honey bee larvae. Chemosphere. 287: 132214.
Khoury, D. S., M. R. Myerscough, and A. B. Barron. **2011**. A quantitative model of honey bee colony population dynamics. PLoS One. 6: 2–7.
Kolics, É., K. Mátyás, J. Taller, A. Specziár, and B. Kolics. **2020**. Contact effect contribution to the high efficiency of lithium chloride against the mite parasite of the honey bee. Insects. 11.
Kolics, É., Z. Sajtos, K. Mátyás, K. Szepesi, I. Solti, G. Németh, J. Taller, E. Baranyai, A. Specziár, and B. Kolics. **2021**. Changes in lithium levels in bees and their products following anti-varroa treatment. Insects. 12.
Kolics, É., A. Specziár, J. Taller, K. K. Mátyás, and B. Kolics. **2020**. Lithium chloride outperformed oxalic acid sublimation in a preliminary experiment for Varroa mite control in pre-wintering honey bee colonies. Acta Vet. Hung. 68.
Kuan, A. C., G. DeGrandi-Hoffman, R. J. Curry, K. V. Garber, A. R. Kanarek, M. N. Snyder, K. L. Wolfe, and S. T. Purucker. **2018**. Sensitivity analyses for simulating pesticide impacts on honey bee colonies. Ecol. Modell. 376: 15–27.
LaLone, C. A., D. L. Villeneuve, J. Wu-Smart, R. Y. Milsk, K. Sappington, K. V. Garber, J. Housenger, and G. T. Ankley. **2017**. Weight of evidence evaluation of a network of adverse outcome pathways linking activation of the nicotinic acetylcholine receptor in honey bees to colony death. Sci. Total Environ. 584–585: 751–775.
Laurino, D., A. Manino, A. Patetta, and M. Porporato. **2013**. Toxicity of neonicotinoid insecticides on different honey bee genotypes. Bull. Insectology. 66: 119–126.
Leita, L., G. Muhlbachova, S. Cesco, R. Barbattini, and C. Mondini. **1996**. Investigation of the use of honey bees and honey bee products to assess heavy metals contamination. Environ. Monit. Assess. 43: 1–9.
Lenth, R. V. 2016. Least-squares means: The R package lsmeans. J. Stat. Softw. 69.
Li, X., M. A. Schuler, and M. R. Berenbaum. **2007**. Molecular Mechanisms of Metabolic Resistance to Synthetic and Natural Xenobiotics. Annu. Rev. Entomol. 52: 231–53.
Long, E. Y., and C. H. Krupke. **2016**. Non-cultivated plants present a season-long route of pesticide exposure for honey bees. Nat. Commun. 7: 11629.
López-Osorio, F., and Y. Wurm. **2020**. Healthy Pollinators: Evaluating Pesticides with Molecular Medicine Approaches. Trends Ecol. Evol. 35: 380–383.
Manjon, C., B. J. Troczka, M. Zaworra, K. Beadle, E. Randall, G. Hertlein, K. S.

Singh, C. T. Zimmer, R. A. Homem, B. Lueke, R. Reid, L. Kor, M. Kohler, J. Benting, M. S. Williamson, T. G. E. Davies, L. M. Field, C. Bass, and R. Nauen. **2018**. Unravelling the Molecular Determinants of Bee Sensitivity to Neonicotinoid Insecticides. Curr. Biol. 28: 1137-1143.e5.

Mao, W., M. A. Schuler, and M. R. Berenbaum. **2011**. CYP9Q-mediated detoxification of acaricides in the honey bee (Apis mellifera). Proc. Natl. Acad. Sci. U. S. A. 108: 12657–12662.

Mao, W., M. A. Schuler, and M. R. Berenbaum. **2017**. Disruption of quercetin metabolism by fungicide affects energy production in honey bees (Apis mellifera). Proc. Natl. Acad. Sci. U. S. A. 114: 2538–2543.

Martin, B. T., T. Jager, R. M. Nisbet, T. G. Preuss, M. Hammers-Wirtz, and V. Grimm. **2013**. Extrapolating ecotoxicological effects from individuals to populations: A generic approach based on Dynamic Energy Budget theory and individual-based modeling. Ecotoxicology. 22: 574–83.

Matuszewska, E., A. Klupczynska, K. Maciołek, Z. J. Kokot, and J. Matysiak. **2021**. Multielemental analysis of bee pollen, propolis, and royal jelly collected in west-central poland. Molecules. 26: 2415.

Meikle, W. G., T. Colin, J. J. Adamczyk, M. Weiss, and A. B. Barron. **2022**. Traces of a neonicotinoid pesticide stimulate different honey bee colony activities, but do not increase colony size or longevity. Ecotoxicol. Environ. Saf. 231: 113202.

Meindl, G. A., and T. L. Ashman. **2014**. Nickel Accumulation by Streptanthus polygaloides (Brassicaceae) Reduces Floral Visitation Rate. J. Chem. Ecol. 40: 128–35.

Milone, J. P., P. Chakrabarti, R. R. Sagili, and D. R. Tarpy. **2021**. Colony-level pesticide exposure affects honey bee (Apis mellifera L.) royal jelly production and nutritional composition. Chemosphere. 263: 128183.

Milone, J. P., and D. R. Tarpy. **2021**. Effects of developmental exposure to pesticides in wax and pollen on honey bee (Apis mellifera) queen reproductive phenotypes. Sci. Rep.

Mokkapati, J. S., A. J. Bednarska, M. Choczyński, and R. Laskowski. **2022**. Toxicokinetics of three insecticides in the female adult solitary bee Osmia bicornis. Environ. Pollut. 293: 118610.

Monchanin, C., A. Blanc-Brude, E. Drujont, M. M. Negahi, C. Pasquaretta, J. Silvestre, D. Baqué, A. Elger, A. B. Barron, J. M. Devaud, and M. Lihoreau. **2021**. Chronic exposure to trace lead impairs honey bee learning. Ecotoxicol. Environ. Saf. 212: 112008.

Monchanin, C., J. M. Devaud, A. B. Barron, and M. Lihoreau. **2021**. Current permissible levels of metal pollutants harm terrestrial invertebrates. Sci. Total Environ. 779: 146398.

Moncharmont, F. X. D., A. Decourtye, C. Hennequet-Hantier, O. Pons, and M. H. Pham-Delègue. **2003**. Statistical analysis of honeybee survival after chronic exposure to insecticides. Environ. Toxicol. Chem. 22: 3088–94.

More, S., V. Bampidis, D. Benford, C. Bragard, T. Halldorsson, A. Hernández-Jerez, S. H. Bennekou, K. Koutsoumanis, K. Machera, H. Naegeli, S. S. Nielsen,

J. Schlatter, D. Schrenk, V. Silano, D. Turck, M. Younes, G. Arnold, J. Lou Dorne, A. Maggiore, S. Pagani, C. Szentes, S. Terry, S. Tosi, D. Vrbos, G. Zamariola, and A. Rortais. **2021**. A systems-based approach to the environmental risk assessment of multiple stressors in honey bees. EFSA J. 19.

Moroń, D., H. Szentgyörgyi, P. Skórka, S. G. Potts, and M. Woyciechowski. **2014**. Survival, reproduction and population growth of the bee pollinator, Osmia rufa (Hymenoptera: Megachilidae), along gradients of heavy metal pollution. Insect Conserv. Divers. 7: 113–121.

Mullin, C. A., M. Frazier, J. L. Frazier, S. Ashcraft, R. Simonds, D. VanEngelsdorp, and J. S. Pettis. **2010**. High Levels of Miticides and Agrochemicals in North American Apiaries: Implications for Honey Bee Health. PLoS One. 5: e9754.

Murashova, E. A. A., Tunikov G M, Byshova N G, and Serebryakova O V. **2019**. Major Factors Determining Accumulation of Toxic Elements By Bees and Honey Products. Int. Trans. J. Eng. Manag. Appl. Sci. Technol. 11.

Myerscough, M. R., D. S. Khoury, S. Ronzani, and A. B. Barron. **2017**. Why Do Hives Die? Using Mathematics to Solve the Problem of Honey Bee Colony Collapse. *In* Role Importance Math. Innov.

Naranjo, E., M. V. Merfa, S. Santra, A. Ozcan, E. Johnson, P. A. Cobine, and L. De La Fuente. **2020**. Zinkicide is a ZnO-based nanoformulation with bactericidal activity against liberibacter crescens in batch cultures and in microfluidic chambers simulating plant vascular systems. Appl. Environ. Microbiol. 86: e00788-20.

Nauen, R., U. Ebbinghaus-Kintscher, V. L. Salgado, and M. Kaussmann. **2003**. Thiamethoxam is a neonicotinoid precursor converted to clothianidin in insects and plants. Pestic. Biochem. Physiol. 76: 55–69.

Niell, S., F. Jesús, R. Díaz, Y. Mendoza, G. Notte, E. Santos, N. Gérez, V. Cesio, H. Cancela, and H. Heinzen. **2018**. Beehives biomonitor pesticides in agroecosystems: Simple chemical and biological indicators evaluation using Support Vector Machines (SVM). Ecol. Indic. 91: 149–154.

Nikolić, T. V., D. Kojić, S. Orčić, D. Batinić, E. Vukašinović, D. P. Blagojević, and J. Purać. **2016**. The impact of sublethal concentrations of Cu, Pb and Cd on honey bee redox status, superoxide dismutase and catalase in laboratory conditions. Chemosphere. 164: 98–105.

Nikolić, T. V., D. Kojić, S. Orčić, E. L. Vukašinović, D. P. Blagojević, and J. Purać. **2019**. Laboratory bioassays on the response of honey bee (Apis mellifera L.) glutathione S-transferase and acetylcholinesterase to the oral exposure to copper, cadmium, and lead. Environ. Sci. Pollut. Res. 26: 6890–6897.

Ockleford, C., P. Adriaanse, P. Berny, T. Brock, S. Duquesne, S. Grilli, A. F. Hernandez-Jerez, S. H. Bennekou, M. Klein, T. Kuhl, R. Laskowski, K. Machera, O. Pelkonen, S. Pieper, R. H. Smith, M. Stemmer, I. Sundh, A. Tiktak, C. J. Topping, G. Wolterink, N. Cedergreen, S. Charles, A. Focks, M. Reed, M. Arena, A. Ippolito, H. Byers, and I. Teodorovic. **2018**. Scientific Opinion on the state of the art of Toxicokinetic/Toxicodynamic (TKTD) effect models for regulatory risk assessment of pesticides for aquatic organisms. EFSA J. 16.

OECD. **2017**. Test No. 245. Honey bee (Apis mellífera L.), chronic oral toxicity test (10-day feeding). OECD Guidel. Test. Chem.

de Oliveira, R. C., S. C. do N. Queiroz, C. F. P. da Luz, R. S. Porto, and S. Rath. **2016**. Bee pollen as a bioindicator of environmental pesticide contamination. Chemosphere. 163: 525–534.

Ostiguy, N., F. A. Drummond, K. Aronstein, B. Eitzer, J. D. Ellis, M. Spivak, and W. S. Sheppard. **2019**. Honey bee exposure to pesticides: A four-year nationwide study. Insects. 10: 13.

Papa, G., G. Capitani, E. Capri, M. Pellecchia, and I. Negri. **2021**. Vehicle-derived ultrafine particulate contaminating bees and bee products. Sci. Total Environ. 750: 141700.

Plummer, M. 2021. rjags: Bayesian Graphical Models using MCMC.

Prešern, J., U. Kur, J. Bubnič, and M. Šala. **2020**. Lithium contamination of honeybee products and its accumulation in brood as a consequence of anti-varroa treatment. Food Chem.

Purać, J., T. V. Nikolić, D. Kojić, A. S. Ćelić, J. J. Plavša, D. P. Blagojević, and E. T. Petri. **2019**. Identification of a metallothionein gene in honey bee Apis mellifera and its expression profile in response to Cd, Cu and Pb exposure. Mol. Ecol. 28: 731–745.

Quinn, C. F., C. N. Prins, J. L. Freeman, A. M. Gross, L. J. Hantzis, R. J. B. Reynolds, S. in Yang, P. A. Covey, G. S. Bañuelos, I. J. Pickering, S. C. Fakra, M. A. Marcus, H. S. Arathi, and E. A. H. Pilon-Smits. **2011**. Selenium accumulation in flowers and its effects on pollination. New Phytol. 192: 727–37.

R Core Team. **2021**. R: A language and environment for statistical computing.

Reffstrup, T. K., J. C. Larsen, and O. Meyer. **2010**. Risk assessment of mixtures of pesticides. Current approaches and future strategies. Regul. Toxicol. Pharmacol. 56: 174–192.

Reid, R. J., B. J. Troczka, L. Kor, E. Randall, M. S. Williamson, L. M. Field, R. Nauen, C. Bass, and T. G. E. Davies. **2020**. Assessing the acute toxicity of insecticides to the buff-tailed bumblebee (Bombus terrestris audax). Pestic. Biochem. Physiol. 166: 104562.

Reilly, J. R., D. R. Artz, D. Biddinger, K. Bobiwash, N. K. Boyle, C. Brittain, J. Brokaw, J. W. Campbell, J. Daniels, E. Elle, J. D. Ellis, S. J. Fleischer, J. Gibbs, R. L. Gillespie, K. B. Gundersen, L. Gut, G. Hoffman, N. Joshi, O. Lundin, K. Mason, C. M. McGrady, S. S. Peterson, T. L. Pitts-Singer, S. Rao, N. Rothwell, L. Rowe, K. L. Ward, N. M. Williams, J. K. Wilson, R. Isaacs, and R. Winfree. **2020**. Crop production in the USA is frequently limited by a lack of pollinators. Proc. R. Soc. B Biol. Sci. 287: 20200922.

Ricke, D. F., C. H. Lin, and R. M. Johnson. **2021**. Pollen Treated with a Combination of Agrochemicals Commonly Applied during Almond Bloom Reduces the Emergence Rate and Longevity of Honey Bee (Hymenoptera: Apidae) Queens. J. Insect Sci. 21: 5.

Robinson, A., H. Hesketh, E. Lahive, A. A. Horton, C. Svendsen, A. Rortais, J. Lou Dorne, J. Baas, M. S. Heard, and D. J. Spurgeon. **2017**. Comparing bee species

responses to chemical mixtures: Common response patterns? PLoS One. 12: e0176289.

Roeben, V., S. Oberdoerster, K. J. Rakel, D. Liesy, Y. Capowiez, G. Ernst, T. G. Preuss, A. Gergs, and C. Oberdoerster. **2020**. Towards a spatiotemporally explicit toxicokinetic-toxicodynamic model for earthworm toxicity. Sci. Total Environ. 722: 137673.

Rondeau, G., F. Sánchez-Bayo, H. A. Tennekes, A. Decourtye, R. Ramírez-Romero, and N. Desneux. **2014**. Delayed and time-cumulative toxicity of imidacloprid in bees, ants and termites. Sci. Rep. 4: 1–8.

Rortais, A., G. Arnold, J. Lou Dorne, S. J. More, G. Sperandio, F. Streissl, C. Szentes, and F. Verdonck. **2017**. Risk assessment of pesticides and other stressors in bees: Principles, data gaps and perspectives from the European Food Safety Authority. Sci. Total Environ. 587–588: 524–537.

Rumkee, J. C. O., M. A. Becher, P. Thorbek, and J. L. Osborne. **2017**. Modeling Effects of Honeybee Behaviors on the Distribution of Pesticide in Nectar within a Hive and Resultant in-Hive Exposure. Environ. Sci. Technol. 51: 6908–6917.

Sánchez-Bayo, F. 2009. From simple toxicological models to prediction of toxic effects in time. Ecotoxicology. 18: 343–54.

Sánchez-Bayo, F., and H. A. Tennekes. **2020**. Time-cumulative toxicity of neonicotinoids: Experimental evidence and implications for environmental risk assessments. Int. J. Environ. Res. Public Health. 17: 1629.

Schmehl, D., S. Hinarejos, J. Ellis, and S. Clark. **2018**. Validation of the 22-day Honey Bee Larval Toxicity, Repeated (Chronic) Exposure Study Design. Julius-Kühn-Archiv. 462: 99–103.

Schmehl, D. R., H. V. V Tomé, A. N. Mortensen, G. F. Martins, and J. D. Ellis. **2016**. Protocol for the in vitro rearing of honey bee (Apis mellifera L.) workers. J. Apic. Res. 55: 113–129.

Schmolke, A., F. Abi-Akar, and S. Hinarejos. **2019**. Honey bee colony-level exposure and effects in realistic landscapes: An application of BEEHAVE simulating clothianidin residues in corn pollen. Environ. Toxicol. Chem. 38: 423–435.

Schrauzer, G. N. 2002. Lithium: Occurrence, Dietary Intakes, Nutritional Essentiality. J. Am. Coll. Nutr. 21.

Schuehly, W., U. Riessberger-Gallé, and J. Hernández López. **2021**. Sublethal pesticide exposure induces larval removal behavior in honeybees through chemical cues. Ecotoxicol. Environ. Saf. 228.

Shimshoni, J. A., R. Sperling, M. Massarwa, Y. Chen, V. Bommuraj, M. Borisover, and S. Barel. **2019**. Pesticide distribution and depletion kinetic determination in honey and beeswax: Model for pesticide occurrence and distribution in beehive products. PLoS One. 14: e0212631.

Simon-Delso, N., G. S. Martin, E. Bruneau, C. Delcourt, and L. Hautier. **2017**. The challenges of predicting pesticide exposure of honey bees at landscape level. Sci. Rep. 7: 1–10.

Simon-Delso, N., G. San Martin, E. Bruneau, and L. Hautier. **2018**. Time-to-death approach to reveal chronic and cumulative toxicity of a fungicide for honeybees not

revealed with the standard ten-day test. Sci. Rep. 8: 1–11.
Simsek, I., O. Kuzukiran, B. Yurdakok-Dikmen, U. T. Sireli, M. Beykaya, and A. Filazi. **2021**. Comparison of selected lipophilic compound residues in honey and propolis. J. Food Compos. Anal. 102: 104068.
Sivakoff, F. S., S. P. Prajzner, and M. M. Gardiner. **2020**. Urban heavy metal contamination limits bumblebee colony growth. J. Appl. Ecol. 57: 1561–1569.
Smirle, M. J., and M. L. Winston. **1987**. Intercolony Variation in Pesticide Detoxification by the Honey Bee (Hymenoptera: Apidae). J. Econ. Entomol. 80: 5–8.
Smith, K. E., D. Weis, M. Amini, A. E. Shiel, V. W. M. Lai, and K. Gordon. **2019**. Honey as a biomonitor for a changing world. Nat. Sustain. 2: 223–232.
Soetaert, K., T. Petzoldt, and R. W. Setzer. **2010**. Solving differential equations in R: Package deSolve. J. Stat. Softw. 33.
Solayman, M., M. A. Islam, S. Paul, Y. Ali, M. I. Khalil, N. Alam, and S. H. Gan. **2016**. Physicochemical Properties, Minerals, Trace Elements, and Heavy Metals in Honey of Different Origins: A Comprehensive Review. Compr. Rev. Food Sci. Food Saf. 15: 219–233.
Søvik, E., C. J. Perry, A. LaMora, A. B. Barron, and Y. Ben-Shahar. **2015**. Negative impact of manganese on honeybee foraging. Biol. Lett. 11: 20140989.
Spivak, M., S. Becker, and G. Reuter. **1994**. Successful Queen Rearing, 2nd ed. University of Minnesota.
Sponsler, D. B., and R. M. Johnson. **2017**. Mechanistic modeling of pesticide exposure: The missing keystone of honey bee toxicology. Environ. Toxicol. Chem. 36: 871–881.
Steen, J. J. M. Van der, J. de Kraker, and T. Grotenhuis. **2015**. Assessment of the Potential of Honeybees (Apis mellifera L.) in Biomonitoring of Air Pollution by Cadmium, Lead and Vanadium. J. Environ. Prot. (Irvine,. Calif). 06.
Van Der Steen, J. J. M., J. De Kraker, and T. Grotenhuis. **2012**. Spatial and temporal variation of metal concentrations in adult honeybees (Apis mellifera L.). Environ. Monit. Assess. 184.
Stocker, A., P. Schramel, A. Kettrup, and E. Bengsch. **2005**. Trace and mineral elements in royal jelly and homeostatic effects. J. Trace Elem. Med. Biol. 19: 183–9.
Stoner, K. A., and B. D. Eitzer. **2013**. Using a Hazard Quotient to Evaluate Pesticide Residues Detected in Pollen Trapped from Honey Bees (Apis mellifera) in Connecticut. PLoS One. 8: e77550.
Suchail, S., D. Guez, and L. P. Belzunces. **2001**. Discrepancy between acute and chronic toxicity induced by imidacloprid and its metabolites in Apis mellifera. Environ. Toxicol. Chem. 20: 2482–6.
Therneau, T. M. 2021. A Package for Survival Analysis in R.
Thompson, H. M. 2021. The use of the Hazard Quotient approach to assess the potential risk to honeybees (Apis mellifera) posed by pesticide residues detected in bee-relevant matrices is not appropriate. Pest Manag. Sci. 77: 3934–3941.
Thompson, H. M., and T. Pamminger. **2019**. Are honeybees suitable surrogates for use in pesticide risk assessment for non-Apis bees? Pest Manag. Sci. 75: 2549–2557.

Tomé, H. V. V., D. R. Schmehl, A. E. Wedde, R. S. M. M. Godoy, S. V. Ravaiano, R. N. C. C. Guedes, G. F. Martins, J. D. Ellis, H. V. V Tom, S. V. Ravaiano, R. N. C. C. Guedes, G. F. Martins, and J. D. Ellis. **2020**. Frequently encountered pesticides can cause multiple disorders in developing worker honey bees. Environ. Pollut. 256: 113420.

Tosi, S., J. C. Nieh, A. Brandt, M. Colli, J. Fourrier, H. Giffard, J. Hernández-López, V. Malagnini, G. R. Williams, and N. Simon-Delso. **2021**. Long-term field-realistic exposure to a next-generation pesticide, flupyradifurone, impairs honey bee behaviour and survival. Commun. Biol. 4: 805.

Traynor, K. S., J. S. Pettis, D. R. Tarpy, C. A. Mullin, J. L. Frazier, M. Frazier, and D. VanEngelsdorp. **2016**. In-hive Pesticide Exposome: Assessing risks to migratory honey bees from in-hive pesticide contamination in the Eastern United States. Sci. Rep. 6: 1–16.

Traynor, K. S., S. Tosi, K. Rennich, N. Steinhauer, E. Forsgren, R. Rose, G. Kunkel, S. Madella, D. Lopez, H. Eversole, R. Fahey, J. Pettis, J. D. Evans, and Dennis vanEngelsdorp. **2021**. Pesticides in honey bee colonies: Establishing a baseline for real world exposure over seven years in the USA. Environ. Pollut. 279: 116566.

Traynor, K. S., D. VanEngelsdorp, and Z. S. Lamas. **2021**. Social disruption: Sublethal pesticides in pollen lead to Apis mellifera queen events and brood loss. Ecotoxicol. Environ. Saf. 214: 112105.

Tremolada, P., I. Bernardinelli, B. Rossaro, M. Colombo, and M. Vighi. **2011**. Predicting pesticide fate in the hive (part 2): Development of a dynamic hive model. Apidologie. 42: 439–456.

Troczka, B. J., R. A. Homem, R. Reid, K. Beadle, M. Kohler, M. Zaworra, L. M. Field, M. S. Williamson, R. Nauen, C. Bass, and T. G. E. Davies. **2019**. Identification and functional characterisation of a novel N-cyanoamidine neonicotinoid metabolising cytochrome P450, CYP9Q6, from the buff-tailed bumblebee Bombus terrestris. Insect Biochem. Mol. Biol. 111: 103171.

USEPA. **2014**. Guidance for Assessing Pesticide Risks to BeesU.S. Environmental Protection Agency (USEPA) Health Canada Pest Management Regulatory Agency (PMRA) and California Departament of Pesticide Regulatio. Off. Pestic. Programs USEPA, Heal. Canada PMRA, CDPR.

USEPA. **2021**. Registration Review Process. (https://www.epa.gov/pesticide-reevaluation/registration-review-process).

vanEngelsdorp, D., D. R. Tarpy, E. J. Lengerich, and J. S. Pettis. **2013**. Idiopathic brood disease syndrome and queen events as precursors of colony mortality in migratory beekeeping operations in the eastern United States. Prev. Vet. Med. 108: 225–233.

Vareda, J. P., A. J. M. Valente, and L. Durães. **2019**. Assessment of heavy metal pollution from anthropogenic activities and remediation strategies: A review. J. Environ. Manage.

Vighi, M., A. Barsi, A. Focks, and F. Grisoni. **2019**. Predictive models in ecotoxicology: Bridging the gap between scientific progress and regulatory applicability—Remarks and research needs. Integr. Environ. Assess. Manag. 15:

345–351.
Walsh, E. M., S. Sweet, A. Knap, N. Ing, and J. Rangel. **2020**. Queen honey bee (Apis mellifera) pheromone and reproductive behavior are affected by pesticide exposure during development. Behav. Ecol. Sociobiol.
Wang, Y., L. Ma, W. Zhang, X. Cui, H. Wang, and B. Xu. **2016**. Comparison of the nutrient composition of royal jelly and worker jelly of honey bees (Apis mellifera). Apidologie. 47.
Winston, M. L. 1987. The Biology of the Honey Bee, 1st ed. Harvard University Press, Cambridge, MA.
Woodcock, B. A., L. Ridding, S. N. Freeman, M. Gloria Pereira, D. Sleep, J. Redhead, D. Aston, N. L. Carreck, R. F. Shore, J. M. Bullock, M. S. Heard, and R. F. Pywell. **2018**. Neonicotinoid residues in UK honey despite European Union moratorium. PLoS One. 13: e0189681.
Wuana, R. A., and F. E. Okieimen. **2011**. Heavy Metals in Contaminated Soils: A Review of Sources, Chemistry, Risks and Best Available Strategies for Remediation. ISRN Ecol. 2011: 402647.
Xun, E., Y. Zhang, J. Zhao, and J. Guo. **2017**. Translocation of heavy metals from soils into floral organs and rewards of Cucurbita pepo: Implications for plant reproductive fitness. Ecotoxicol. Environ. Saf. 145: 235–243.
Zaworra, M., H. Koehler, J. Schneider, A. Lagojda, and R. Nauen. **2019**. Pharmacokinetics of Three Neonicotinoid Insecticides upon Contact Exposure in the Western Honey Bee, Apis mellifera. Chem. Res. Toxicol. 32: 35–37.
Zeaiter, Z., and M. R. Myerscough. **2020**. Poor hive thermoregulation produces an Allee effect and leads to colony collapse. J. Theor. Biol. 503: 110361.
Zhang, Q., and C. Wang. **2020**. Natural and Human Factors Affect the Distribution of Soil Heavy Metal Pollution: a Review. Water. Air. Soil Pollut.
Zhu, W., D. R. Schmehl, C. A. Mullin, and J. L. Frazier. **2014**. Four common pesticides, their mixtures and a formulation solvent in the hive environment have high oral toxicity to honey bee larvae. PLoS One. 9: e77547.
Ziegelmann, B., E. Abele, S. Hannus, M. Beitzinger, S. Berg, and P. Rosenkranz. **2018**. Lithium chloride effectively kills the honey bee parasite Varroa destructor by a systemic mode of action. Sci. Rep. 8: 683.
Zioga, E., R. Kelly, B. White, and J. C. Stout. **2020**. Plant protection product residues in plant pollen and nectar: A review of current knowledge. Environ. Res.

Appendix A. Metal concentrations in colony matrices reported from past field studies.

Metal	Honey*	Pollen or Bee Bread	Bee bodies	Site Description	Reference
As	ND-0.10		0.00151 - 0.00456	Industrial	Matin et al. (2016)
			0.011 - 0.160	Urban and mining areas	Zhou et al. (2018)
			0.66 - 0.83	Mixed	Van der Steen et al. (2012)
		< 0.2	< 1	Mixed, some sites near mines	Maragou et al. (2017)
			< 12.5	Puget Sound, downwind from smelters	Bromenshenk et al. (1985)
			< 13.9	Puget Sound, downwind from smelters	Bromenshenk et al. (1991)
		< 0.01 - 1.38		Rural and urban	Morgano et al. (2010)
Cd	1.7E-5 - 0.373	< 0.091	< 0.00423	Extraurban and urban	Conti and Botrè (2001)
			~ 0.14	Urban	Zarić et al. (2017)
		0.003- 1.798		Mixed	Roman (2009)
			0.01 - 0.21	Urban areas including near an airport and wildlife reserves	Perugini et al. (2011)
			0.01 - 0.39	Nature reserves	Ruschioni et al. (2013)
			0.07 - 0.75	Mixed	Van der Steen et al. (2012)
			0.03 - 0.96	Mixed	Dżugan et al. (2018)
		0.01 - 0.15	0.05 - 1.2	Mixed	Fakhimzadeh and Lodenius (2000)
		0.067 - 1.4	0.07 - 1.6	Mixed	Al Naggar et al. (2013)
			0.63775 - 1.636	Industrial	Matin et al. (2016)
			0.02 - 1.75	Mixed	Velemínský and Stary (1990)
			< 1.8	Puget Sound, downwind from smelters	Bromenshenk et al. (1985)

Table A1. Metal concentrations (in mg/kg) from field studies. *Honey concentrations taken from review paper by Solayman et al. (2016). Continued on next page.

Table A1 continued

Metal	Honey	Pollen or Bee Bread	Bee bodies	Site Description	Reference
Cd	1.7E-5 - 0.373		0.03 - 2.93	Mixed	Goretti et al. (2020)
			ND - 3.19	Mixed	Tomzyk et al. (2020)
			< 4.07	Puget Sound, downwind from smelters	Bromenshenk et al. (1991)
			0.00045 - 0.00766	Near thermal power plants	Silici et al. (2016)
		0.003 - 0.233		Rural and urban	Morgano et al. (2010)
		1.8 - 2.3		Extraurban crossroad	Leita et al. (1996)
		0.89 - 9.31**		Urbanization gradients approaching smelters	Moroń et al. (2012)
Li	NA	NA	0.01 - 0.05	Mixed	Van der Steen et al. (2012)
Pb	6.3E-4 - 3.23	< 0.332	< 0.00125	Extraurban and urban	Conti and Botrè (2001)
			0.03036 - 0.05206	Industrial	Matin et al. (2016)
			ND - 0.58	Mixed	Dżugan et al. (2018)
			~ 0.65	Urban	Zarić et al. (2017)
			ND - 0.77	Mixed	Tomzyk et al. (2020)
		0.007-3.9		Mixed	Roman (2009)
			0.075 - 1.1450	Mixed	Gutiérrez et al. (2015)
			< 1.20	Nature reserves	Ruschioni et al. (2013)
			0.17 - 1.34	Urban areas, including near an airport, and wildlife reserves	Perugini et al. (2011)
		< 0.2 - 0.37	0.33 - 1.5	Mixed	Fakhimzadeh and Lodenius (2000)
			0.13 - 1.53	Mixed	Goretti et al. (2020)

Continued

** These pollen concentrations were measured from the nests of red mason bees (*O. bicornis*).

Table A1 Continued

Metal	Honey	Pollen or Bee Bread	Bee bodies	Site Description	Reference
Pb	6.3E-4 - 3.23		0.19 - 1.67	Mixed	Van der Steen et al. (2012)
			0.026 - 3.1	Urban and mining areas	Zhou et al. (2018)
			< 0.25 - 7.8	Mixed	Velemínský et al. (1990)
		0.65 - 14.23	2.32 - 11.23	Mixed	Al Naggar et al. (2013)
			0.00401 - 0.0241	Near thermal power plants	Silici et al. (2016)
		< 0.01 - 0.44		Rural and urban	Morgano et al. (2010)
		3.2 - 4.6		Extraurban crossroad	Leita et al. (1996)
		42.05 - 356.16**		Urbanization gradients approaching smelters	Moroń et al. (2012)
Zn	0.23 - 73.60		8.56 - 17.0	Near thermal power plants	Silici et al. (2016)
			31 - 58	Urban and mining areas	Zhou et al. (2018)
			14.15 - 68.20	Mixed	Dżugan et al. (2018)
		7.13 - 42.42	13.8 - 77.95	Mixed	Al Naggar et l. (2013)
			59.18 - 100.46	Mixed	Van der Steen et al. (2012)
		29 - 49	55 - 101	Mixed	Fakhimzadeh and Lodenius (2000)
			~103	Urban	Zarić et al. (2017)
			8.8 - 204.4	Mixed	Velemínský et al. (1990)
			87.91 - 210.55	Mixed	Goretti et al. (2020)
		89.8 - 108.2		Extraurban crossroad	Leita et al. (1996)
		55.90 - 440.11**		Urbanization gradients approaching smelters	Moroń et al. (2011)

** These pollen concentrations were measured from the nests of red mason bees (*O. bicornis*).

References not appearing in main text:

Fakhimzadeh, K., and M. Lodenius. **2000**. Heavy metals in Finnish honey, pollen and honey bees. Apiacta. 35.

Maragou, N. C., G. Pavlidis, H. Karasali, and F. Hatjina. **2017**. Major and minor element levels in Greek apicultural products. Glob. Nest J. 19.

Morgano, M. A., M. C. Teixeira Martins, L. C. Rabonato, R. F. Milani, K. Yotsuyanagi, and D. B. Rodriguez-Amaya. **2010**. Inorganic contaminants in bee pollen from southeastern Brazil. J. Agric. Food Chem. 58.

Moroń, D., I. M. Grześ, P. Skórka, H. Szentgyörgyi, R. Laskowski, S. G. Potts, and M. Woyciechowski. **2012**. Abundance and diversity of wild bees along gradients of heavy metal pollution. J. Appl. Ecol. 49: 118–125.

Perugini, M., M. Manera, L. Grotta, M. C. Abete, R. Tarasco, and M. Amorena. **2011**. Heavy metal (Hg, Cr, Cd, and Pb) contamination in urban areas and wildlife reserves: Honeybees as bioindicators. Biol. Trace Elem. Res.

Roman, A. 2009. Concentration of chosen trace elements of toxic properties in bee pollen loads. Polish J. Environ. Stud. 18.

Ruschioni, S., P. Riolo, R. L. Minuz, M. Stefano, M. Cannella, C. Porrini, and N. Isidoro. **2013**. Biomonitoring with honeybees of heavy metals and pesticides in nature reserves of the Marche region (Italy). Biol. Trace Elem. Res. 154.

Van Der Steen, J. J. M., J. De Kraker, and T. Grotenhuis. **2012**. Spatial and temporal variation of metal concentrations in adult honeybees (Apis mellifera L.). Environ. Monit. Assess. 184.

Tomczyk, M., G. Zaguła, C. Puchalski, and M. Dżugan. **2020**. Transfer of Some Toxic Metals from Soil to Honey Depending on Bee Habitat Conditions. Acta Univ. Cibiniensis. Ser. E Food Technol. 24.

Veleminsky, M., P. Laznicka, and P. Stary. **1990**. Honeybees (Apis mellifera) as environmental monitors of heavy metals in Czechoslovakia. Acta Entomol. Bohemoslov. 87.

Zarić, N. M., K. Ilijević, L. Stanisavljević, and I. Gržetić. **2017**. Use of honeybees (Apis mellifera L.) as bioindicators for assessment and source appointment of metal pollution. Environ. Sci. Pollut. Res. 24.

Zhou, X., M. P. Taylor, P. J. Davies, and S. Prasad. **2018**. Identifying Sources of Environmental Contamination in European Honey Bees (Apis mellifera) Using Trace Elements and Lead Isotopic Compositions. Environ. Sci. Technol. 52.

Appendix B. Description of GUTS

The General Unified Thresholds Model of Survival (GUTS) is a mechanistic model of toxicity that was designed to analyze survival data from standard laboratory bioassays (Jager et al. 2011). Unlike curve-fitting models such as probit models, whose parameters have no fixed biological meaning, GUTS makes explicit assumptions about the mechanisms by which toxicants are taken into organisms (toxicokinetics) and cause damage (toxicodynamics), which ultimately leads to effects on survival.

The creation of GUTS was motivated by the existence of a variety of preexisting toxicokinetic-toxicodynamic (TKTD) models of survival that lacked a common theoretical framework (Ashauer and Brown 2008). Most of these earlier models were subsequently shown to be special cases of GUTS (Jager et al. 2011). GUTS was recently approved for aquatic risk assessment at the regulatory level in the European Union (Ockleford et al. 2018). Although GUTS was largely developed in the context of aquatic risk assessment, it has been applied to a variety of organisms, including honey bees (Hesketh et al. 2016, Heard et al. 2017, Robinson et al. 2017).

In the full version of GUTS (GUTS-FULL), toxicokinetics and toxicodynamics are represented in individual compartments, forming a two-compartment model (Fig. B1, part A). First, chemical concentrations in the organism's environment and/or diet (C_{ext}) are converted into some internal concentration within the organism (C_i). The equation for this and most other GUTS equations are given in Fig. B1. The meanings of all variables and parameters are given in Table B1. The chemical's internal concentration is then converted into a metric of damage known as scaled internal damage (D_i). Once damage exceeds a certain tolerance threshold (z_i)

specific to the given organism and chemical, the probability of death, or the hazard rate (h_z), increases at a linear rate (Fig. B2).

GUTS-FULL requires information on the internal concentration of the chemical within the organism, which is rarely measured during standard honey bee bioassays. In contrast, a reduced version of GUTS (GUTS-RED, Fig. B1 part B) can be used with survival data, alone. GUTS-RED represents toxicokinetics and toxicdynamics as occurring together, forming a one-compartment model. The overall rate that the chemical's external concentration is translated into damage is represented by a single, dominant rate constant (k_d). The utilization of k_d relies on a key assumption: Because toxicodynamics follows from toxicokinetics in a linear chain, the slower of the two processes will constitute the rate-limiting step and will drive the overall rate that external concentrations are translated into damage. For this reason, in GUTS-RED, k_d is assumed to approximate the slower of the two processes. This obviates the need for additional rate constants and associated parameters in this version of the model.

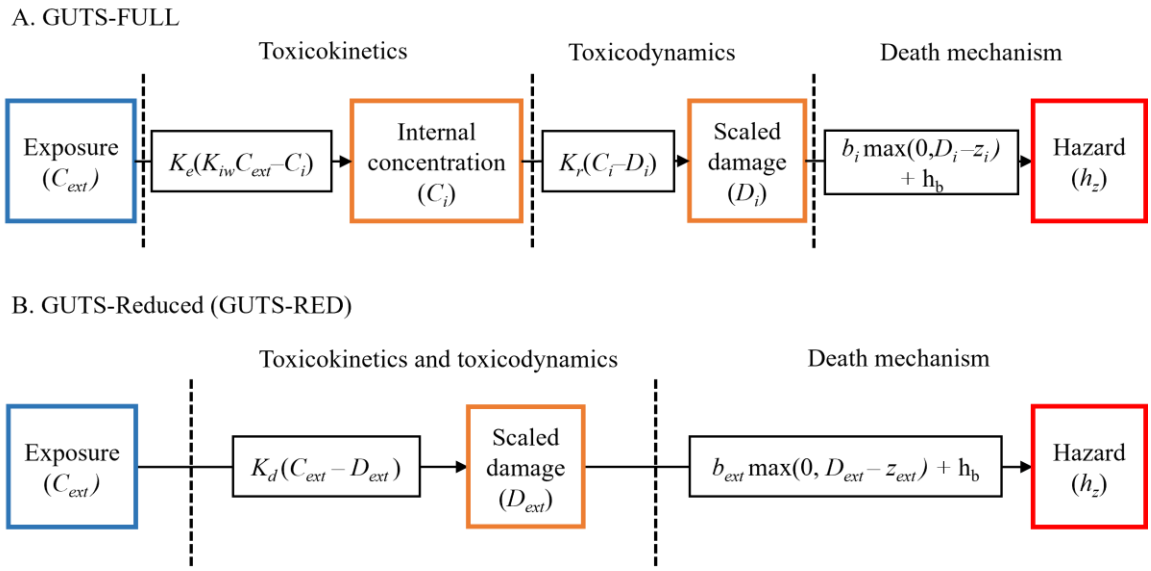

Figure 28. Diagrams of GUTS. (A) The full version of GUTS (GUTS-FULL) includes a toxicokinetic compartment, which represents the uptake and elimination of the chemical from the organism, followed by a toxicodynamic compartment, which represents the accrual of chemical-induced damaged. (B) The reduced version of GUTS (GUTS-RED) represents toxicokinetics and toxicodynamics in a single compartment.

Symbol	Description	Model version	Death mechanism	Example Units
$\boldsymbol{k_e}$	Elimination rate constant of chemical from the organism	FULL	Both	d^{-1}
$\boldsymbol{K_{iext}}$	Bioconcentration factor of chemical into organism from source of exposure	FULL	Both	mL/mg
$\boldsymbol{k_r}$	Damage repair rate constant	FULL	Both	d^{-1}
C_i	Internal chemical concentration	FULL	Both	mg/L
$\boldsymbol{k_d}$	Dominant rate constant of all TKTD processes	RED	Both	d^{-1}
$\boldsymbol{h_b}$	Baseline hazard	Both	Both	d^{-1}
D_i*	Scaled internal damage	Both	Both	mg/L
h_z	Total hazard for individual with tolerance threshold *z*	Both	Both	d^{-1}
C_{ext}	Chemical concentration in organism's diet or media	Both	Both	mg/L
$\boldsymbol{F_s}$	Spread factor of distribution of tolerance thresholds	Both	IT	-
m*	Median of distribution of tolerance thresholds	Both	IT	mg/L
b*	Killing rate	Both	SD	$L\ mg^{-1}\ d^{-1}$
z*	Tolerance threshold	Both	SD	mg/L

Table 18. All constants, variables, and parameters in either version of GUTS (FULL or RED) representing either death mechanism (SD or IT). Parameters that are estimated during model calibration are presented in bold. All other symbols represent state variables. * These symbols have different subscripts depending on the version of GUTS being used: "i" (internal concentrations) is used in GUTS-FULL, whereas "ext" (external concentrations) is used in GUTS-RED. Unlike previous publications on GUTS, the subscript "ext" is used rather than "w," which stands for "water" and is a vestige of GUTS history of use with aquatic organisms.

In addition to the full and reduced versions of GUTS, there are also two subtypes of GUTS that convert damage into survival probabilities differently (Fig. B2). In the "stochastic death" version of GUTS (GUTS-SD), death is represented as a stochastic event whose probability increases linearly once the tolerance threshold is exceeded, and every individual in the population is assumed to have the same threshold. In the "individual tolerance" version (GUTS-IT), individuals are allowed to have varying tolerance thresholds, but the probability of death is infinite (certain) once that threshold is reached. These different "death mechanisms"

have their roots in the toxicological literature (Ashauer et al. 2015). Neither version is universally better and either version may fit a particular dataset more closely than the other, though data from certain chemicals can be expected to fit one version better than the other.

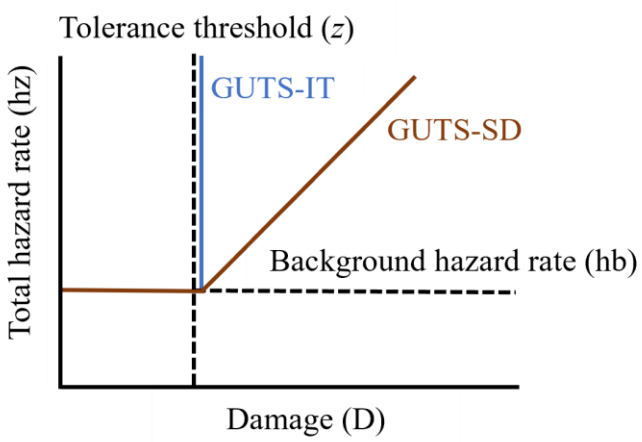

Figure 29. Diagram of GUTS death mechanisms. GUTS assumes that the hazard rate or probability of death (h_z) increases above its baseline value (h_b) once damage exceeds the organism's tolerance threshold (z). In GUTS-SD (orange), z is the same for all members of the study population and once it is exceeded, h_z increases linearly at a rate dependent on the killing rate parameter (b). In GUTS-IT (blue), z varies among individuals, and once it is exceeded, the hazard rate becomes infinite, represented by a vertical line in the above diagram. Figure modified with permission from (Jager and Ashauer 2018).

GUTS parameters can be estimated by a variety of independent modeling approaches. This includes Bayesian (Delignette-Muller et al. 2017) and frequentist approaches (Jager and Ashauer 2018, Jager 2021). For the current study, the *survFit* function in the R package 'morse' was used to fit the parameters of GUTS-RED-SD and GUTS-RED-IT to experimental data for each metal and assay (Baudrot et al. 2021). 'morse' uses the input data for each chemical to infer reasonable prior distributions for each GUTS parameter (Delignette-Muller et al. 2017). These prior values are iteratively refined through a Bayesian Gibbs sampling algorithm implemented in the R package 'RJAGS' (Plummer 2021). This results in posterior probability distributions for each parameter that are used to calculate median estimates for each parameter and their 95%

confidence intervals. These posterior distributions were used to predict survival during colony level simulations (main text, section 2.2.5).

To cross-check the parameter values estimated by *morse*, GUTS parameters were also estimated using the OpenGUTS software, which implements a frequentist maximum likelihood parameter estimation procedure (Jager 2021). This software does not rely on prior information during model fitting and can be considered a more conservative approach than 'morse'. For this reason, only its parameter estimates are provided in the main text (Table 5). OpenGUTS was also used to determine the best-fitting version of GUTS-RED (SD or IT) for each metal (main text, Table 4).

Appendix C. Supplementary Figures and Tables

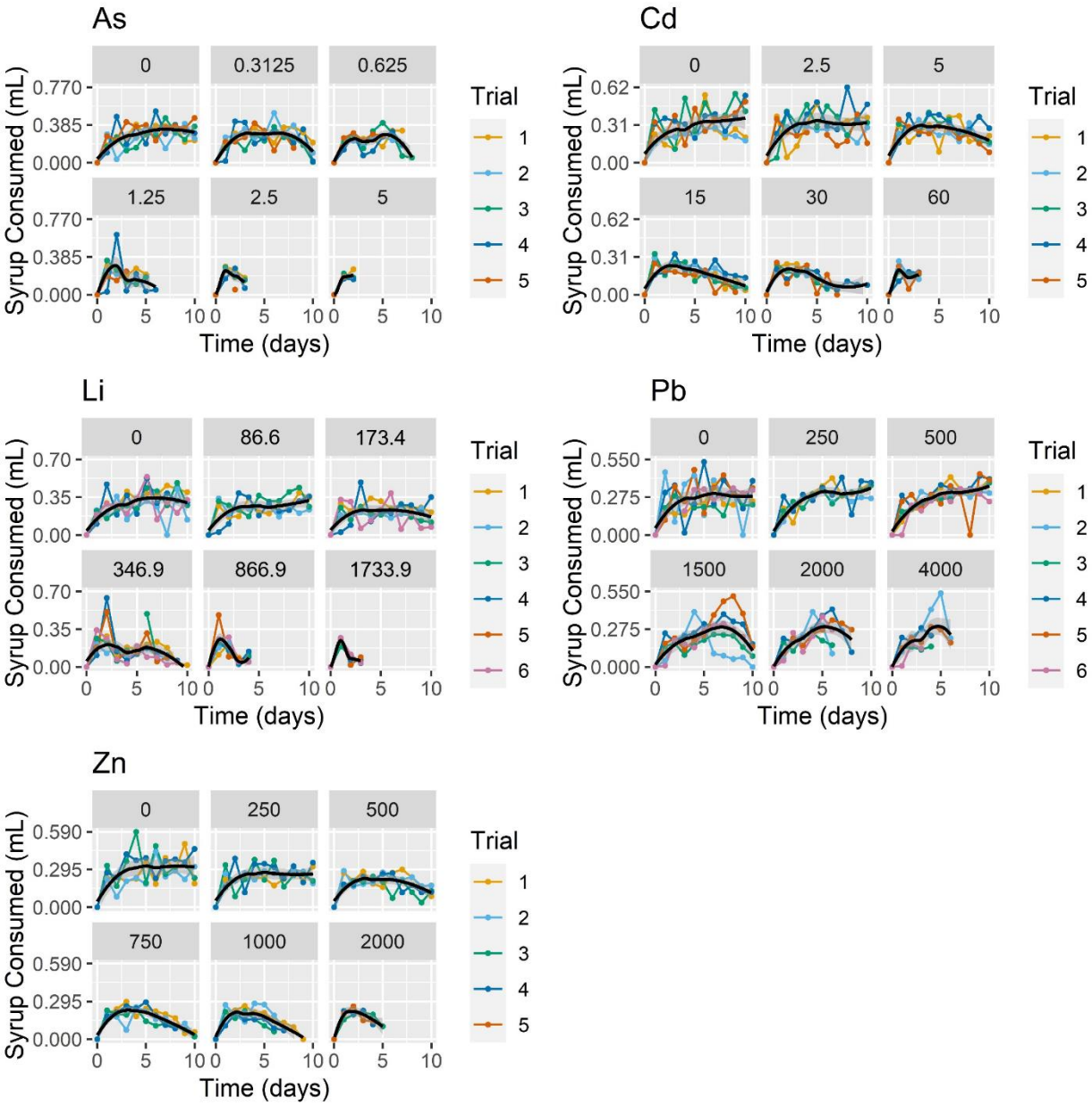

Figure 30. Food consumption data from calibration assays for each metal, after correcting for evaporation. Curves are Loess models of food consumption for each concentration.

GUTS Model	Parameter	Unit	As	Cd	Li*	Pb	Zn
SD	Dominant rate (*kd*)	day^{-1}	0.015	0.096	0.021	0.081	0.064
	Killing rate (bw)	$mg\ L^{-1}$	10.782	0.040	0.002	0.000	0.001
	Threshold (z)	$mg\ L^{-1}\ day^{-1}$	0.022	0.639	70.378	106.344	65.735
IT	Dominant rate (*kd*)	day^{-1}	0.005	0.006	0.004	0.007	0.013
	Median of threshold distribution (mw)	$mg\ L^{-1}\ day^{-1}$	0.023	0.685	69.042	90.324	70.114
	Spread of threshold (Fs)	--	3.581	2.908	4.131	4.316	4.632

Table 19. Median estimates of GUTS parameters (SD or IT) for each metal, fitted to the calibration data. Values were estimated with the R package 'morse.' * Values for Li are in terms of concentrations of LiCl.

Metal	Assay	n	Probit Models	GUTS-RED-SD
As	Calibration	29	0.24 (0.19-0.28)	0.33 (0.31-0.34)
Cd	Calibration	29	10.33 (7.50-14.64)	6.77 (6.10-7.46)
Li	Calibration	32	183.6 (161.9-208.5)	172.2 (163.6-184.3)
Pb	Calibration	31	1011.26 (885.01-1149.15)	853.62 (787.51-928.00)
Zn	Calibration	23	473.12 (431.81-514.43)	408.65 (382.72-437.04)
Cd	Corroboration	13	2.5 (1.78-3.57)	2.26 (1.97-2.65)
Li	Corroboration	18	353.8 (11.4-170.5)	58.5 (51.6-66.9)
Zn	Corroboration	18	177.07 (139.73-221.57)	150.82 (138.38-164.97)

Table 20. LC_{50} estimates (medians and 95% confidence intervals) for each metal and modeling approach, using data from calibration assays or corroboration assays.

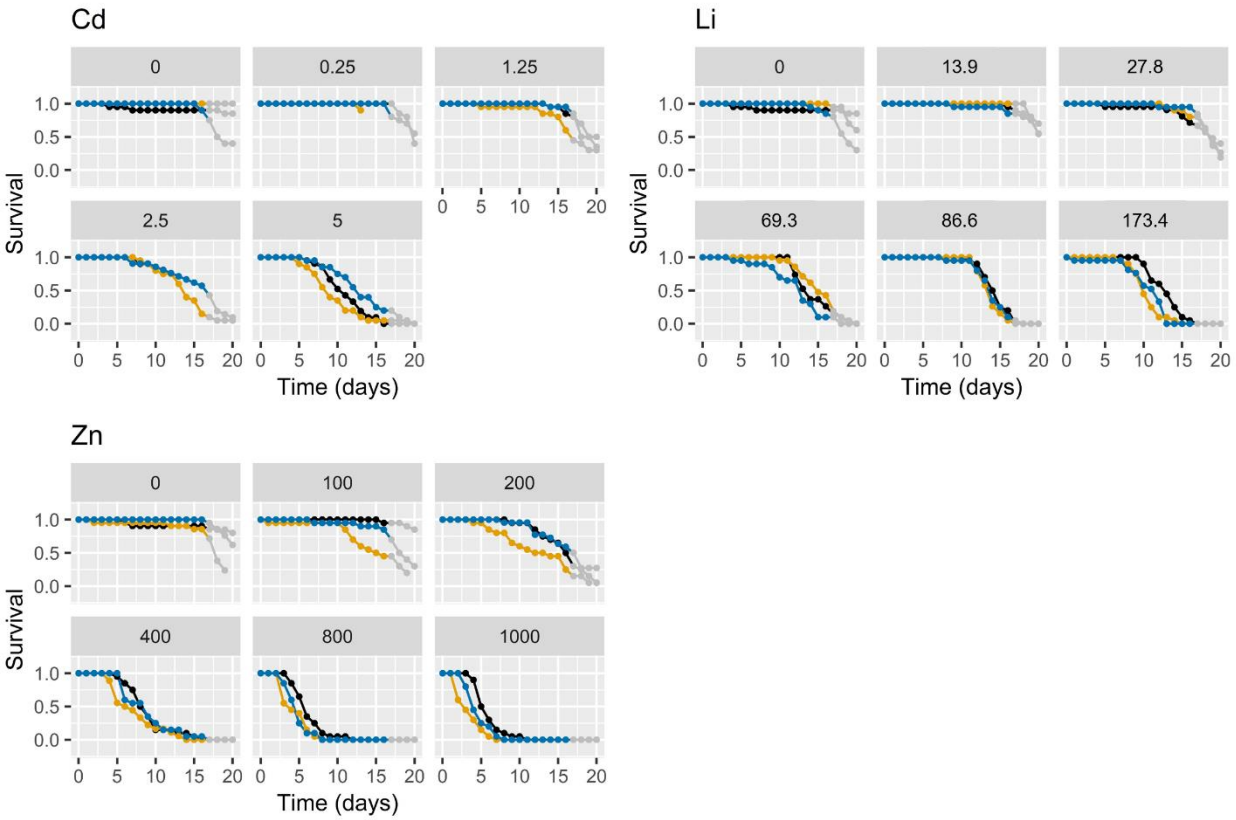

Figure 31. Survival observed during corroboration assays for each metal and treatment group. Concentrations are given in mg/L. Lines are colored by trial. Datapoints and lines in grey (days 17-20) were omitted from the analysis because at least one cup from the negative control groups for each metal exhibited mortality ≥20% by those times.

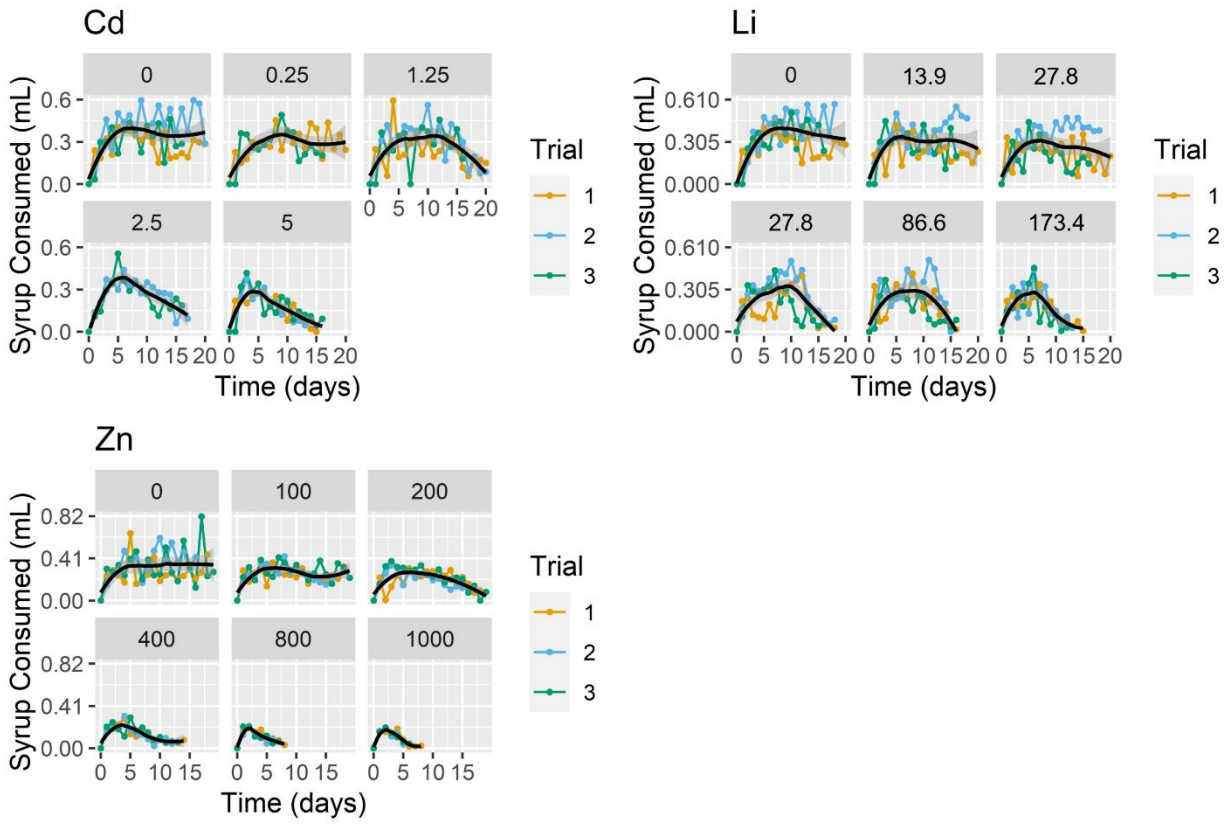

Figure 32. Food consumption data from corroboration assays for each metal, after correcting for evaporation. Curves are Loess models of food consumption for each concentration.

Comparison	P value	t ratio	Estimate	SE	df
As - Cd	1.000	0.142	0.031	0.218	16
As - LiCl	1.000	-0.093	-0.019	0.207	16
As - Pb	0.845	-1.014	-0.435	0.429	16
As - Zn	0.463	-1.697	-0.398	0.234	16
Cd - LiCl	0.999	-0.265	-0.050	0.191	16
Cd - Pb	0.801	-1.107	-0.466	0.421	16
Cd - Zn	0.332	-1.952	-0.429	0.220	16
LiCl - Pb	0.851	-1.001	-0.416	0.416	16
LiCl - Zn	0.400	-1.814	-0.378	0.209	16
Pb - Zn	1.000	0.087	0.037	0.430	16

Table 21. Pairwise comparisons of Haber constants for each metal. No pair of Haber constants were significantly different from each other (Tukey's HSD, $p < 0.05$).